Affordable Adsorbent for Arsenic Removal from Rural Water Supply Systems in Newfoundland

By

Javid Shadbahr

A thesis submitted to the School of Graduate Studies in partial fulfilment of the requirements for the degree of

Master of Engineering

Faculty of Engineering and Applied Science

Memorial University of Newfoundland

September 2017

St. John’s Newfoundland

Abstract

Fly ash from the Corner Brook Pulp and Paper (CBPP) mill was used in this study as the raw material for preparation of a low-cost adsorbent for arsenic removal from the well water in the Bell Island. The CBPP was physically activated in two different ways: (a) activation with pure CO_2 (CAC) with the iodine number and methylene value of 704.53 mg/g and 292.32 mg/g, respectively; and (b) activation with the mixture of CO_2 and steam (CSAC) with the iodine number and methylene value of 1119.98 mg/g and 358.95 mg/g, respectively, at the optimized temperature of 850ºC and the contact time of 2 hours of activation. The surface area of CAC and CSAC, at the optimized conditions, was 847.26 m^2/g and 1146.25 m^2/g, respectively. The optimized CSAC was used for impregnation with iron (III) chloride ($FeCl_3$) with different concentrations (0.01M to 1M). The study showed that the adsorbent impregnated with 0.1M $FeCl_3$ was the most efficient one for arsenic removal. According to the scanning electron microscopy images and BET surface area analysis, it was revealed that the impregnation with 0.1M $FeCl_3$ would not significantly decrease the surface area and pore blockage was also negligible.

Isotherm analysis showed that the Langmuir model better described the equilibrium behavior of the arsenic adsorption for both local well water and synthesized water than the other models. Based on this model, the maximum arsenic adsorption capacity was 35.6 µg/g of carbon for local well water and 1428.6 µg/g of carbon for synthesized water. Furthermore, the kinetic data of the arsenic adsorption from synthesized and local well water was best fitted with the pseudo-second order kinetic model.

Acknowledgement

The author would like to express his appreciation to Dr. Tahir Husain, Professor, Memorial University of Newfoundland, for his great support, help, and contribution through this study. The author would also like to thank his family and friends for their never-ending support and help.

Table of Contents

List of Figures

List of Tables

1. Introduction

1.1. Background Information

Arsenic (As) is one of the most toxic heavy metals and it is a regulated contaminant in the drinking water (U.S.EPA, 2016). There is a high level of arsenic in the ground water in countries, listed in Figure 1-1. The Bengal Basin, covering a part of India and Bangladesh, is severely affected region with high level of arsenic in the ground water (Smedley & Kinniburgh, 2002). Around 30–35 million people in Bangladesh and 6 million in West Bengal in India are estimated to be exposed to arsenic in the drinking water at concentrations above 50 µg/L (Kinniburgh & Smedley, 2001).

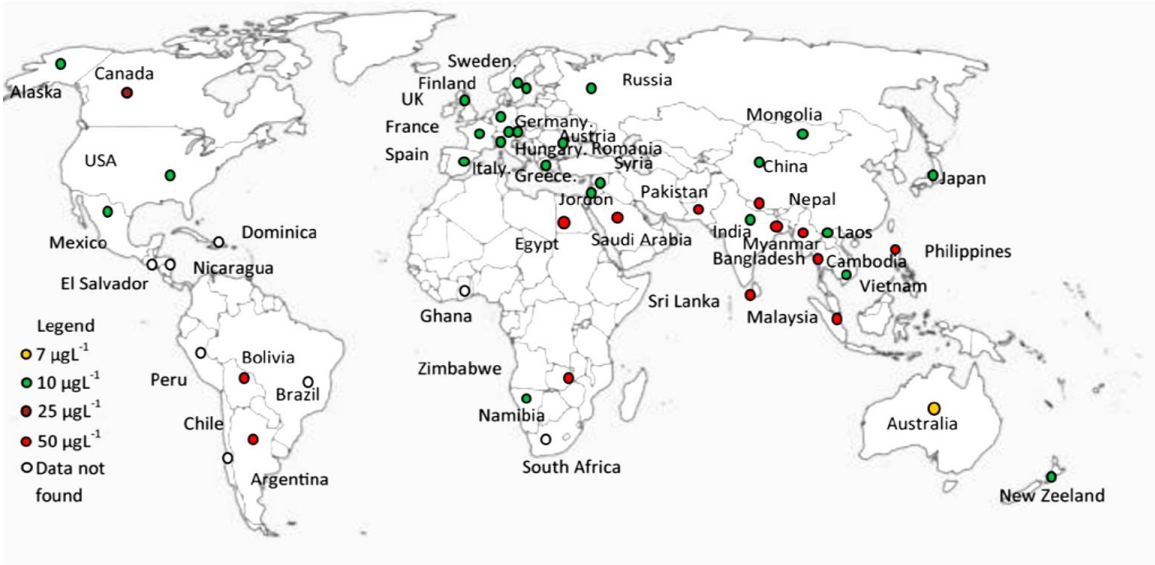

Figure 1-1: Arsenic concentration in different countries (Mondal *et al.*, 2013)

Arsenic commonly appears in both organic and inorganic forms in the natural waters. Organic arsenic is less of a concern because it is transformed into nontoxic forms

through methylation (Yao *et al.*, 2014). In the water systems, the arsenic usually occurs in the arsenate, As (V), and arsenite, As(III), forms (Lorenzen *et al.*, 1995, Rageh *et al.*, 2007). Comparing to arsenic (V), arsenic (III) is more soluble, mobile, and toxic.

Long term exposure to inorganic arsenic can significantly increase the risk of skin, lung, liver, bladder, and kidney cancer (Rohail, 2012, Yao et al., 2014). Since the drinking water is considered as the major source of exposure to inorganic arsenic, finding a simple, economic, and efficient solution for arsenic removal is critical.

30% of residents in the rural areas in Newfoundland and Labrador use groundwater and 75% of these wells are private wells (Sarkar *et al.*, 2012, Department of Municipal Affairs and Environment, 2010). While the maximum acceptable concentration of arsenic in drinking water is (MAC) of 10µg/L (U.S.EPA, 2016), the study shows that most of these wells have arsenic level above the MAC and the background concentration of arsenic in these wells can reach as high as 60µg/L. The Town of Wabana on Bell Island and the Town of Freshwater in Carbonear, shown in Figure 1-2, have been found previously to contain high level of arsenic in the wells with mean values as 62.0µg/L and 29.7µg/L, respectively (Rohail, 2012).

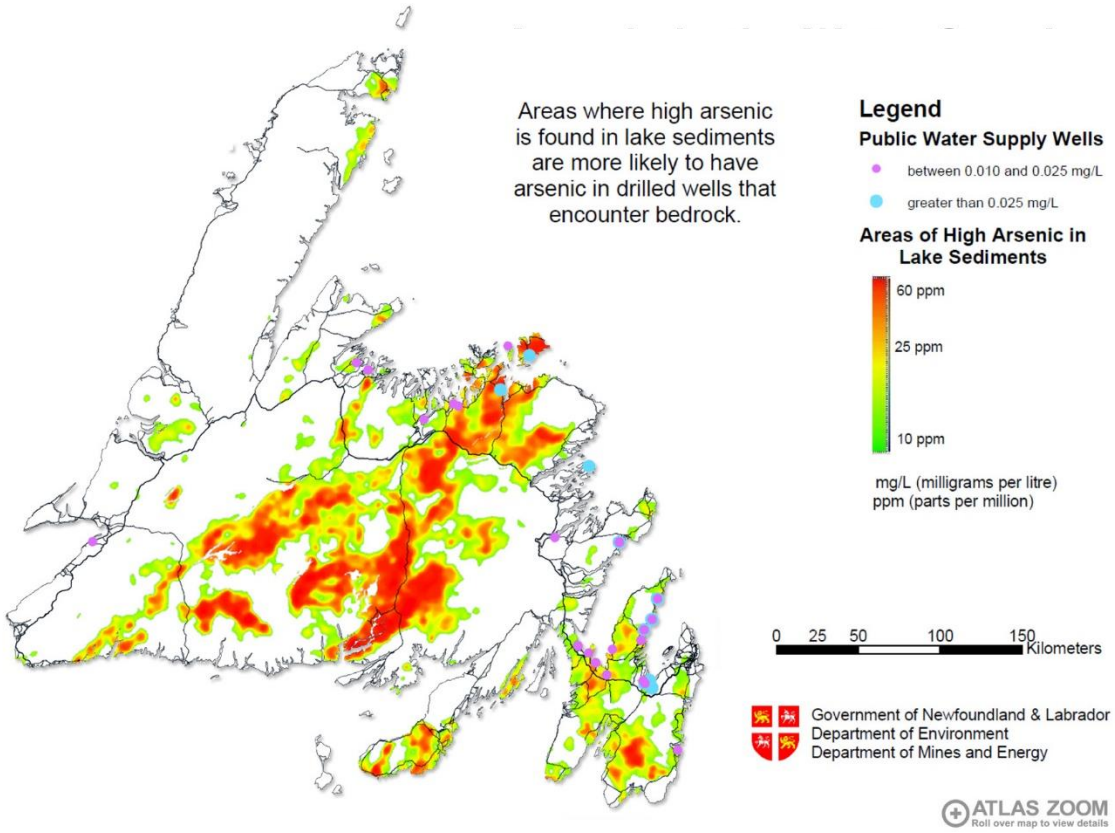

Figure 1-2: Areas of potential arsenic concentration in well water (Department of Municipal Affairs and Environment, 2016)

Arsenic can enter the water body through natural processes and anthropogenic activities. In the province, the arsenic in the groundwater is mainly from the natural sources, which typically include weathering, erosion from rock and soil, and rainwater. Two main categories of rocks containing arsenic in the province are igneous and sedimentary rocks. Igneous rocks have arsenic concentrations in the range of 0.2 to 13.8mg/kg, while sedimentary rocks hold a wider range from 0.3 to 500mg/kg (Salbu & Steinnes, 1994, Rohail, 2012). The release of arsenic from natural sources is primarily led by the interfacial interactions between solids, liquids, and gases. More precisely, the

interaction between natural solids (rock) and water bodies has the most contribution in the arsenic release into the water wells. The arsenic tends to appear in those wells which have been drilled into bedrocks with high levels of natural arsenic (Ray & Shipley, 2015).

Drinking-water quality issues are of great concern, and, as a result, billions of dollars are being spent worldwide annually to address this issue. As a main drinking water source, groundwater, especially well water contaminated by arsenic, has been documented in many communities in Newfoundland and Labrador. Certain systems such as arsenic adsorption package unit have been installed for the water source purification. However, the cost of installation and maintenance is rather high, thus the well owners find it difficult to afford. Besides, some of the techniques are relatively complex and not easy to operate, which can add difficulties to the well owners.

1.2. Study structure and objectives

The technologies used to treat arsenic from water supply systems are ion exchange, chemical precipitation, electrochemical, reverse osmosis, membrane filtration, floatation and adsorption (Yao et al., 2014, Ray & Shipley, 2015). Among these, adsorption is a simple and efficient method to remove low concentration pollutants. For rural and small communities, it is simple to install and operate and does not require skill operator. Due to the high surface area, porous structure, ad high adsorption capacity, the activated carbon (AC) is proved to be one of the most effective and reliable adsorbent. In order to

enhance the removal efficiency of arsenic, synthetically amended activated carbon by coating with metallic compounds has recently gained recognition (Ghanizadeh *et al.*, 2010, Yao et al., 2014). Iron compounds including hematite, goethite, iron oxide and ferric hydroxide are more preferred to combine with activated carbon due to their high affinity to arsenic adsorption (Zhang & Itoh, 2006, Ghanizadeh et al., 2010).

Some of the commercial activated carbon is usually manufactured using raw materials such as petroleum coke, bituminous and lignite coal, wood products, and coconut shells but due to the high cost of these raw materials, the activated carbon from these materials is not economical and small communities cannot afford (Streat *et al.*, 1995).

The Corner Brook Pulp and Paper (CBPP) mill, located in Western Newfoundland, generates approximate 10,000 metric tons of boiler ash and bottom ash on a yearly basis. This ash is mainly wood ash and is currently dumped into the landfills. The ash from CBPP has very high carbon content (around 90%). It has high pH (above 12) with 80% of CBPP ash has the particle size between 15 and 352 microns (µm) with mean value as 70 µm. According to Chen et al. (2007) and Jahan et al. (2008), a higher micro pore volume could increase not only the iron loading on the activated carbon surface but also the adsorption of arsenic species (Chen *et al.*, 2007, Jahan *et al.*, 2008).

In this study, CBPP fly ash was activated at different activation conditions and the optimized conditions for better activating the CBPP fly ash was obtained. Then, the

activated CBPP fly ash was impregnated with different concentrations of iron solution and according to the arsenic removal efficiencies of the impregnated samples, the best concentration for the iron impregnation was obtained. By having the impregnated sample, the developed adsorbent was used for arsenic removal from the local well water of Bell Island.

The main objective of this study is to develop a filter technology using a metal impregnated activated carbon by extracting carbon from CBPP fly ash as this type of carbon is cheaply available and such filters will be easy to install and operate. Commercialized activated carbon products are usually costly due to the high cost of raw materials. Converting the CBPP fly ash into valuable activated carbon product will not only provide affordable adsorbents to rural communities but it will also save money in the CBPP waste management.

2. Literature review

The study of Mondal et al. (2013) reviewed different technologies such as adsorption, ion exchange, coagulation, oxidation, and membrane processes, used for arsenic removal from the groundwater and discussed their applications and drawbacks. While it was recommended to use the combination of two technologies instead of using one single technology, such as the combination of membrane processes with iron based technologies, membrane distillation and forward osmosis was mentioned as the efficient technologies in case of arsenic removal. The main concern of these technologies is the high cost. Adsorption was also reviewed in this study as one of the useful methods for arsenic removal because of its high removal efficiency and being comparatively cheap (Mondal et al., 2013). Hence, there is a review in section 2-1 about the adsorbent preparation and its characterization, such as surface area and adsorption capacity, in different studies. Moreover, in section 2-2, a review on the important parameters for both preparation of the adsorbent and the arsenic adsorption experiments is presented. The kinetic and equilibrium behaviour of the arsenic adsorption by using different adsorbents are also examined in section 2-2.

2.1. Preparation and characterization of the adsorbent

In the study of González et al. (2006), activated carbon was prepared from shredded scrap tires by using carbon dioxide activation and the steam activation, and the differences between these two activations were compared and the best one as an efficient method for activation of this material was identified. The procedure of these activations was using the nitrogen flow at 800^{o}C in a cylindrical stainless steel atmospheric pressure reactor to purge the air from the reactor and continuing the carbonization stage to remove all the volatiles from the system. After that, the activation stage started at 850^{o}C and 900^{o}C by applying carbon dioxide or steam/nitrogen (85/15 v/v) flow. It was reported that at a constant temperature, there is a relationship between burn-off and activation time of the raw material. Moreover, it was presented that the burn-off during the activation through carbon dioxide was much lower than the activation through steam, which means the steam is more reactive compared with the carbon dioxide. It was reported that the reason for lower reaction rate for carbon dioxide might be the formation of oxygen groups on the carbon surface. In addition, the steam activation was found more efficient due to its higher nitrogen adsorption in comparison to carbon dioxide activation (González *et al.*, 2006).

According to the average equivalent radius of micropores for those two types of activation mentioned in González et al. (2006), it was found that for the burn-off values of around 40%, steam activation produces thinner micropores compared to the CO_2

activation and by proceeding the activation, more mesopores are produced, as the micropores become more widened. The external surface area of activated carbon increased as the activation proceeds and that would be because of production of mesopores from the large micropores and also the ignition of the pore walls (González et al., 2006).

Iron-coated Bagasse fly ash (BFA-IC) and sponge iron char (SIC) were used as the adsorbents for arsenic removal in the study of Yadav et al. (2014) and it was concluded that these adsorbents are useful in wastewater industry as the low-cost adsorbents for arsenic removal. The adsorption capacity of these two adsorbents was presented as 39.53 µg As(III)/g and 25.82 µg As(V)/g for BFA-IC and 27.85 µg As(III)/g and 28.58 µg As(V)/g for SIC respectively. Moreover, by applying the Brunauer, Emmett, and Teller (BET) method, the surface area of BFA-IC was determined as 168 m^2/g and SIC as 78.63 m^2/g (Yadav *et al.*, 2014).

Aworn et al. (2008), prepared activated carbon from agricultural waste material by physical activation. The study shows that the activation temperature, the activation agent, the amount of volatile matter in raw materials, and the characteristics of the raw materials are the important factors affecting the procedure of the preparation of an efficient activated carbon. The procedure of activation in this study was also started with carbonization with nitrogen gas as an inert gas to remove volatile matters and moisture, followed by activation with steam or carbon dioxide at different temperatures. It was

reported that in in the carbonization stage, by increasing the temperature, the amount of volatile matter decreases gradually and the amount of fixed carbon increases. Moreover, it was found that mesoporosity and microporosity are related to the ash content, which means that the materials with lower ash content, produce more micropores and high surface area, while materials with higher ash content produce more mesopores (Aworn *et al.*, 2008).

Iron-coated Bagasse fly ash (BFA-IC) and sponge iron char (SIC) were used as the adsorbents for arsenic removal in the study of Yadav et al. (2014) and it was concluded that these adsorbents are useful in wastewater industry as the low-cost adsorbents for arsenic removal. The adsorption capacity of these two adsorbents was presented as 39.53 µg As(III)/g and 25.82 µg As(V)/g for BFA-IC and 27.85 µg As(III)/g and 28.58 µg As(V)/g for SIC respectively. Moreover, by applying the Brunauer, Emmett, and Teller (BET) method, the surface area of BFA-IC was determined as 168 m^2/g and SIC as 78.63 m^2/g (Yadav et al., 2014).

In the study of Meher et al. (2016), removal of arsenate from drinking water by using impregnated fly ash, which was iron enriched aluminosilicate adsorbent (IEASA) prepared using alkali fusion of fly ash with aging and hydrothermal curing, was studied. According to the batch experiments, it was observed that IEASA could remove the arsenate which was from water solution with concentration of 1mg/L more than 99% and this high efficiency could be because of the active sites due to the existence of iron, Si/Al

ratio, and Al-OH groups for arsenate adsorption. Moreover, it was observed that the arsenic adsorption capacity was 0.592 mg/g for this adsorbent (Meher *et al.*, 2016).

In the study of Zhang et al. (2016), an effective method for arsenic removal from water was found. The fly ash of a coal-fired power station in China was used as an adsorbent of alumina/silica oxide hydrate (ASOH) and then impregnated with $FeCl_3.6H_2O$ to achieve a high rate of arsenic removal from water. By following the procedure of this study, the surface area of the treated fly ash increased by 8-12 times compared to the raw fly ash. Moreover, about arsenic removal, it was reported that by using the synthesized water with initial arsenic concentration of 0.1 to 50 mg/L, ASOH, before impregnation, has the ability of removing about 96% of arsenic from water, which is much higher than the raw fly ash. Furthermore, it was found that iron impregnated ASOH removed about 99% of arsenic from the water solution. It was concluded that this low-cost procedure was not only effective for arsenic removal from water but also it was an effective way to recycle the waste of the power station (Zhang *et al.*, 2016).

In the study of Li et al. (2014), coal blending of Shenfu coal (SFC) and Datong coal (DTC) was used as the raw material. This raw material was treated through carbonization process with N_2 and CO_2, followed by 2 stage activation and finally, adsorbent was prepared. According to the good results of iodine number, methylene blue, and pore volume, ash content, and mesoporosity of this adsorbent, that are 1104 mg/g, 251.8 mg/g, and 1.087 cm^3/g, 15.26%, and 64.31% respectively, it was reported that this

adsorbent, with this innovative preparation, is an efficient adsorbent for arsenic removal of water sources with initial low arsenic concentrations (<0.5 mg/L) and low temperatures (Li *et al.*, 2014).

In the study of Asadullah et al. (2014), Jute stick, which is a kind of agricultural residue, was used to be activated both physically (PAC), that developed mainly macropores and meso pores, and chemically (CHAC), which H_3PO_4 was used to produced high number of micro pores for activated carbon. It was reported that by using the water with the initial arsenic concentration of 100 µg/L, physically activated carbon reduced the arsenic concentration to 55 µg/L, while chemically activated carbon reduced it to 45 µg/L. However, iron impregnated CHAC had reduced it to lower than the maximum acceptable concentration of arsenic (10µg/L) and it was only 3 µg/L (Asadullah *et al.*, 2014).

In the study of Chang et al. (2010), granular activated carbon was impregnated with ferrous chloride, due to its high solubility in a wide range of pH. The main effort of this study was to increase the amount of iron impregnated on the activated carbon and stabilizing the iron. Hence, the impregnation was done by mixing and shaking 0.5M ferrous chloride and activated carbon for 24 hours and after the separation of the solution and particles, the particles heated at 105^{o}C for 10 hours to transform the ferrous the ferric, so most of the ferrous chloride transformed in to the form of ferric chloride, ferric hydroxide, and ferric oxide. These steps were repeated several times to increase the amount of impregnated iron. The impregnated activated carbon was mixed with 1N

sodium hydroxide for 24 hours and after that, the particles were made thoroughly wet with hydrochloric acid for another 24 hours. Finally, the adsorbent was washed several times with distilled water and dried in the oven at 105^{o}C. For the arsenic adsorption test in the experiments only the arsenate was investigated. Different concentrations of arsenate were treated with 0.1g of modified adsorbent by shaking with the speed of 30rpm for 48 hours. (Chang *et al.*, 2010).

2.2. Effects of different parameters on arsenic adsorption

According to the study of Chen et al. (2007), the reason activated carbon is suggested to be impregnated with iron is the fact that arsenic oxides would form complexes with the surface sites which contain iron. It was also reported that iron loaded amount and, accessibility and dispersion of preloaded iron are the factors that influence the arsenic removal. However, in the process of impregnating activated carbon with iron in the study, some of the iron ions located in micropores and it means they can not be helpful for arsenic removal. Moreover, the effect of existence of other substance such as silica in contaminated water was examined in this study and it was found that the concentration of silica was reduced during the treatment of that water and it means that some of the sorption sites were occupied with adsorbed silica and the arsenic adsorption capacity of the adsorbent reduced (Chen et al., 2007).

In the study of Raychoundhury et al. (2015), they focused on preparing an impregnated activated carbon which can remove arsenate [As(V)] and arsenite [AS(III) efficiently from synthetized water with the concentration of 1 ppm of $Na_2HAsO_4.7H_2O$ for arsenate removal and 1ppm of Na_2AsO_2 for arsenite removal. The concentration of Fe^{3+} in $Fe(NO_3)_3.9H_2O$, which was found significant to control the arsenic adsorption, was one of the parameters investigated in this study. It was observed that the activated carbon impregnated with the lowest concentration of Fe^{3+} has the highest arsenic removal efficiency among the other concentrations from 0.09 to 3.0 M and it was because of uniform distribution of Fe^{3+} on the activated carbon and not blocking significantly the porous media. This performance was assessed by the adsorption capacity of 125 mg of As(V) per g of Fe and 98.4 mg As(III) per g of Fe (Raychoudhury *et al.*, 2015).

The other parameter, which was assessed in the experiment of Raychoundhury et al. (2015), was pH in the range from 4.2 to 10 and it was found that increasing the pH increases the arsenite removal, however, decreases the arsenate removal. Hence, based on the contaminated water, that includes arsenate or arsenite, pH of the solution can be adjusted for the high capacity of arsenic removal. The effect of Ionic strength (IS) was also found insignificant. It was reported that while the iron content of the activated carbon was low and negligible, after the impregnation with different concentration of iron solution, the iron content was between 1.54% to 6.01% and for the most efficient impregnated adsorbent for arsenic removal, the iron content of impregnated activated

carbon was 1.54%. Langmuir and Freundlich models were used to develop isotherms and it was reported that the Langmuir model fits better to the equilibrium data achieved in this experiment for arsenic removal than the Freundlich model. Furthermore, pseudo first-order and pseudo second-order sorption kinetics was fitted with the kinetic data of modified adsorbent in this study for arsenic removal and it was found that the pseudo first-order sorption kinetic better describes the kinetic of arsenic removal with this impregnated activated carbon (Raychoudhury et al., 2015).

According to the experiments conducted in the study of Chang et al. (2010), it was found that the best pH for arsenate removal is between 2 and 6, since in the pH range of 6-7, arsenate removal rate was decreased slightly and after pH of 7, arsenate removal rate was decreased sharply. Moreover, about the isotherm, it was reported that the Langmuir model better describes the results of arsenate removal through this procedure and with this impregnated activated carbon. It was reported that the parameter “b” in the Langmuir model is an indicator for the affinity of the adsorbent for the adsorbate. The iron use efficiency, which is defined as the amount of adsorbed arsenic (mg) per unit amount of impregnated iron (g), was investigated and found that total surface area and specific surface area of impregnated iron are the representatives of maximum adsorption capacity and iron use efficiency, respectively (Chang et al., 2010).

The study of Chang et al. (2010) showed that for the small amount of impregnated iron, iron ions were placed on a single layer in the interior surface of activated carbon, so

the iron use efficiency is high in that case while the adsorption capacity is still low. By increasing the iron content until the optimum amount, the adsorption capacity increases and iron use efficiency remains high, however after this point and increasing the iron content, iron ions not only block the pores of the activated carbon but also make a multilayer which decreases the iron use efficiency and adsorption capacity (Chang et al., 2010).

The impact of iron content on arsenic removal by iron impregnated granular activated carbon (Fe-GAC) from water was investigated in another study by Chang et al. (2012). The acid extraction method was used to determine the iron content in the GAC. According to the scanning electron microscopy (SEM) and energy dispersion scope (EDS), it was revealed that iron was well distributed in the GAC by following this method. Because of having narrow pores due to the impregnation with iron and in order to give enough time for arsenic to be adsorbed, the equilibrium time was considered as 15 days. The Langmuir model was found a better fit than the other models for describing the equilibrium behavior of Fe-GAC for arsenic adsorption (Chang *et al.*, 2012).

Arcibar-Orozco et al. (2014) studied the influence of different parameters such as iron content, surface area, and charge distribution of raw activated carbon and modified activated carbon with iron oxyhydroxide nanoparticles for arsenate removal. Different activated carbons investigated in this study and it was reported that while the surface area of these activated carbons varies from 388 to 1747m^2/g, after modifying with iron

oxyhydroxide, the surface area reduced for all of them, due to the pore blockage of iron nanoparticles (Arcibar-Orozco *et al.*, 2014).

During the arsenic removal tests of Arcibar-Orozco et al. (2014) study, the pH was kept constant at 7 by using NaOH and HNO_3 solutions and in this pH, all arsenate complexes are in the form of $H_2AsO_4^-$ and $HAsO_2^{2-}$ species. The iron content of the activated carbon samples was reported in the range of 0.21% to 1.9% after applying the procedure of this study for modifying the activated carbon with iron oxyhydroxide nanoparticles. It was also presented that the arsenic adsorption capacity of these adsorbents increased after modifying with iron nanoparticles. Moreover, Langmuir model has reported as the best model describes the equilibrium data of the adsorbent compared to the Freundlich model. Furthermore, it was reported that the mechanism of arsenic adsorption could be described in 2 ways, electrostatic attraction to the surface of activated carbon and the interchange of OH- ligand of the molecules of arsenates (Arcibar-Orozco et al., 2014, Mohan & Pittman, 2007).

Different types of equilibrium models such as Langmuir, Freundlich, Temkin, and Redlich-Peterson were investigated in the study of Yadav et at. (2014). It was reported that by using the BFA-IC Temkin and Freundlich models fit better and by using the SIC, Freundlich and Redlich-Peterson models better describe the equilibrium behavior of arsenic adsorption. About the adsorption kinetic, the pseudo first-order and pseudo-second order kinetic models were investigated and it was reported that pseudo second-

order better describes the kinetic of arsenic removal with SIC and BFA-IC (Yadav et al., 2014).

Granular activated carbon-based adsorbents (As-GAC) was used for arsenic removal from drinking water in the study of Gu et al. (2005). Obstruction of micro pores was the reason mentioned for reduction of BET specific surface area, pore volume, average mesoporous diameter, and porosity. According to the SEM tests of these adsorbents, it was found that in case of impregnating with low concentrations of iron (around 1% Fe), these iron ions settled on the rime of the adsorbent (As-GAC), while for higher concentrations of iron (around 6% Fe), distribution of iron was good in the central spots, and also it was presented that As-GAC with this amount of iron has the most efficacious arsenic removal among higher and lower concentration. Moreover, by increasing the concentration of iron (more than 7% Fe), a ring of iron appears on the rim of the granular activated carbon (GAC) (Gu *et al.*, 2005).

Furthermore, in the Gu et al. (2005) study, the column test was also investigated, and it was presented that by using the groundwater with approximate initial concentration of 50 µg/L, these adsorbents have the capability to reduce the concentration of As(V) and As(III) to lower than the maximum acceptable concentration of arsenic which is 10 µg/L. The effect of pH and ionic strength were also examined in this study and it was reported that for the high amount of arsenate removal, pH should be kept between 4.4 to 9 since by increasing the pH more than 9, the arsenic adsorption was

reduced. About the ionic strength, it was presented that it does not have an efficient effect on arsenic removal from water (Gu et al., 2005).

About the equilibrium data and isotherm, Gu et al. (2005) reported that the Langmuir model was fitted better than the Freundlich model. Moreover, the effect of the presence of three oxyanions, SO_4^{2-}, PO_4^{3-}, and SiO_3^{2-}, and two halide anions, Cl^- and Fe^- examined and it was presented that while the effect of halide anions and sulfate is negligible, phosphate and silicate could significantly decrease the arsenic adsorption, especially for higher pH. It was concluded that the existence of phosphate and silicate would slightly decrease the arsenic removal in the pH of 3 to 6.5, while by increasing the pH, their influence would be higher until the 20% reduction arsenic removal was observed for pH higher than 9. Moreover, the effect of phosphate was reported to be more than silicate in the reduction of arsenate removal (Gu et al., 2005).

To achieve the best condition for arsenic removal, pH was also optimized in the study of Zhang et al. (2016), and the optimum pH was reported between 2 to 4. Moreover, by examining the equilibrium data of arsenic removal with this modified adsorbent, it was reported that the Langmuir model fitted better than the Freundlich model (Zhang et al., 2016).

According to the study of Ghanizadeh et al. (2010), it was revealed that the existence of silicate and phosphate influence the mobility of arsenic and consequently,

the arsenic removal decreases. It was also reported that although impregnation with copper (Cu) also increases the arsenic removal from water, impregnation with iron compounds, due to the high affinity of arsenic for the iron compounds, gives better efficiency in arsenic removal from water. Introducing the film diffusion as the controlling step in the adsorption rate of arsenic, compared to the pore diffusion was the other observation of this study (Ghanizadeh et al., 2010).

The synthesized silicate template SBA-15 was used and treated by polymerization and carbonization process to achieve the ordered mesoporous carbon (OMC) for arsenic removal by Gu et al. (2007). The OMC was impregnated by using ferrous ion (FeOMC), because of its ability to penetrate the holes of the adsorbent. The specific surface area of OMC and FeOMC was determined and reported as $607 m^2/g$ and $466 m^2/g$, respectively. The reduction in the specific surface area of the FeOMC was believed due to iron impregnation and its pore blockage. According to the effect of pH on the removal efficiency, it was concluded that for arsenate removal the optimum pH range is in the range of 3-7, and for arsenite removal, the optimum pH should be in the range of 6 to 9. Other anions such as silica and phosphate could influence the arsenic removal. The adsorption isotherm for arsenic removal was also investigated and found that Langmuir model is a better fit than the other models (Gu *et al.*, 2007).

3. Materials and methods

3.1. Materials

CBPP fly ash obtained from Corner Brook Pulp and Paper mill and the local well water collected from Bell Island's well #16. All chemicals used in this study were reagent grade and the materials and chemicals used are:, sodium arsenate ($Na_2HAsO_4.7H_2O$) as the arsenic (V) source, arsenic oxide (As_2O_3) as the arsenic (III) source, ferric chloride anhydrous ($FeCl_3$), , sodium hydroxide (NaOH), hydrochloric acid (HCl) 5%wt/wt, nitric acid (HNO_3) 5% wt/wt, iodine solution (0.1N), sodium thiosulfate (0.1N), methylene blue solution (1500ppm), nitrogen (N_2) gas, carbon dioxide (CO_2) gas, 0.45µm and 11cm Whatman filter paper, volumetric burette, end-over-end rotator, vertical tube furnace from Carbolite Gero manufacturer, digital shaker from Thermo Fisher Scientific, scanning electron microscopy (SEM), Perkin – Elmer 2400 Series II CHN analyzer, Perkin – Elmer ELAN DRC II Mass Spectrometer, inductively coupled plasma mass spectrometry (ICP-MS), Horiba Particle Laser Scattered Particles Size Analyzer (Model LA-950), Perkin-Elmer Optima 5300 DV Inductively coupled plasma, Cole-Parmer Centrifuge, UV/V spectrophotometer (Thermo Scientific Genesys), 3Flex Surface Characterization Analyzer (Micromeritics Instrument Corporation.

3.2. Elemental analysis of Bell island's well water

The arsenic contaminated well water in Bell Island was collected and in order to find out different elements existed in this well water and their concentrations, it was sent to be analyzed by the Inductively Coupled Plasma Mass Spectrometry (ICP-MS) device in the Earth Resources Research and Analysis Facility (TERRA).

3.3. Preparation of CBPP fly ash

The CBPP carbon-enriched ash obtained from the Corner Brook Pulp and Paper (CBPP) mill. The CBPP fly ash was first grinded. The grinded sample before cleaning is named raw CBPP fly ash in this study. Then, it was washed with hot water to remove volatile organic compounds (VOCs) and other impurities, and then it was acid-washed with HNO_3 5% wt./wt. to remove metals existed in this fly ash. For the acid wash step, CBPP fly ash and acid were mixed with the ratio of 1g of CBPP fly ash to 10ml of acid and then the mixture was placed on the hot plate at 80^{o}C to be heated and rotated for 4 hours.

After that, the mixture was removed from the hot plate and placed at room temperature to be cooled down and filtered through 0.45 µm filter paper. In the last step of washing the fly ash, since CBPP was washed with acid, its pH was around 1, so it was needed to be washed with distilled water to increase the pH until it becomes stable. This step was also done on the hot plate at 80^{o}C and mixing the sample with the magnet. After

the washing process, the sample was placed in the oven to be dried at 110^{o}C overnight. This dried sample, which cleaned with both water and acid, is named cleaned CBPP fly ash in this study.

3.4. Characterization of CBPP fly ash

3.4.1 Particle Size distribution

The particle size of the grinded CBPP fly ash was determined using a Horiba Particle Laser Scattered Particles Size Analyzer (Model LA-950) in the Earth Resources Research and Analysis Facility (TERRA).

3.4.2 pH value

The pH was determined using the ASTM method D3838-05 (2017). 10g of CBPP fly ash was added to 100ml of boiling deionized water and the mixture was kept boiling for 15min. Then, solution and fly ash was separated via filtration system and by using the pH meter, pH of raw and cleaned CBPP fly ash was determined.

3.4.3 Moisture content

The ASTM method D2867-09 (2014) was used to determine the moisture content of raw and clean CBPP fly ash. According to this method, 2g of the fly ash was added to a crucible, that was weighted before, and placed in oven at 110^{o}C for 1 hour. After cooling down, the weight of the crucible was recorded, and this procedure was repeated until the weight of the crucible and fly ash inside remained constant. Moisture content is determined through Equation (3-1):

$$M\% = \frac{W_{wet} - W_{dry}}{W_{Sample}} \times 100 \quad (3\text{-}1)$$

in which,

M% = Moisture content in wt/wt %.

W_{wet}= Weight of crucible and sample, g.

W_{dry} = Weight of crucible and sample after heating, g.

W_{sample} = Weight of the original sample, g.

3.4.4 Ash content

Ash content of raw and cleaned CBPP fly ash was determined by following the ASTM method D2866-11 (2011). An empty and cleaned crucible was placed in the muffle furnace at 650^{o}C for 1hour to remove any remained impurities. After cooling down, the weight of the crucible was recorded. A certain amount of fly ash was added to the crucible and the weight of the fly ash and the crucible with the fly ash, was again recorded. The crucible, then, was placed in the muffle furnace at 650^{o}C for 3 hours. After cooling down, the weight of the crucible with the fly ash was recorded. Then, the crucible with the fly ash were placed into the muffle furnace again for another hour. After cooling down, the weight of the crucible and fly ash was compared the previous weight of them. This

procedure was repeated for several times to achieve a constant weight for crucible with the fly ash. Finally, Equation (3-2) calculated the ash content:

$$\text{Ash}\% = \frac{W_{ash}}{W_{Sample}} \times 100 \quad (3\text{-}2)$$

in which,

Ash% = Ash content, wt/wt %.

W_{ash} = Weight of ash remained in the crucible, g.

W_{Sample}= Weight of the original sample, g.

3.4.5 Carbon content

A Perkin – Elmer 2400 Series II CHN analyzer in Aquatic Research Cluster (ARC) under Core Research Equipment & Instrument Training (CREAIT) Network was used to determine the carbon content of raw and cleaned CBPP fly ash.

3.4.6 Metal content

A Perkin – Elmer ELAN DRC II Mass Spectrometer in TERRA facilities under CREAIT Network was also applied to determine the metal content of raw and cleaned CBPP fly ash.

3.4.7 Iodine number

The iodine number is known as an indicator of micropores and surface area of carbon (Krupa & Cannon, 1996). The ASTM method D4607-1 (2014) was applied to determine the iodine number for fly ash samples. According to this method, 0.2g of fly ash was added to 5ml of 5 wt.% hydrochloric acid and placed on the hot plate. The mixture was heated and remained in boiling state for 30 seconds to remove the sulfurs to prevent any interference of this element. After cooling down, 15ml of iodine solution (0.1N) was added to the mixture and placed on the shaker for 15min with the speed of 200rpm. Then, the solution and the fly ash were separated and 10ml of the solution was titrated with sodium thiosulfate (0.1N). The iodine number was calculated by applying Equation (3-3):

$$\mathrm{IN} = \frac{[(\mathrm{C_0} \times \mathrm{V_0}) - (\mathrm{C_1} \times \mathrm{V_1} \times \mathrm{DF})] \times 126.90}{\mathrm{M_c}} \quad (3\text{-}3)$$

where,

IN= Iodine number, mg/g.

$\mathrm{C_0}$= Concentration of iodine solution, 0.1N.

$\mathrm{V_0}$= Initial volume of iodine solution, ml.

$\mathrm{C_1}$= Concentration of sodium thiosulfate, 0.1N.

$\mathrm{V_1}$= Volume of sodium thiosulfate used for titration, ml.

DF= Dilution factor, equals to the summation of iodine solution volume and hydrochloric acid volume divided by the volume of filtrate for titration (10ml)

M_c= Weight of the sample, g.

3.4.8 Methylene blue value

Since the molecule sizes of the methylene blue, as a kind of organic dyes, are more than 1nm, methylene blue value typically is known as an indicator for mesopores of the tested sample (Yan *et al.*, 2009). The procedure of determining the methylene blue value was derived from GB/T 7702.6 (2008). According to this method, 0.1g of the fly ash was mixed with 10ml of methylene blue stock solution with the concentration of 1500mg/L and shaken for 30min with the speed of 200rpm. The fly ash and solution, then, was separated and the solution was transferred to a 10-mm cuvette and placed in the UV/V spectrophotometer (Thermo Scientific Genesys) at the wavelength of 665nm to analyze the UV absorbance. Equation (3-4) calculated the methylene blue value:

$$MBV=\frac{(C_0\text{-}C_1)\times V}{M_c} \quad (3\text{-}4)$$

in which,

MBV= Methylene blue value, mg/g.

C_0= Concentration of methylene blue tock solution, mg/g.

V= Initial volume of methylene blue solution, ml.

C_1= Concentration of methylene blue solution after filtration, mg/L.

M_c= Weight of the sample, g.

3.5. Carbonization and Activation of CBPP fly ash

Carbonization and activation are the major stages in the activation of raw materials. In the carbonization stage, 10g of the cleaned CBPP was placed in a programmable vertical tube furnace from Carbolite Gero Manufacturer, which provides the versatility and control accuracy to meet the critical temperatures required for the system. The furnace programmed under nitrogen flow (500cc/min) at 15^{o}C/min heating rate until the final selected temperature reached. After that, the furnace was kept at the final temperature and under the nitrogen flow of 500cc/min to complete the carbonization stage.

The activation stage carried out immediately after carbonization, using the CO_2 flow of 500cc/min and the temperature was kept at final temperature. This activation is called pure CO_2 activation of fly ash. In this study, in order to find out the optimum condition for activation of CBPP fly ash, the effects of both final temperature, and the activation time were examined. The final temperature of the furnace for activation of CBPP fly ash was changed from 650^{o}C to 900^{o}C and the CO_2 flow was in the range of 1 to 3 hours.

Moreover, another type of activation was also carried out in this study and it was the activation with the mixture of CO_2 and steam. The main difference of this activation with the pure CO_2 activation is in the CO_2 flow section that in this activation, CO_2 flow of

500cc/min was passed through the steam, that was generated in a bottle of distilled water that was continuously heated to be stabled at 90^{o}C. The mixture of CO_2 and steam was then passed through the activation tube to activate the CBPP fly ash. In this type of activation, also, temperature and CO_2 flow hours were changed to obtain the optimum condition of activation. Finally, the activated fly ash was cooled down to room temperature and became ready for iron impregnation.

3.6. Iron impregnation of activated CBPP fly ash

After activating the CBPP fly ash and cooling it in a desiccator, iron was coated on the activated CBPP fly ash through the impregnation method by using iron (III) chloride ($FeCl_3$) solution, prepared from ferric chloride anhydrous. Based on the results achieved in the study of Ray et al. the procedure of impregnation used in their study was also followed in this study with some modification, such as decreasing the range of iron solution while in high concentrations of iron surface reduction and iron leaching during the water treatment was significant (Raychoudhury et al., 2015). The procedure of this impregnation is as follows:

1. The activated CBPP fly ash was added to a series of flasks containing $FeCl_3$ solution with different concentrations of $FeCl_3$, from 0 to 1M, with the ratio of 1g of activated CBPP fly ash to 20ml of $FeCl_3$ solution.
2. The samples were mixed on the shaker for 1 hour and the speed of 50 rpm at room temperature.
3. In order to give enough time for iron ions to spread out into the pores of activated CBPP fly ash, mixtures were kept in room temperature for 24 hours.
4. The excess iron solution of each flask was taken out.
5. To impregnate activated CBPP fly ash with iron, the mixture was put in the oven at 110^{O}C for 24 hours to start hydrolysis and drying.

6. After drying, the mixture of each sample was washed several times to remove the excess iron of each sample.

7. Finally, each sample placed in the oven at 110^{O}C for 24 hours to be dried.

3.7. Characterization of activated and impregnated CBPP fly ash

3.7.1 Scanning electron microscopy (SEM)

The inner faces and surface microstructure of carbon samples before and after activation and after impregnation was observed by using the scanning electron microscopy (SEM) instrument from TERRA facilities.

3.7.2 Iron content

The amount of iron existed in each batch of activated CBPP fly ash could be determined through incineration method (Xu & Teja, 2006), incineration plus acid digestion (Chen et al., 2007), and acid extraction (Gu et al., 2005) which was used in this study due to its simplicity. According to the acid extraction method, the adsorbents and hydrochloric acid (1:1) were mixed with the ratio of 0.1 gram of adsorbent to 20ml of acid. Then the mixture was shaken overnight (18hr) at room temperature with the speed of 120rpm. After that, the mixture was kept at the oven with the temperature of 70^{O}C for 4

hours. Finally, the adsorbents were separated from the solution by using the centrifuge with the speed of 6000 rpm for 1 hour and the solution was sent for ICP-OES analysis using a Perkin-Elmer Optima 5300 DV Inductively coupled plasma instrument as a part of CREAIT facilities in Memorial University of Newfoundland.

3.7.3 Specific surface area

The specific surface area and porosity analysis of cleaned, activated, and impregnated activated CBPP fly ash were measured at the Centre for Catalysis Research and Innovation (CCRI) of the University of Ottawa. The surface area and pore volume of the samples were determined by N_2 sorption-desorption isotherms at 77K by applying a 3Flex Surface Characterization Analyzer (Micromeritics Instrument Corporation), following the Brunauer, Emmett, and Teller (BET) method.

3.8. Sorption experiments

3.8.1 Arsenic removal experiment

The developed absorbent was applied to measure the performance of arsenic removal from synthetic water. All chemicals used for the solutions were reagent grades in distilled water with electrical conductivity (EC) less than 3µmohs/cm. The stock solution of arsenate, As(V), and arsenite, As(III), were prepared from sodium arsenate ($Na_2HAsO_4.7H_2O$) and arsenic (III) oxide (As_2O_3), respectively, with concentration of 1000mg/L. For this experiment, the stock solutions were diluted to the concentration of 1mg/L. The next step was the batch experiments that were continued by using 0.1g of the developed adsorbents, impregnated with different concentration of iron solution, in a series of glass containers that each contained 200ml of As(V) or As(III) solutions. By using an end-over-end rotator, containers were mixed for 24 hours at room temperature.

Finally, samples were filtered through the 11cm filter paper and sent for ICP-MS analysis. The activated CBPP fly ash was impregnated with different concentrations of $FeCl_3$ from 0.01M to 1M and each of these impregnated adsorbents were used for arsenic removal through this procedure and under the same conditions in order to find out the efficiency of these adsorbents and finally to determine the efficient one. The efficient impregnated activated CBPP fly ash, which is the sample impregnated with 0.1M $FeCl_3$, was used for sorption kinetic tests and equilibrium sorption experiments.

3.8.2 Sorption kinetic test

The adsorption of arsenic from both local well water of Bell Island and synthesized water, using the prepared iron impregnated activated CBPP fly ash was investigated and the efficient impregnated activated CBPP fly ash was used for sorption kinetic experiments. For these experiments, also, synthesized water with concentration of 1ppm of sodium arsenate ($Na_2HAsO_4.7H_2O$) was prepared. For kinetic sorption tests, 200ml of local well water (or synthesized water) was added to a series of glass bottles that contained 0.1g of the developed and efficient adsorbent. Each of these bottles, then, was mixed by an end-over-end rotator at room temperature for specific time, from 5 minutes to 24 hours to ensure that the equilibrium state was reached for the adsorbent and arsenic contaminated water. All samples were then filtered through the 11cm filter paper and sent for ICP-MS analysis. The results were then compared with different models to find the best model fitted with these kinetic results.

3.8.3 Equilibrium sorption experiments

The equilibrium sorption experiments were also conducted for both synthesized water with the concentration of 1ppm prepared by using sodium arsenate ($Na_2HAsO_4.7H_2O$) and local well water of Bell Island. To find out the equilibrium condition and sorption isotherm, a series of glass bottles, with the amount of 0.1g of the efficient adsorbent from CBPP fly ash inside, was prepared. Then, from 50ml to 1000ml of arsenic

contaminated local well water (or synthesized arsenic contaminated water) added to these bottles and mixed for 24 hours at room temperature with an end-over-end rotator. All samples were then filtered through the 11cm paper and sent for ICP-MS analysis. The results were then compared with different models to find the best model fitted with these results.

3.9. Quality Control and Quality Assurance

About the quality control and quality assurance some actions were taken in this study:

1) Water samples collected from the local well water in Bell Island were acidified to keep ions in the solution moving and preventing them to precipitate and producing errors in finding the accurate concentrations and maximizing the removal.
2) Before using any kind of glassware and container such as beaker or different parts of filtration systems, after regular washing, they were in contact with HNO_3 10% wt./wt. for 24 hours to remove any possible remained ions on them to minimize the error and then rinsed with distilled water.
3) The activation of CBPP fly ash was done in triplicate and the results of methylene blue value and Iodine number reported in next chapter are the average value of those three activations.
4) The iron impregnation on activated CBPP fly ash was done in duplicate and the results reported in next chapter are the averaged values.
5) The arsenic removal experiments were done in duplicate and the reported results in next chapter are the averaged values.
6) About the accuracy and precision of ICP-MS analyses, the percentage of relative standard deviation (RSD), which is the standard deviation of a group of numbers

divided by the average of them and then multiplying this product by 100, is usually reported (Jenner *et al.*, 1990). The standard deviation describes the difference of each individual number with the average of them. For the accuracy of ICP-MS, there are some reference samples that contain most of the elements and for each element, the most probable value (MPV) has been reported. Each time for starting the experiment, these reference samples are analyzed with the device and the concentration of each sample is determined and compared with the reported values of them and the RSD of them is calculated. In this study and specifically for arsenic, the RSD and difference of determined concentration and MPV of arsenic reported as 1.20% and 5.62% respectively, which shows the high accuracy of the reported values of ICP-MS. For the precision, also, samples analyzed in duplicate or triplicate and then %RSD is reported. In this study and for arsenic, the RSD reported for all samples analyzed was less than 6% and it shows the high precision of ICP-MS reported values.

4. Results and discussion

4.1. Elemental analysis of Bell island's well water

Water samples from the well water of Bell Island analyzed for metal concentration using ICP-MS and the results are reported in Table 4-1. According to these results, the concentration of arsenic in this water is higher than the maximum acceptable concentration of arsenic which is 10 µg/L and the treatment is required for this water prior to being used. Moreover, the existence of other elements, with relatively high concentrations, are representing that the arsenic adsorption capacity of the modified adsorbent in this study would be lower than the other adsorbents reported in other studies applied synthesized water contained arsenic. Moreover, pH of this water was also determined, and it was 7.32.

Table 4-1: Concentrations of different elements existed in the raw Bell island's well water

Element	**Concentration (ppb)**	**Element**	**Concentration (ppb)**
Li	15.3	Rb	1.35
Be	0.342	Sr	340
Pb	0.175	Mo	0.3
P	365	I	1.64
Ti	0.600	Cs	0.032
Al	11.7	Ni	0.102
Cr	2.48	Ba	53.1
Mn	256	Ce	0.1
Fe	50	Mg	5974
Cu	4.24	Si	6939
As	15.7	Cl	18404
Br	50.5	Ca	32126

4.2. Characterization of raw and clean CBPP fly ash

4.2.1 Particle size distribution

According to Figure 4-1, which is the particle size distribution of CBPP fly ash after grinding, the size of the CBPP fly ash particles are from 7.8 to 710 µm. Most of them have the size of between 37 to 300 µm, and about 25% is below 30 µm (Zhang *et al.*, 2017).

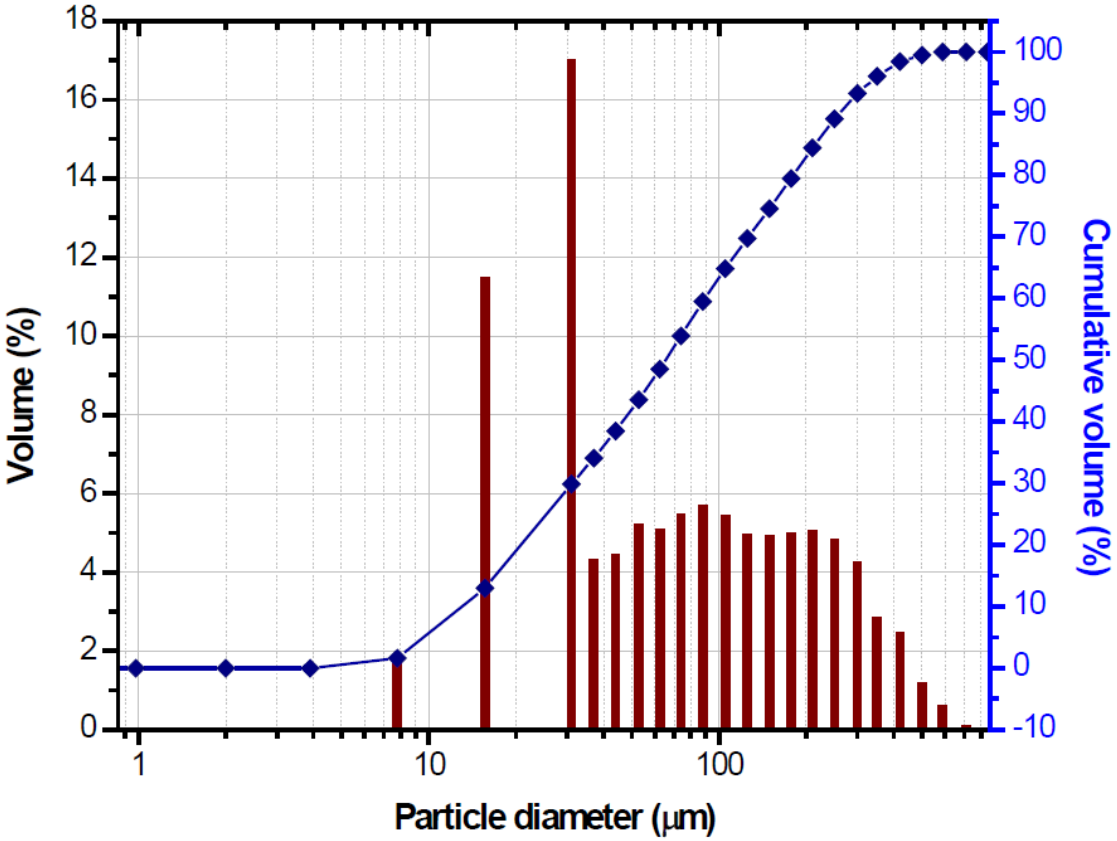

Figure 4-1: particle size distribution of CBPP fly ash after grinding (Zhang et al., 2017)

4.2.2 Ash content, moisture content, carbon content, pH, IN, and MBV

The pH, ash content, moisture content, carbon content, iodine number (IN), and methylene blue value (MBV) of the raw and cleaned CBPP fly ash is reported in Table 4-2. According to these results, the pH of the raw CBPP fly ash is in the alkaline range while using the nitric acid for removing the impurities, has reduced the pH of cleaned CBPP fly ash to the acidic range. Furthermore, the carbon content was increased after cleaning as the result of decreasing the moisture content and ash content. Moreover, after cleaning, the methylene blue value was increased and the iodine number decreased (Zhang et al., 2017).

Table 4-2: pH, Moisture content, ash content, carbon content, iodine number, and methylene blue value of raw and cleaned CBPP fly ash (Zhang et al., 2017)

Parameters	**Raw CBPP fly ash**	**Cleaned CBPP fly ash**
pH	11.44	3.4
Moisture content (%)	1.67	0.35
Ash content (%)	14.04	4.05
Carbon content (%)	78.68	82.79
Iodine number (mg/g)	444.56	57.42
Methylene blue value (mg/g)	57.42	61.89

4.2.3 Metal Content of CBPP fly ash

Different metals existed in the raw and cleaned CBPP fly ash are reported in Table 4-3. According to these results, while high amount of calcium, aluminum, iron, and magnesium are presented in raw CBPP fly ash, the removal rate of these elements after acid washing is 44.2%, 70.3%, 77.7%, and 63.8% , respectively, which means that this acid washing is appropriate and necessary for preparing the fly ash for activation process (Zhang et al., 2017).

Table 4-3: Metal content in raw and cleaned CBPP fly ash (Zhang et al., 2017)

Metal Element	**Raw fly ash (ppm)**	**Cleaned fly ash (ppm)**	**Removal rate (%)**
Magnesium (Mg)	511.65	185.33	63.8
Aluminum (Al)	947.025	281.31	70.3
Iron (Fe)	784.202	175.19	77.7
Zinc (Zn)	11.724	9.07	22.6
Copper (Cu)	7.280	1.75	76
Lead (Pb)	2.252	0	100
Arsenic (As)	< detection limit		
Vanadium (V)	15.460	2.57	83.4
Nickel (Ni)	15.962	3.74	76.6
Calcium (Ca)	2656.356	1481.50	44.2

4.3. Activated CBBP fly ash

Before starting any treatment for arsenic removal, preparation of an efficient adsorbent was sufficient and in order to achieve this goal, different parameters were optimized. There are some simple methods for analyzing different types of activated carbons to find out the adsorption capacity, such as methylene blue test and iodine adsorption test, that are usually used for assessing the performance of the adsorbent and we applied them in this study as a rough estimate of the adsorption capacity of the activated CBPP fly ash. However, to find out the best condition for activation of CBPP fly ash, another parameter, that is the percentage of fly ash burn off during the activation, should also be considered because it is not cost-effective to produce an adsorbent with high energy consumption and ignition loss. Thus, the effect of temperature and activation time was examined by using the results of methylene blue value, iodine number, and the burn off rate.

4.3.1 Effect of activation temperature

In this study CBPP fly ash was activated with the pure CO_2 (CAC) at different temperatures: 650^{o}C, 700^{o}C, 750^{o}C, 800^{o}C, 850^{o}C and 900^{o}C and activation time was kept same for activation in different temperatures. The percentage of fly ash burn off, methylene blue value (MBV), and iodine number (IN) of each sample after activation is

presented in Table 4-4. According to these data and Figure 4-2, that is the trend of changing iodine number (IN) and methylene blue value (MBV) by temperature, it was found that by increasing the temperature, methylene blue value and iodine number, that are the indicators of mesoporosity and microporosity, respectively, increased.

Thus, the optimum temperature was found as 850^{o}C while at the 900^{o}C, the iodine number results were slightly better. One of the reasons for this recommendation is that by considering the ignition loss at 900^{o}C and the energy consumption for activation in this temperature, the activation of CBPP fly ash at 900 ^{o}C is costly and not economical.

Table 4-4: Percentage of fly ash burn off, MBV, and IN of CAC at different temperatures (constant time) (Zhang et al., 2017)

Sample name	**Temperature (ºC)**	**Activation time (hr)**	**MBV (mg/g)**	**Iodine number (mg/g)**	**Burn-off (%)**
CAC	650	1	71.57	529.66	7.79
CAC	700	1	73.84	552.92	14.29
CAC	750	1	76.7	469.26	13.7
CAC	800	1	107.19	502	22.22
CAC	850	1	147.523	515.16	36.84
CAC	900	1	169.33	760.91	53.57

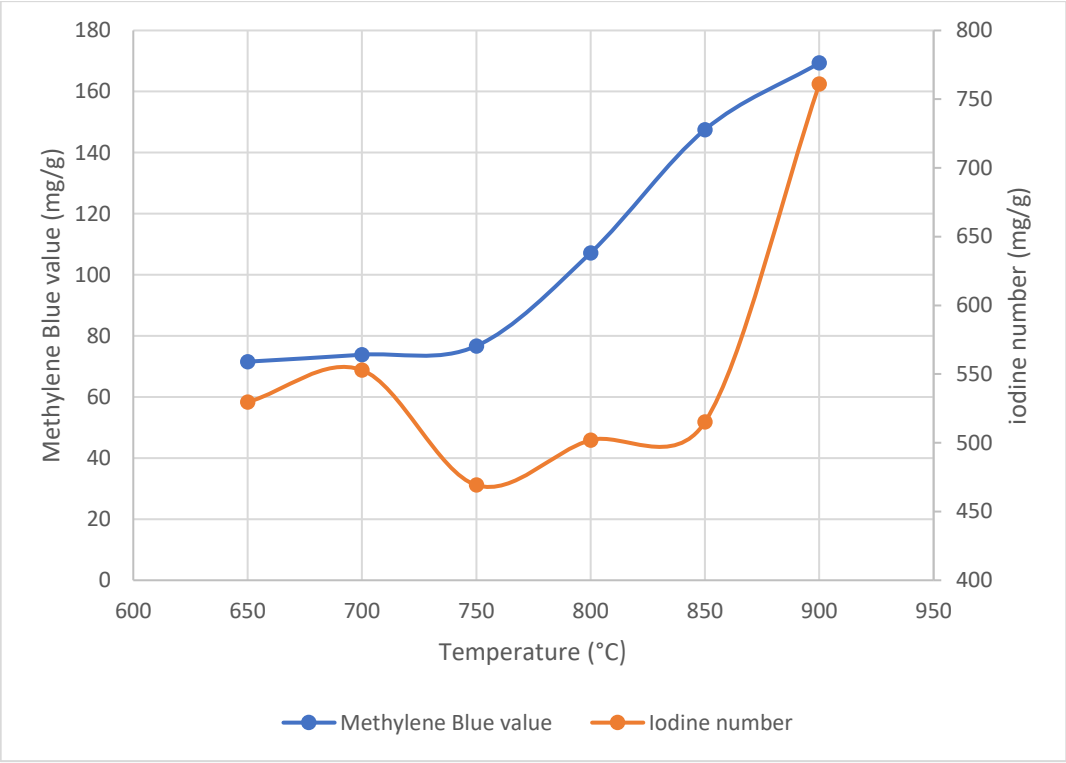

Figure 4-2: MBV and IN of CSA at different temperatures (constant time) (Zhang et al., 2017)

According to these values in Table 4-4, it was decided to run the activation system by applying steam to the system in the last three temperatures that showed higher values of methylene blue and iodine number. Therefore, methylene blue value (MBV), the percentage of fly ash burn-off, and iodine number (IN) of the mixture of CO_2 and steam activated samples (CSAC) are shown in Table 4-5 and Figure 4-3. It is cleared that applying steam to the activation is more efficient in activating the CBPP fly ash compared with pure CO_2 activation due to the development of more micro and meso-pores based on IN and

MBV values, respectively. The reason could be the formation of stronger oxygen groups at carbon surface during the CO_2 activation (González et al., 2006).

The highest results related to the 900^{o}C, but as it was mentioned, it is not cost-effective to activate the CBPP fly ash with the high amount of ignition loss and energy consumption for this activation. Thus, according to these results and figures and also considering the economic aspects, for the mixture of CO_2 and steam activation, also, 850^{o}C is recommended as the best temperature for the steam activation due to its high iodine number and methylene blue value.

Table 4-5: Percentage of fly ash burn off, MBV, and IN of the CSAC at different temperatures (constant time)

Sample name	**Temperature (ºC)**	**Activation time (hr)**	**MBV (mg/g)**	**Iodine number (mg/g)**	**Burn-off (%)**
CSAC	800	1	120.36	580.14	34.15
CSAC	850	1	234.29	717.73	47.62
CSAC	900	1	256.32	792.56	71.26

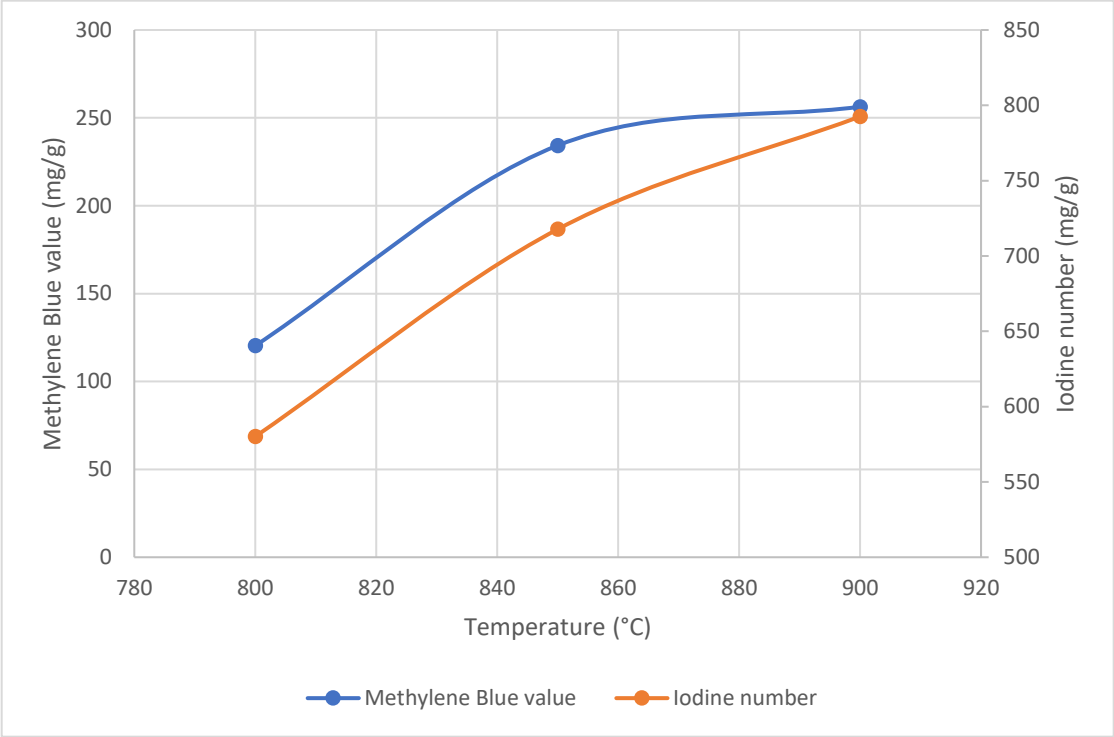

Figure 4-3: MBV and IN of CSAC at different temperatures (constant time)

4.3.2 Effect of activation time

After optimizing the activation temperature, the CBPP fly ash was activated in different time periods at the optimized temperature. Hence, CBPP fly ash was activated with the mixture of CO_2 and steam (CSAC), and pure CO_2 (CAC) for 1, 2, and 3 hours separately and the results of methylene blue value (MBV), iodine number (IN) and ignition loss for CAC and CSAC are presented in Table 4-6 and Table 4-7, respectively. Figure 4-4 and Figure 4-5 are showing the trend of methylene blue value (MBV) and iodine number

(IN) changes with time after activation with pure CO_2 and the mixture of CO_2 and steam, respectively. Thus, CSAC at 850^{o}C for 2 hours was selected as the efficient adsorbent for impregnation because of its high adsorption capacity due to the high iodine number (IN) and methylene blue value (MBV) of the adsorbent.

Table 4-6: Percentage of fly ash burn off, MBV, and IN of the CAC at different activation times (constant temperature) (Zhang et al., 2017)

Sample name	Temperature (°C)	Activation time (hr)	MBV (mg/g)	Iodine number (mg/g)	Burn-off (%)
CAC	850	1	147.523	515.16	36.84
CAC	850	2	292.317	704.53	41.12
CAC	850	3	236.094	617.63	65.59

Table 4-7: Percentage of fly ash burn off, MBV, and IN of the CSAC at different activation times (constant temperature)

Sample name	Temperature (°C)	Activation time (hr)	MBV (mg/g)	Iodine number (mg/g)	Burn-off (%)
CSAC	850	1	234.29	580.14	32.18
CSAC	850	2	358.95	1119.98	47.62
CSAC	850	3	374.69	1069.92	72.29

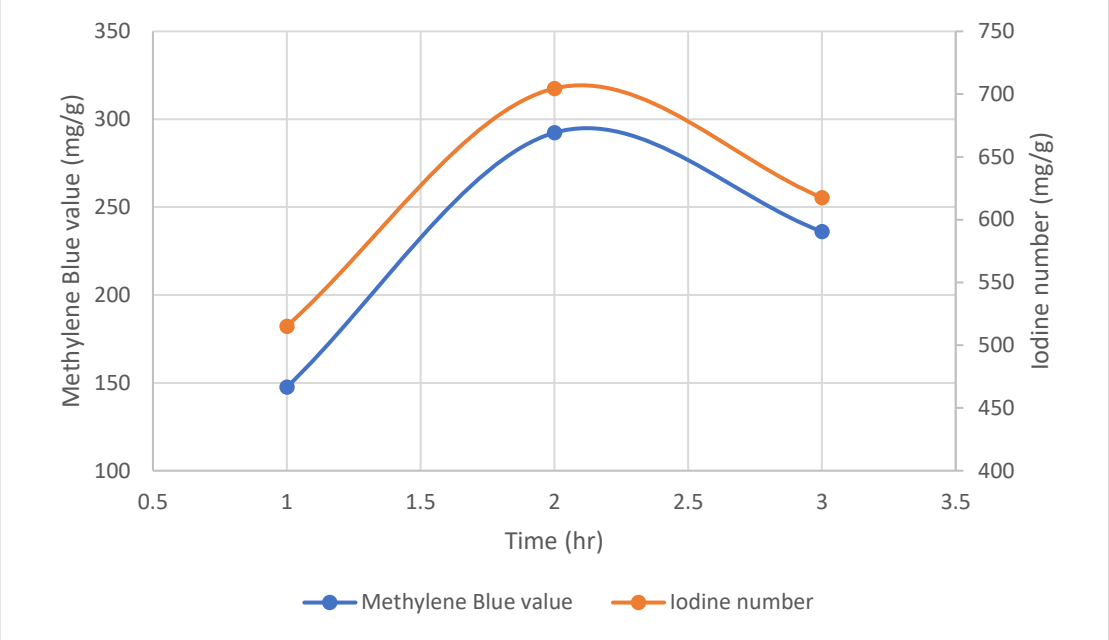

Figure 4-4: MBV and IN changes with time for CAC at 850°C (Zhang et al., 2017)

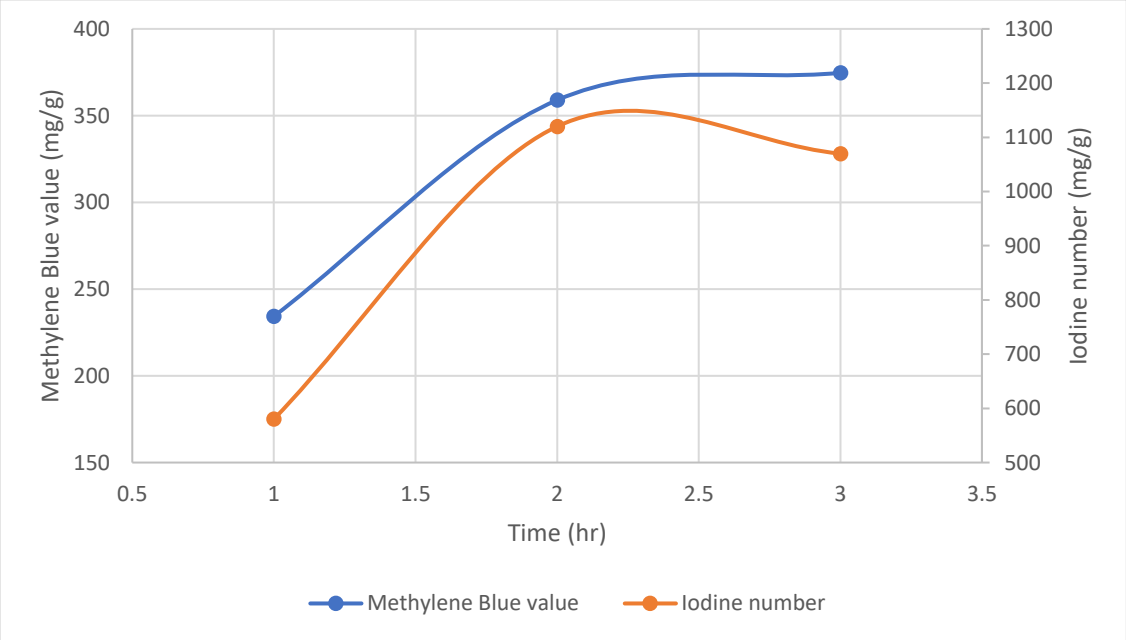

Figure 4-5: MBV and IN changes with time for CSAC at 850°C

4.4. Iron impregnated activated CBPP fly ash

Based on the study conducted by Raychounhury et al. (2015) for removing arsenate and arsenite from drinking water, it was decided to follow their procedure of impregnation in this study. Hence, activated CBPP fly ash with the mixture of CO_2 and steam (CSAC) was impregnated with iron (III) chloride (anhydrous). Different adsorbents prepared from CSAC samples impregnated with different concentrations of iron chloride from 0.01M to 1M. In order to find the best concentration to apply for impregnation of CSAC for arsenic removal from rural water, each sample after impregnation was tested for arsenic removal from synthesized water with the concentration of 1ppm of sodium arsenate ($Na_2HAsO_4.7H_2O$) or arsenic (III) oxide (As_2O_3). The percentage of arsenic (V) removal and leached iron concentrations in treated waters with samples impregnated with different iron chloride concentration are shown in Table 4-8.

Table 4-8: Percentage of arsenic (V) removal and leached iron concentrations in treated waters with CSAC samples impregnated with different iron chloride concentration

Sample#	Iron chloride concentration for impregnation (M)	% removal of As(V)	Leached iron concentration (ppb)
1	1	98.34	1364
2	0.5	98.13	1490
3	0.4	98.44	1324
4	0.3	98.08	424
5	0.20	99.42	<detection Limit
6	0.10	99.63	<detection Limit
7	0.05	98.63	<detection Limit
8	0.02	97.62	<detection Limit
9	0.01	94.11	<detection Limit
10	0	80.43	<detection Limit

According to the ICP-MS results of the treated water with each of these impregnated adsorbents, it was observed that for first 4 samples (impregnated with iron chloride concentrations between 0.3M to 1M), even after washing for several times, a considerable amount of iron leached to the water in high concentrations. Hence, it was

concluded that samples impregnated with iron chloride with concentration 0.01M to 0.2M give better results in arsenic removal without iron leaching in water. Therefore, these samples were tested to treat synthesized water contaminated with arsenic (III) oxide (As_2O_3) and the percentage of arsenic (III) removal by using these adsorbents is reported in Table 4-9.

Table 4-9: Percentage of arsenic (III) removal using CSAC samples impregnated with different iron chloride concentration

Sample#	Iron chloride concentration for impregnation (M)	% removal of As (III)
0	0	59.18
1	0.01	81.45
2	0.02	82.84
3	0.05	84.51
4	0.075	85.53
5	0.1	86.64
6	0.2	85.52

Based on the results listed in tables and figures above, it is clear, that the best concentration of iron (III) chloride for the activated CBPP fly ash impregnation is 0.1M, as this concentration showed the most efficient ability in arsenic removal from water. Hence, this modified adsorbent was used to treat the local well water of Bell Island with the ratio of 0.1g of adsorbent to 200ml of well water and the concentration of different elements are presented in Table 4-10.

Table 4-10: Concentration of different elements in local Well water of Bell Island before and after treatment (with 0.1M iron impregnated CSAC)

Element	Concentration in well water (ppb)	Concentration after treatment (ppb)
Li	15.3	13.1
Be	0.342	<DL
Pb	0.175	0.03
P	365	<DL
Ti	0.6	0.314
Cr	2.48	<Dl
Mn	256	76.7
Fe	50	<Dl
Cu	4.24	6.13
As	15.7	3.7
Br	50.5	47.7
Zn	<DL	<DL
Sr	340	276
Ni	0.102	<DL
I	1.64	1.17
V	<DL	<DL
Ba	53.1	31.8
Al	11.7	13.3
Mg	5974	5076
Si	6939	6405
Cl	18404	25236
Ca	32126	26236
Rb	1.35	1.24
Cs	0.035	0.032
Be	0.342	<DL
Ce	0.1	<DL

As shown in Table 4-10, applying this adsorbent for the treatment of Bell Island's well water, not only reduced the arsenic from the water, but also it reduced the concentration of almost all of the other metals in the water. For instance, concentration of Cl was slightly increased after treatment because the adsorbent was prepared by impregnation with iron (III) chloride and Cl could leach during the treatment. Hence, it is concluded that this method for preparation of the adsorbent is good for arsenic and other metals removal from drinking water and the adsorbent prepared by using 0.1M of iron chloride solution for impregnation of activated CBPP fly ash was used for other experiments and analyses.

4.5. Iron content and SEM images

The SEM images of carbon samples before and after activation, Figure 4-6 and Figure 4-7, respectively, reveal that this type of activation with the mixture of CO_2 and steam (CSAC) produces more pores, especially micropores on CBPP fly ash that is lead to achieving an adsorbent with high surface area and it is in good agreement with the values of iodine number and methylene blue.

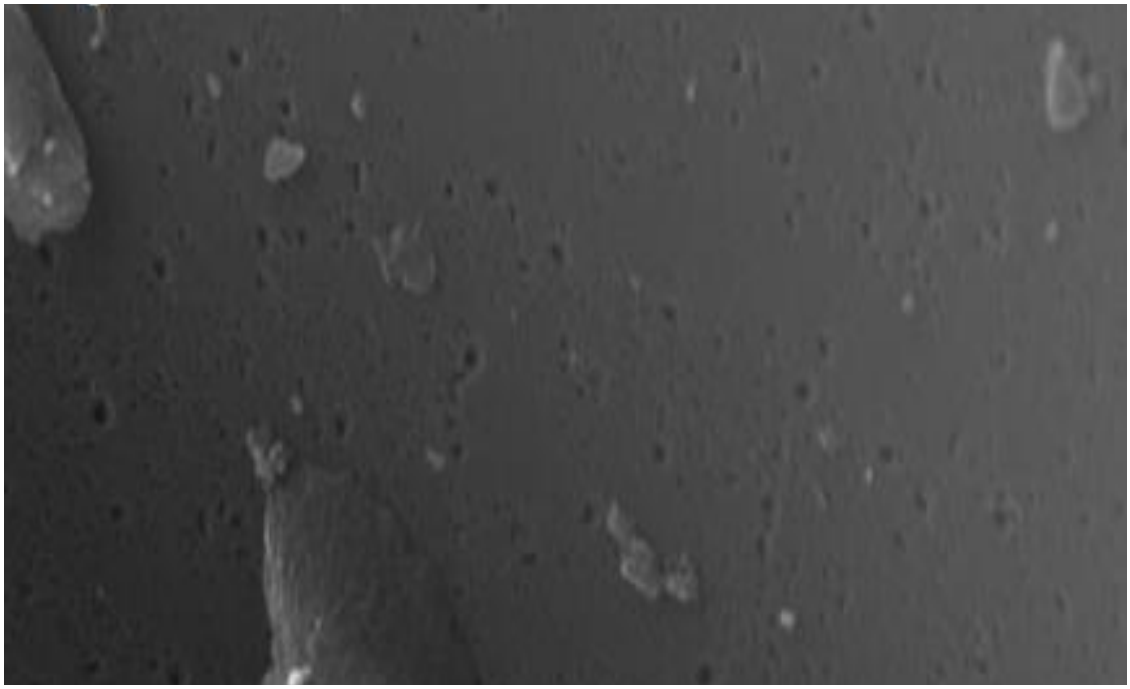

Figure 4-6: SEM image of CBPP fly ash before activation

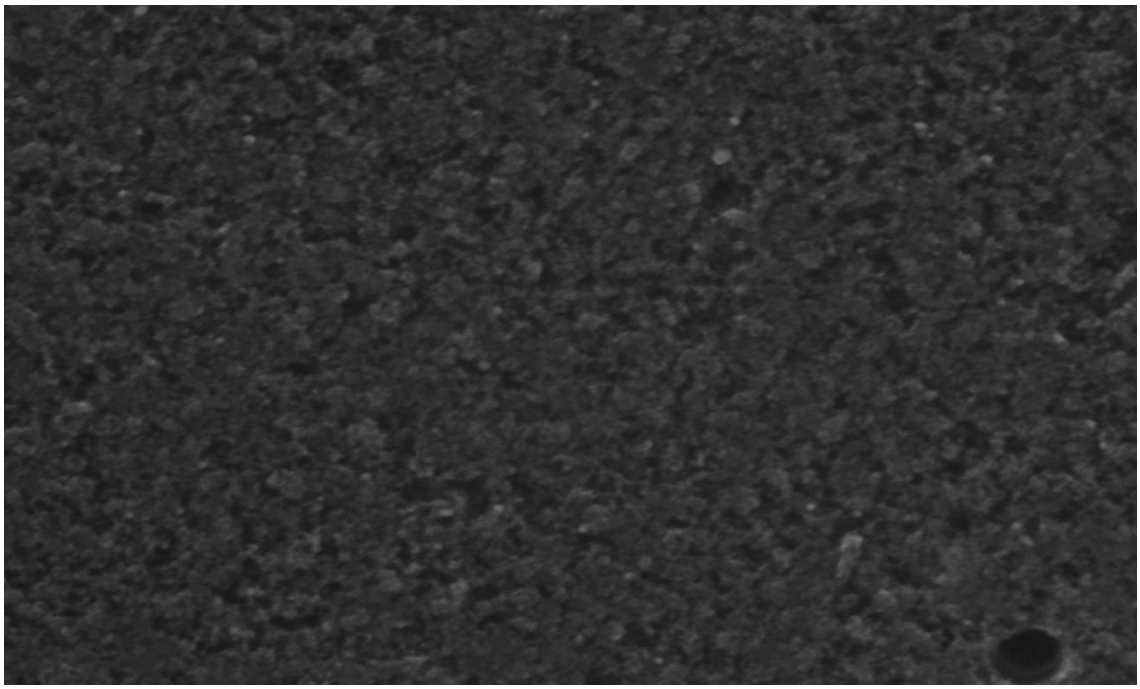

Figure 4-7: SEM image of CSAC after activation at 850^{o}C

Furthermore, according to the SEM images of the impregnated samples in Figure 4-8 to Figure 4-10, it is clear that by increasing the iron content, more pore blockage occurred, and for higher iron concentrations, clusters of iron particles were presented on the surface of the sample, that reduce the surface area of the adsorbent. For higher contents of iron, the surface of the adsorbent is covered by the iron particles and then, more iron particles accumulate on the iron particles attached to the adsorbent and these accumulated particles are not attached strong enough and leach to the solution through the adsorption process.

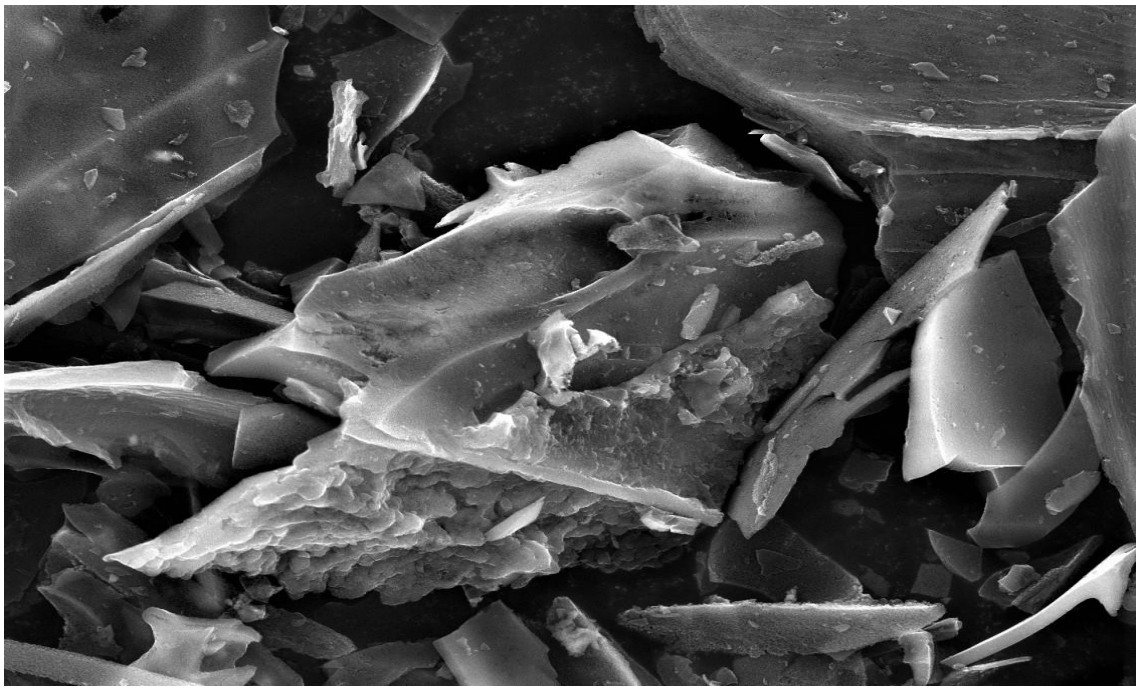

Figure 4-8: SEM image of CSAC impregnated with 0.01M $FeCl_3$

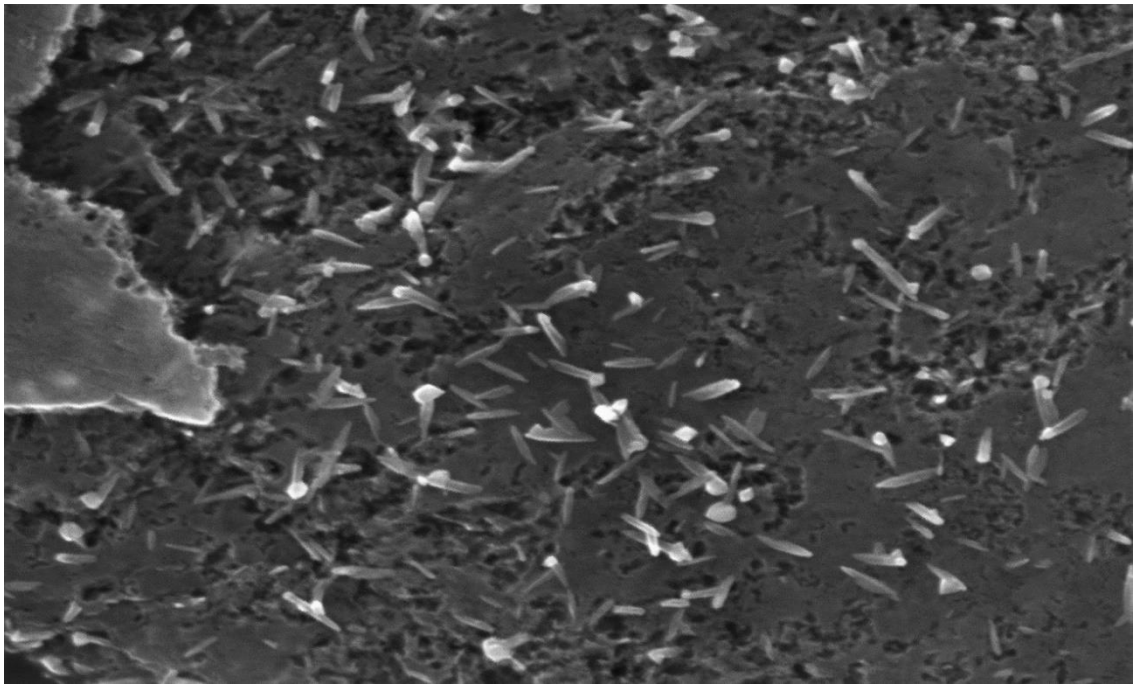

Figure 4-9: SEM image of CSAC impregnated with 0.1M $FeCl_3$

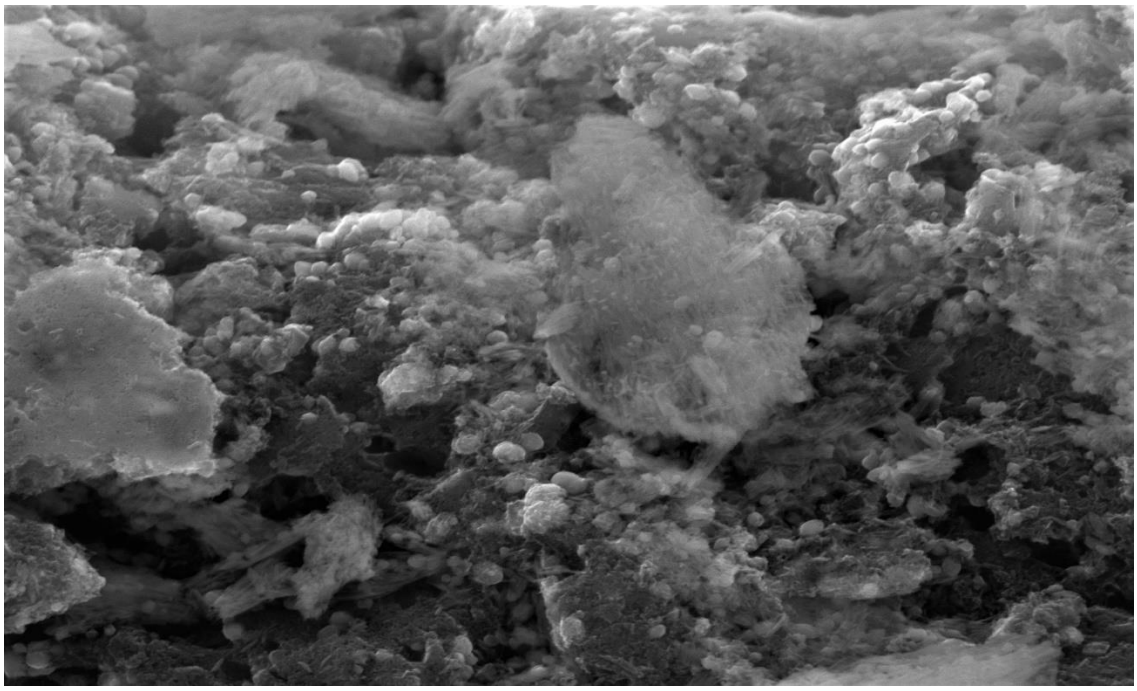

Figure 4-10: SEM image of activated CBPP fly ash impregnated with 1M $FeCl_3$

Having described the procedure of determining the iron content in the previous chapter, after separation of adsorbents from the acid solution, the amount of iron in the solutions was determined. The concentration of iron in each of these solutions, prepared by acid extraction of the iron impregnated samples with concentrations from 0.01 to 1M of iron (III) chloride, are shown in Table 4-11. According to the Table 4-11, and the SEM images of different adsorbents presented above, it is concluded that by increasing the amount of iron, the distribution of iron impregnated on the carbon sample changes from uniform to uneven and non-uniform that causes the pore blockage, reduction of surface area, and iron leaching for higher iron contents during the adsorption process for arsenic

removal. The iron content of the most efficient adsorbent for arsenic removal, that was determined in the previous section and it is the sample impregnated with iron chloride with the concentration of 0.1 M, is 1.97%. This modified adsorbent was used for the kinetic and equilibrium experiments.

Table 4-11: Iron content and concentration of impregnated CSAC with different concentrations of $FeCl_3$ from 0.01 to 1M

Sample name	**Iron concentration (ppm)**	**Iron content (%)**
Impregnated with 0.01M $FeCl_3$	4.67	0.19
Impregnated with 0.02M $FeCl_3$	6.21	0.25
Impregnated with 0.05M $FeCl_3$	19.26	0.77
Impregnated with 0.1M $FeCl_3$	49.10	1.97
Impregnated with 0.2M $FeCl_3$	158.53	6.31
Impregnated with 0.3M $FeCl_3$	244.94	9.71
Impregnated with 0.4M $FeCl_3$	336.80	13.50
Impregnated with 0.5M $FeCl_3$	435.03	17.28
Impregnated with 1M $FeCl_3$	631.93	25.17

4.6. Surface area and pore volume

According to the BET results reported in Table 4-12, about the surface area and porosity of the cleaned, pure CO_2 activated CBBP fly ash (CAC), mixture of CO_2 and steam activated CBPP fly ash (CSAC), and impregnated CSAC with 0.1M $FeCl_3$ solution, which was revealed that it is the most efficient adsorbent for arsenic removal in section 4-4, it was found that while activation of CBBP fly ash with both pure CO_2 and the mixture of CO_2 and steam improve the surface area and micro porosity of the CBPP fly ash, using the mixture of steam and CO_2 in activation, increases the surface area more effectively than using the pure CO_2. Moreover, according to the Table 4-12, the impregnation of the steam and CO_2 activated CPP fly ash with 0.1M $FeCl_3$ not significantly decreases the surface area, and pore blockage is negligible.

N_2 adsorption- desorption isotherms are plotted for the cleaned CBPP fly ash, the pure CO_2 activated CBPP fly ash (CAC), the mixture of CO_2 and steam activated CBPP fly ash (CSAC), and the impregnated CSAC in Figure 4-11, Figure 4-12, Figure 4-13, and Figure 4-14, respectively. It is obvious from these plots that the adsorption rate of activated samples, especially sample activated with the mixture of CO_2 and steam, is significantly increased compared to the cleaned carbon and it is in a good agreement with the methylene blue and iodine number results. About the N_2 adsorption- desorption isotherm of the impregnated sample, Figure 4-14, it is revealed that the impregnation of the steam and CO_2 activated CPP fly ash with 0.1M $FeCl_3$, did not decrease the adsorption rate

significantly compared to the activated CBPP fly ash with the mixture of steam and CO2 while it is still notably higher than the cleaned and pure CO_2 activated samples. The detailed information and data about the porosity and BET surface area of these samples are presented in appendixes A to D.

Table 4-12: Surface area and micropore volume of cleaned CBPP fly ash, CAC, CSAC, and impregnated CSAC

CBPP Sample	**Surface area (m^2/g)**	**Micropore area (m^2/g)**	**Micropore volume (cm^3/g)**
Cleaned	486.44	402.5	0.18
2 hours pure CO_2 activated @850^oC	847.26	619.49	0.28
2 hours (Steam+CO_2) activated @850^oC	1146.25	648.90	0.29
2 hours (Steam+CO_2) activated @850^oC-impregnated with 0.1M $FeCl_3$	1074.45	572.84	0.26

Note: The results of surface area, micropore area, and micropore volume of cleaned and 2 hours pure CO_2 activated CBPP fly ash at 850 °C was obtained from the report of Zhang et al. (2017)

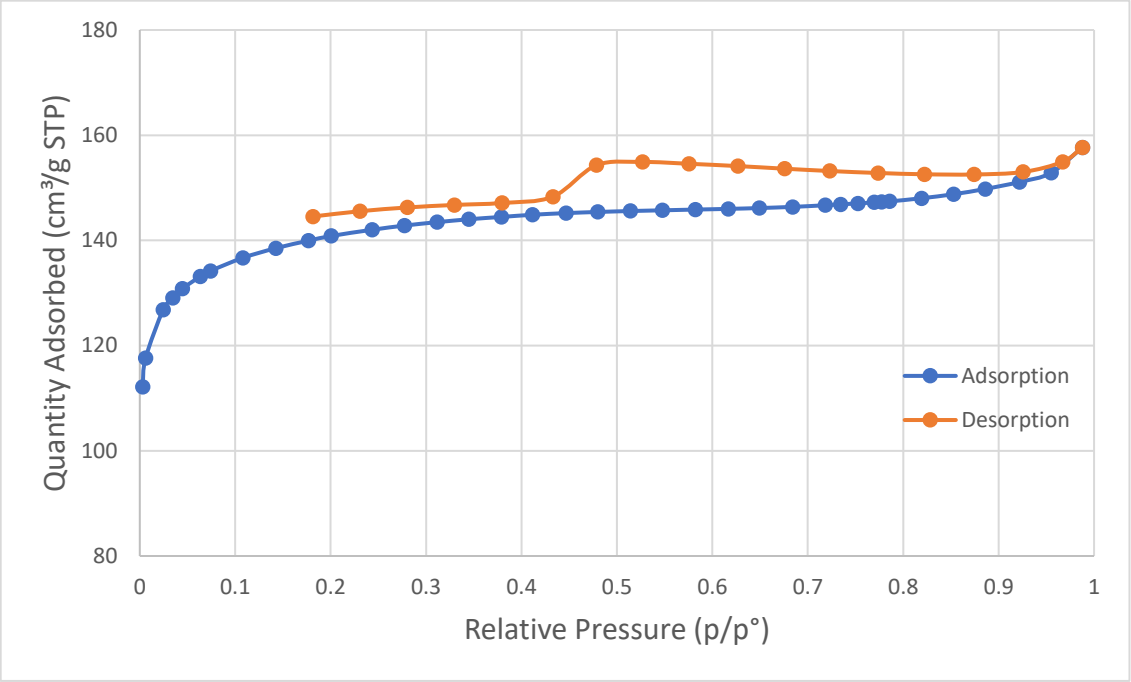

Figure 4-11: N_2 adsorption-desorption isotherm linear plot of raw and cleaned CBPP fly ash (Zhang et al., 2017)

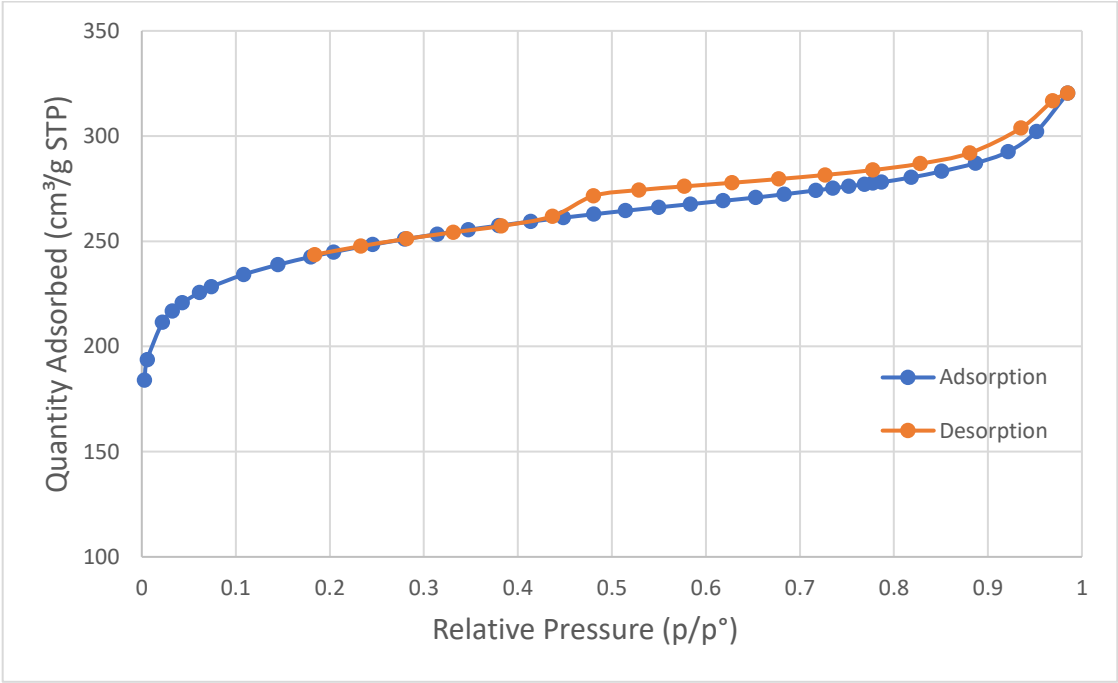

Figure 4-12: N_2 adsorption-desorption isotherm linear plot of CSA (Zhang et al., 2017)

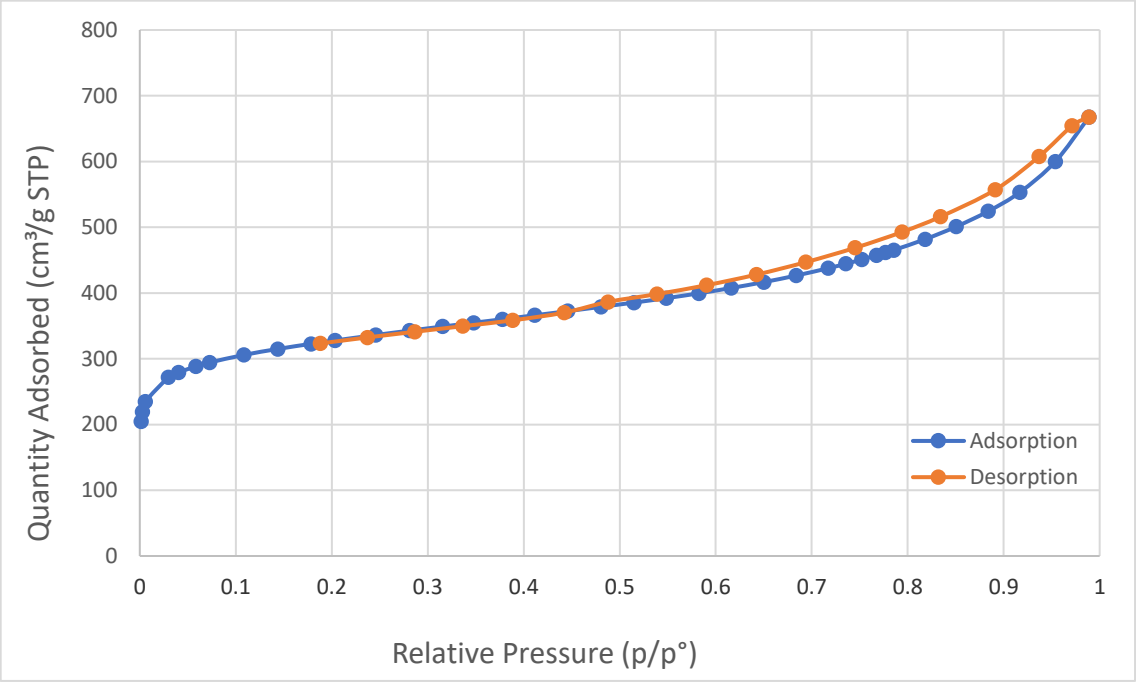

Figure 4-13: N_2 adsorption-desorption isotherm linear plot of CSAC

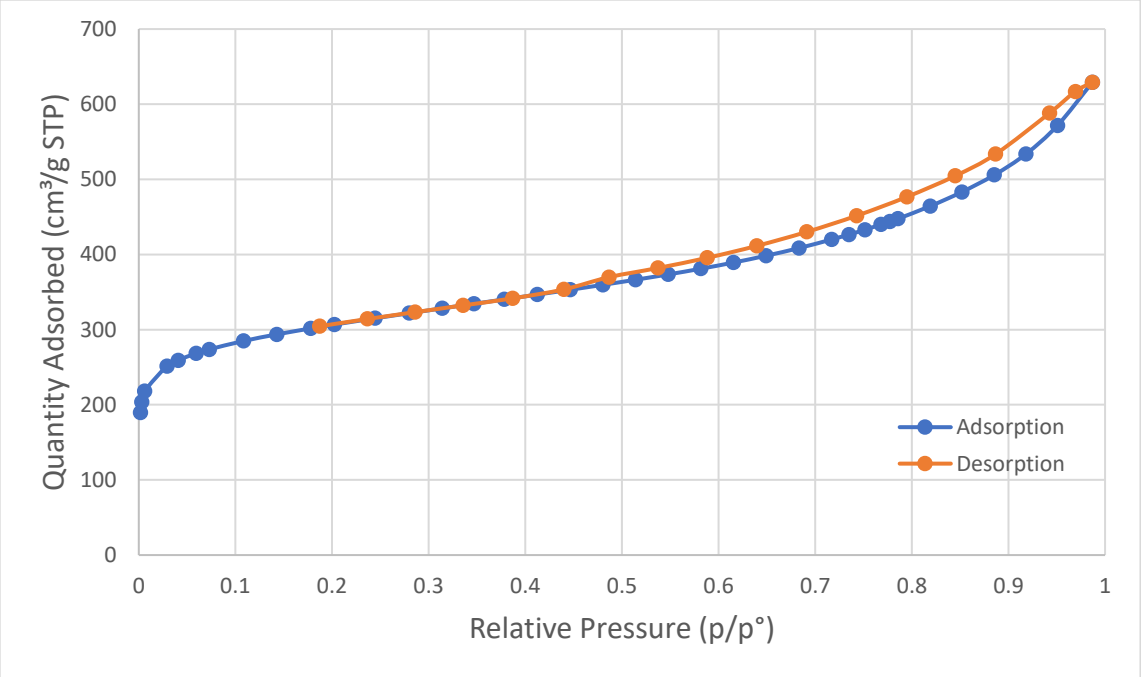

Figure 4-14: N_2 adsorption-desorption isotherm linear plot of CSAC impregnated with 0.1M $FeCl_3$

4.7. Equilibrium sorption isotherms

To understand the mechanism of the adsorption process, sorption isotherms are essential. Sorption isotherms give an equilibrium relationship of arsenic concentration between liquid phase and adsorbents, which are the solid phase, at a constant temperature. The results achieved from the equilibrium sorption experiments of arsenic removal from the local well water and synthesized water with $Na_2HAsO_4.7H_2O$ (1 ppm), using the CSAC sample impregnated with the 0.1M $FeCl_3$ solution, are presented in Figure 4-15 and Figure 4-16, respectively. According to the previous studies on arsenic removal using the adsorption method, Freundlich, Langmuir, and Temkin adsorption isotherm models were commonly used to introduce the mechanism of arsenic adsorption and these models were also examined in this study (Ananta *et al.*, 2015, Dehghani *et al.*, 2017).

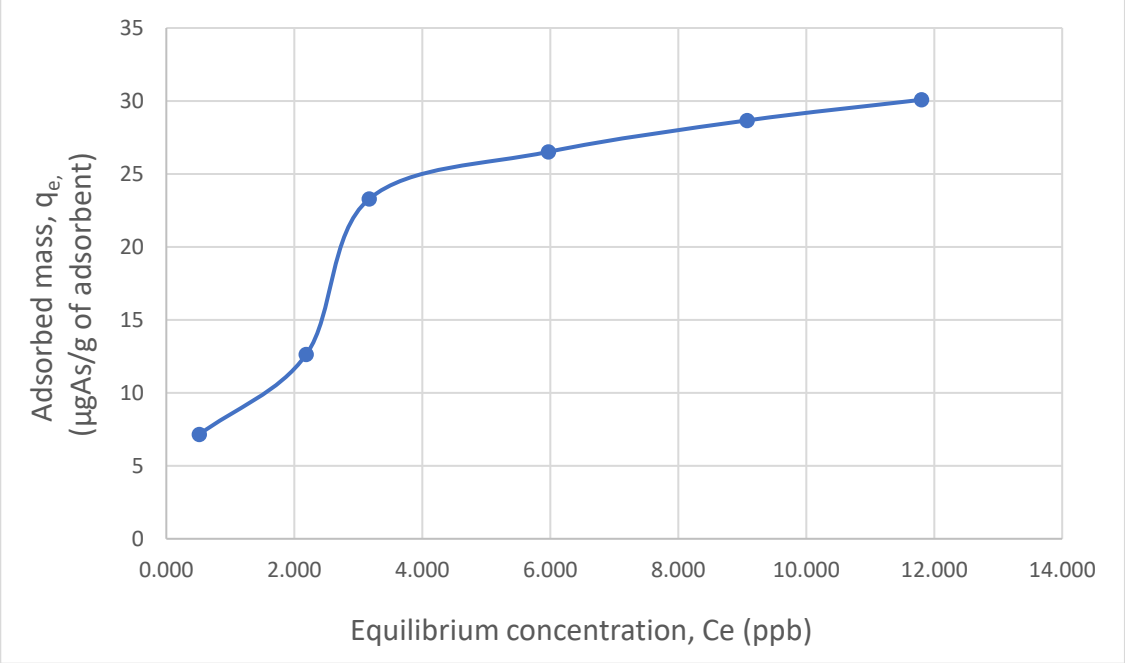

Figure 4-15: Isotherm curve of arsenic removal from local well water

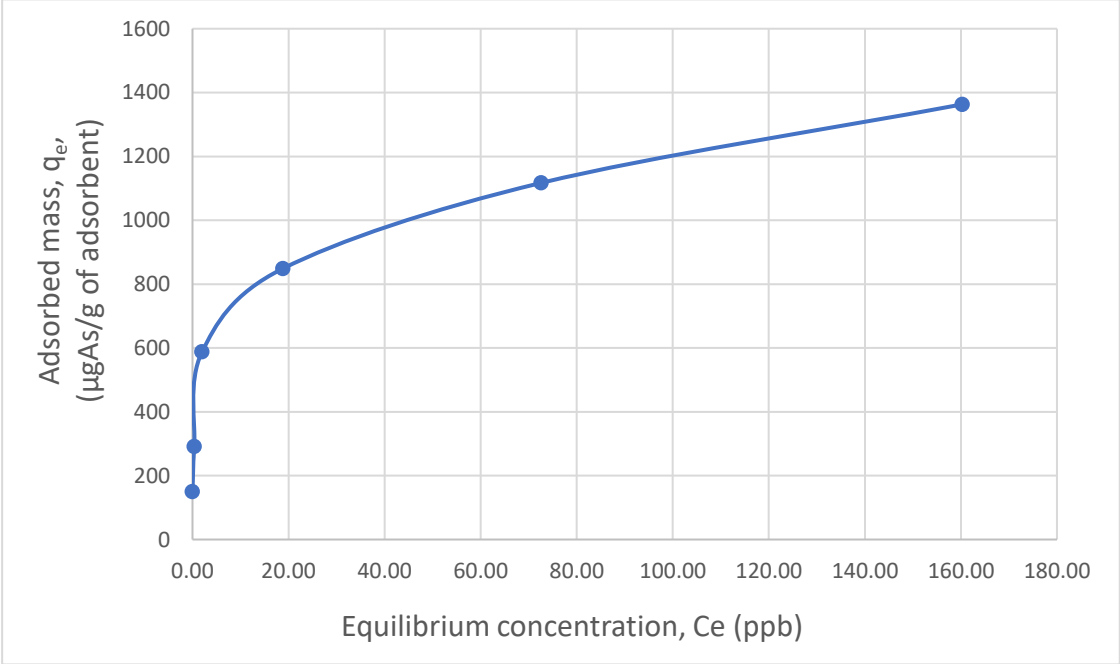

Figure 4-16: Isotherm curve of arsenic removal from synthesized water ($Na_2HAsO_4.7H_2O$,1 ppm)

4.7.1 Freundlich isotherm model

This model is generally used to describe the adsorption behavior of systems with low adsorption capacities and it is reported by applying the empirical Equation (4-1) (Dada *et al.*, 2012, Erhayem *et al.*, 2015).

$$q_e = K_f \times C_e^{1/n} \quad (4\text{-}1)$$

In which,

q_e = the amount of adsorbed arsenic per gram of adsorbent at equilibrium, µg/g

K_f = Freundlich isotherm constant

n = adsorption intensity

C_e = the equilibrium concentration of adsorbate, µg/L

The linearized form of Equation (4-2), is shown as the Equation (4-2):

$$\mathrm{Ln}(q_e) = \mathrm{Ln}(K_f) + \frac{1}{n}\,\mathrm{Ln}(C_e) \quad (4\text{-}2)$$

K_f, is the representative of adsorption capacity and n, indicates the strength of the adsorption. By plotting $\mathrm{Ln}(q_e)$ versus $\mathrm{Ln}(\mathrm{C_e})$, the slope of this plot is n^{-1} and the intercept is $\mathrm{Ln}(K_f)$, so n and K_f could be calculated (Erhayem et al., 2015). While n is between 1 to 10, it was reported that the reaction is favorable between the 2 phases

(Dada et al., 2012). The equilibrium sorption experiments were done with the adsorbent impregnated with 0.1M iron (III) chloride for local well water and synthesize water and the results of these experiments were fitted with linearized Freundlich model, that are shown in Figure 4-17 and Figure 4-18 for local well water and synthesized water, respectively. The parameters of this model and the value of the correlation coefficient (R^2) were calculated and reported in Table 4-13.

Table 4-13: The parameters of Freundlich model for arsenic removal from local well water and synthesized water ($Na_2HAsO_4.7H_2O$, 1 ppm)

Parameter	**Value for local well water**	**Value for synthesized water**
K_f	10.22	413.5
n	2.07	3.92
R^2	0.93	0.96

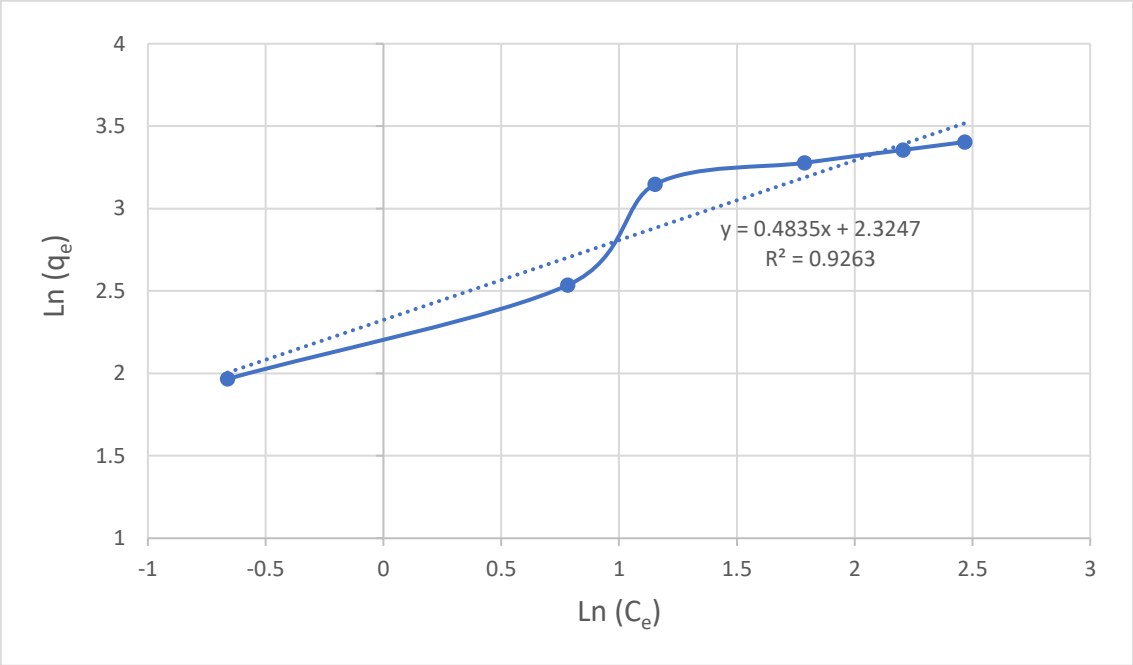

Figure 4-17: Equilibrium data of arsenic removal from local well water fitted with linearized Freundlich model

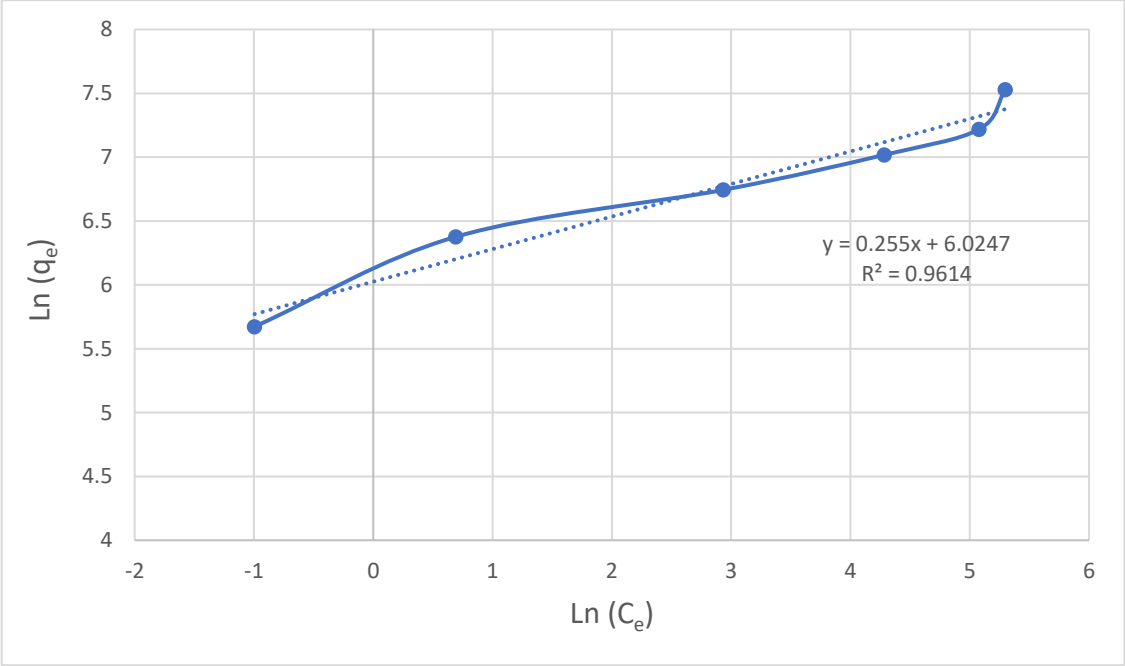

Figure 4-18: Equilibrium data of arsenic removal from synthesized water ($Na_2HAsO_4.7H_2O$, 1 ppm) fitted with linearized Freundlich model

4.7.2 Langmuir model

This model is usually used for monolayer adsorption and estimation of maximum adsorption capacity of the adsorbent. In monolayer adsorption, despite multilayer adsorption, the adsorbed molecules are in contact with the surface layer of the adsorbent (Ananta et al., 2015, Dada et al., 2012). Equation (4-3) is used for the Langmuir model, which is called Langmuir equation:

$$q_e = \frac{q_{max} K_L C_e}{1 + K_L C_e} \quad (4\text{-}3)$$

In which,

q_e = the amount of adsorbed arsenic per gram of adsorbent at equilibrium, µg/g

C_e = the equilibrium concentration of adsorbate, µg/L

q_{max} = maximum monolayer adsorption capacity, µg/g

K_L = Langmuir equilibrium constant, L/µg

Equation (4-4) is the linearized form of Langmuir equation.

$$\frac{C_e}{q_e} = \frac{1}{q_{max} K_L} + \frac{C_e}{q_{max}} \quad (4\text{-}4)$$

By plotting C_e/q_e versus C_e, Figure 4-19 and Figure 4-20 for local well water and synthesized water, respectively, maximum adsorption capacity, from the slope of the

plots, Langmuir constant, from the intercept of the plots, and the value of the correlation coefficient (R^2) calculated and the results are reported in Table 4-14.

Table 4-14: The Langmuir calculated parameters for arsenic removal from local well water and synthesized water ($Na_2HAsO_4.7H_2O$, 1 ppm)

Parameter	Value for local well water	Value for synthesized water
K_L	0.482	0.18
q_{max}	35.46	1428.6
R^2	0.997	0.99

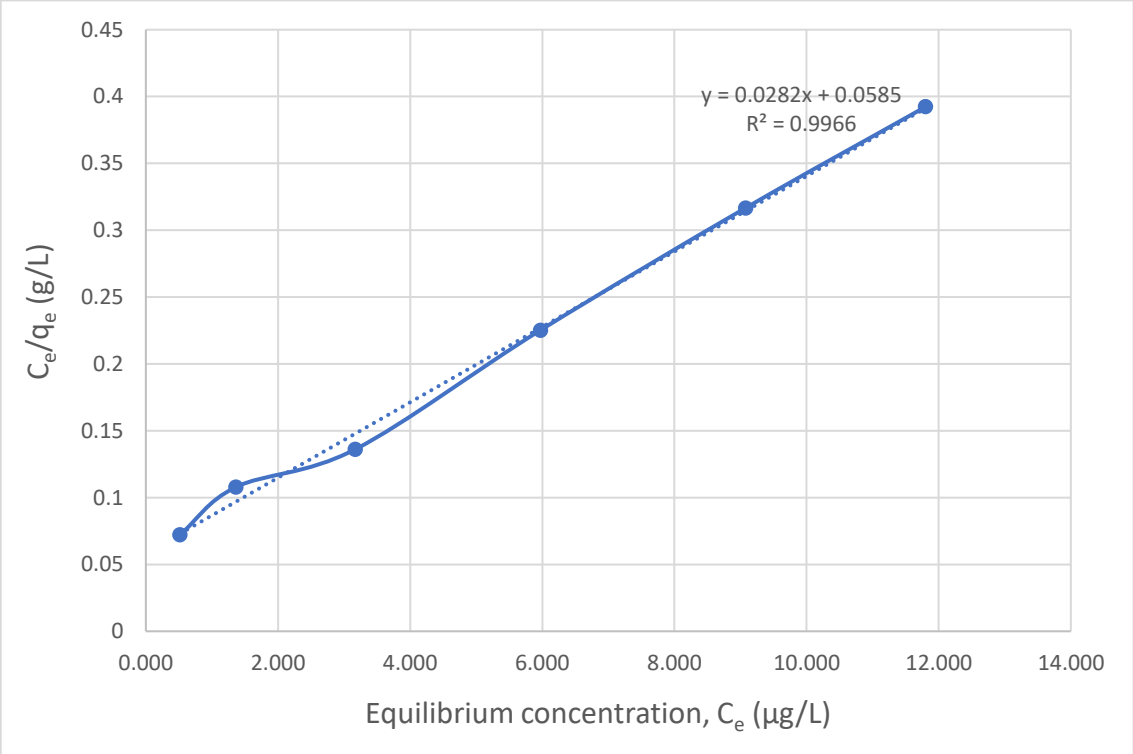

Figure 4-19: Equilibrium data of arsenic removal from local well water fitted with linearized Langmuir model

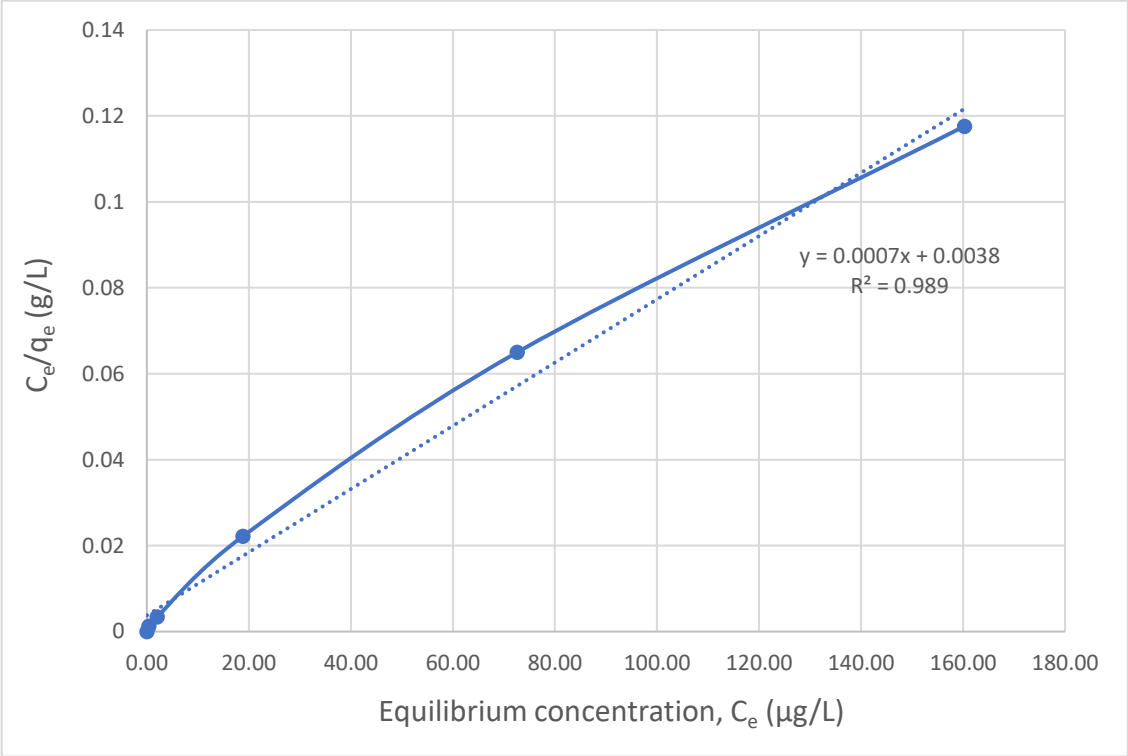

Figure 4-20: Equilibrium data of arsenic removal from synthesized water ($Na_2HAsO_4.7H_2O$, 1 ppm) fitted with linearized Langmuir model

4.7.3 Temkin model

This model is usually used to define both the interactions between the adsorbate and the adsorbent, and the heat of adsorption and also it is based on the assumption that the heat of adsorption decreases linearly with the surface coverage rather than logarithmic (Wang & Qin, 2005). Equation (4-5) is the Temkin expression (Dada et al., 2012, Erhayem et al., 2015, Ananta et al., 2015).

$$q_e = \frac{RT}{b} Ln(K_T . C_e) \quad (4\text{-}5)$$

In which,

B = $\frac{RT}{b}$ = Constant related to heat of sorption, J/mol

K_T = Temkin isotherm equilibrium binding constant, L/µg

b = Temkin isotherm constant

q_e = the amount of adsorbed arsenic per gram of adsorbent at equilibrium, µg/g

C_e = the equilibrium concentration of adsorbate, µg/L

R= Universal gas constant (8.314 J/mol.K)

T = Temperature, K

Equation (4-6) is the linearized form of Temkin model equation.

$$q_e = B . Ln(K_T) + B . Ln(C_e) \quad (4\text{-}6)$$

By plotting q_e versus Ln(C_e), Figure 4-21 and Figure 4-22 for local well water and synthesized water, respectively, parameters of Temkin model, B as the slope of the plot, BLn(K_T) as the intercept, and the value of the correlation coefficient (R^2) determined and are reported in Table 4-15.

Table 4-15: The Temkin calculated parameters for arsenic removal from local well water and synthesized water ($Na_2HAsO_4.7H_2O$, 1 ppm)

Parameter	Value for local well water	Value for synthesized water
K_T	4.21	7.60
B	7.84	205.95
R^2	0.92	0.87

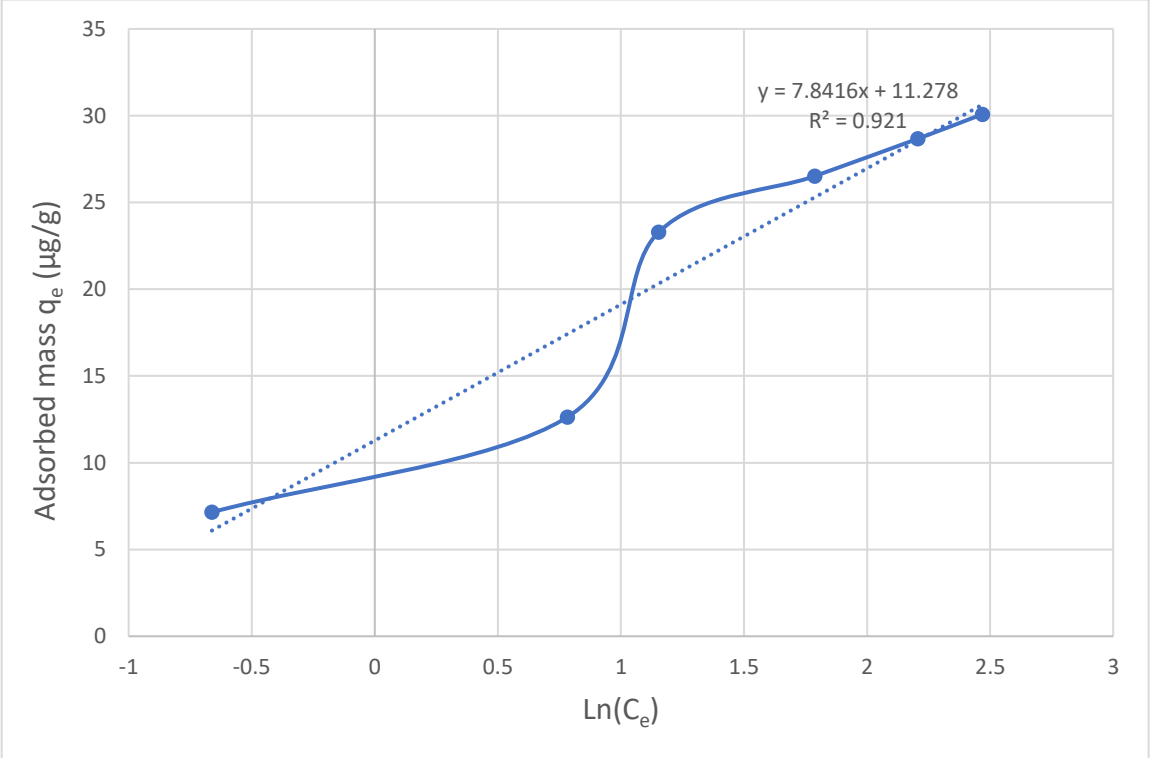

Figure 4-21: Equilibrium data of arsenic removal from local well water fitted with linearized Temkin model

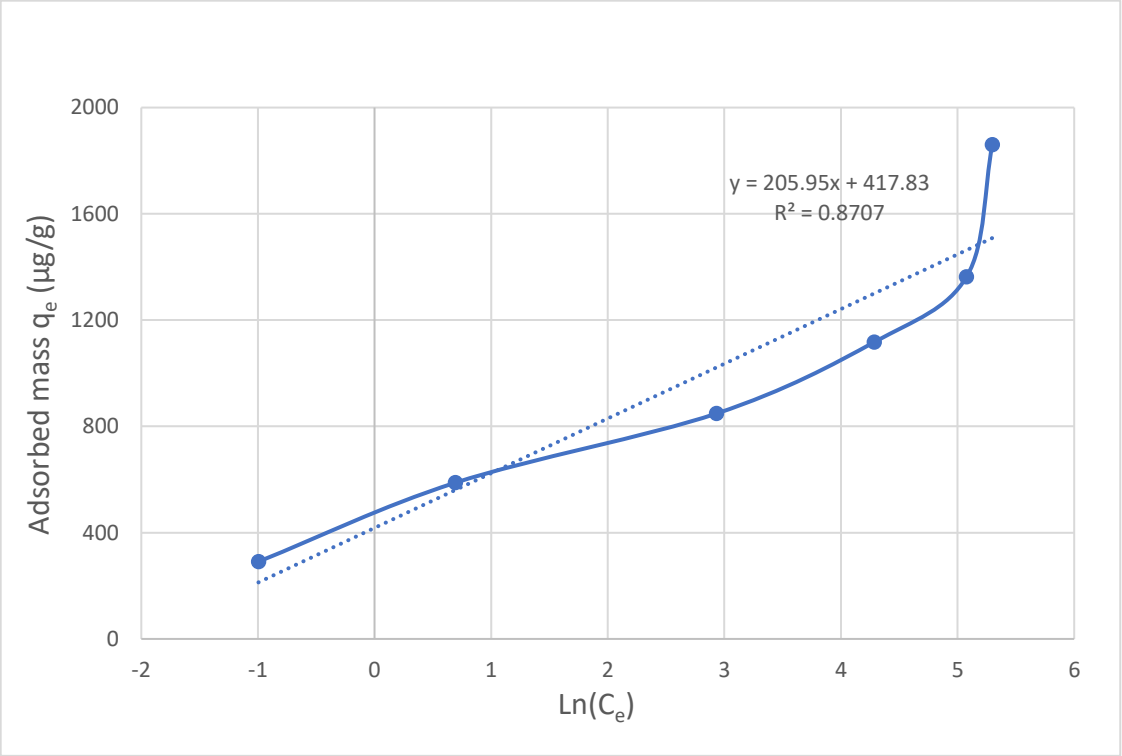

Figure 4-22: Equilibrium data of arsenic removal from synthesized water ($Na_2HAsO_4.7H_2O$, 1 ppm) fitted with linearized Temkin model

Among the different isotherm models fitted in this study, it is obvious that the Langmuir model is the best model for describing the equilibrium behavior of arsenic adsorption by iron impregnated CSAC ($R^2 \geq 0.99$) for both local well water and synthesized water with $Na_2HAsO_4.7H_2O$ (1ppm), indicating that the monolayer of arsenic ions covers the adsorbent surface. Hence, according to the results of Langmuir fitting, maximum adsorption capacity of this modified adsorbent in removing the arsenic was 35.46µg/g from the local well water and 1428.6µg/g from synthesized water with $Na_2HAsO_4.7H_2O$ (1ppm) that is higher than the other adsorbents previously used for arsenic removal and

their results are presented in Table 4-16. Furthermore, the maximum iron use efficiency or the maximum adsorption capacity with respect to iron is 1.8 mg/gFe and 72.67 mg/gFe in removing the arsenic from the local well water and synthesized water with $Na_2HAsO_4.7H_2O$ (1ppm), respectively.

According to the Table 4-16, it is obvious that while using natural or well water for arsenic removal, the adsorption capacity significantly decreases. It should be considered that these reported values are only the adsorption capacity for arsenic, and in the case of natural and local well waters, which have a wide range of elements with different concentrations that affect and decrease maximum arsenic adsorption capacity, it would be a competition between elements presented in these waters to reach to the active sites of the adsorbent surface and this is known as the effect of multi component adsorption. By comparing the surface area of the adsorbents in Table 4-16, it is observed that the surface area of the mixture of CO_2 and steam activated CBPP fly ash (CSAC) impregnated with 0.1M $FeCl_3$ is higher than most of adsorbents reported in this table while it has the highest arsenic adsorption capacity for both synthesized and well water. Based on the results of this table, it is notable that high surface area is only one of the factors for having a proper adsorbent and the effect other parameters such as surface charge distribution, iron content, and constituents of adsorbent are also significant.

Table 4-16: Comparison of various adsorbents surface area (SA) and their arsenic adsorption capacity (Q)

Adsorbent base	Water sample	Impregnation	SA[1] (m^2/g)	Q (mg/g)	Reference
Commercial activated carbon	Synthesized	-	1223	0.675	*(Li et al., 2014)*
Commercial activated carbon	Synthesized	$FeCl_3$	478	0.024	*(Ghanizadeh et al., 2010)*
bituminous Filtrasorb-400	Synthesized	$FeCl_3$	864	1.26	*(Arcibar-Orozco et al., 2014)*
Coconut shell	Synthesized	$FeCl_3$	491	0.5	*(Arcibar-Orozco et al., 2014)*
Jute stick	Synthesized	$FeSO_4$	1266	1.320	*(Asadullah et al., 2014)*
Bagasse fly ash	Synthesized	$FeCl_3$	168	0.025	*(Yadav et al., 2014)*
Sponge iron char	Synthesized	-	78.63	0.028	*(Yadav et al., 2014)*
Bituminous Filtrasorb-400	Synthesized	$FeCl_3.6H_2O$	1045	0.847	*(Vitela-Rodriguez & Rangel-Mendez, 2013)*
Commercial activated carbon	Well water	$FeCl_3$	1575	0.028	*(Fierro et al., 2009)*
Commercial activated carbon	Well water	$FeCl_2$	NA[2]	0.036	*(Muniz et al., 2009)*
Red flint filter sand	Natural water	$Fe(NO_3)_3.9H_2O$	NA[2]	0.018	*(Thirunavukkarasu et al., 2001)*
Manganese oxide	Synthesized	-	NA[2]	0.172	*(Ouvrard et al., 2002)*
`	Synthesized	$FeCl_3$	1074.5	1.43	*This study*
CBPP fly ash	Well water	$FeCl_3$	1074.5	0.035	*This study*

[1]Note: The values of surface area in this table for the impregnated samples represent the values of the adsorbent surface area after impregnation.

[2]NA = Not available

In addition, according to the results of other studies for arsenic removal, it was found that increasing the pH from 3 to 7 does not significantly affect the arsenate removal. For the arsenite, the optimum pH was reported between 6 and 9.5. Hence, the optimum pH, in this study, for adsorption of arsenate and arsenite was set between 6 and 7, at which arsenate existed mainly as its active species $H_2AsO_4^-$ and $HAsO_4^{2-}$ and arsenite is mostly as un-dissociated species, and also recommended in other studies (Di Natale *et al.*, 2009, Gu et al., 2007, Li et al., 2014, Raychoudhury et al., 2015).

4.8. Sorption Kinetics

Sorption kinetics are usually used to examine the adsorption behavior and mechanism and, to find out the steps controlling the reaction rate. Moreover, by using the kinetic models, it is possible to find out the equilibrium time of the reaction (Ho & McKay, 1998). The sorption kinetic results of arsenic removal, using the CSAC impregnated with 0.1M $FeCl_3$, from synthesized water with $Na_2HAsO_4.7H_2O$ (1 ppm) and the local well water were determined in a time zone of 5 minutes to 24 hours and shown in Figure 4-23 and Figure 4-24, respectively. According to Figure 4-23, after 300 minutes, arsenic adsorption on the iron impregnated CSAC reached to the equilibrium, since after 300 minutes the adsorbed mass of arsenic per gram of adsorbent remained constant. For synthesized water, also, it seems that after 20 hours the adsorption of arsenic on the modified adsorbent was reached to the equilibrium.

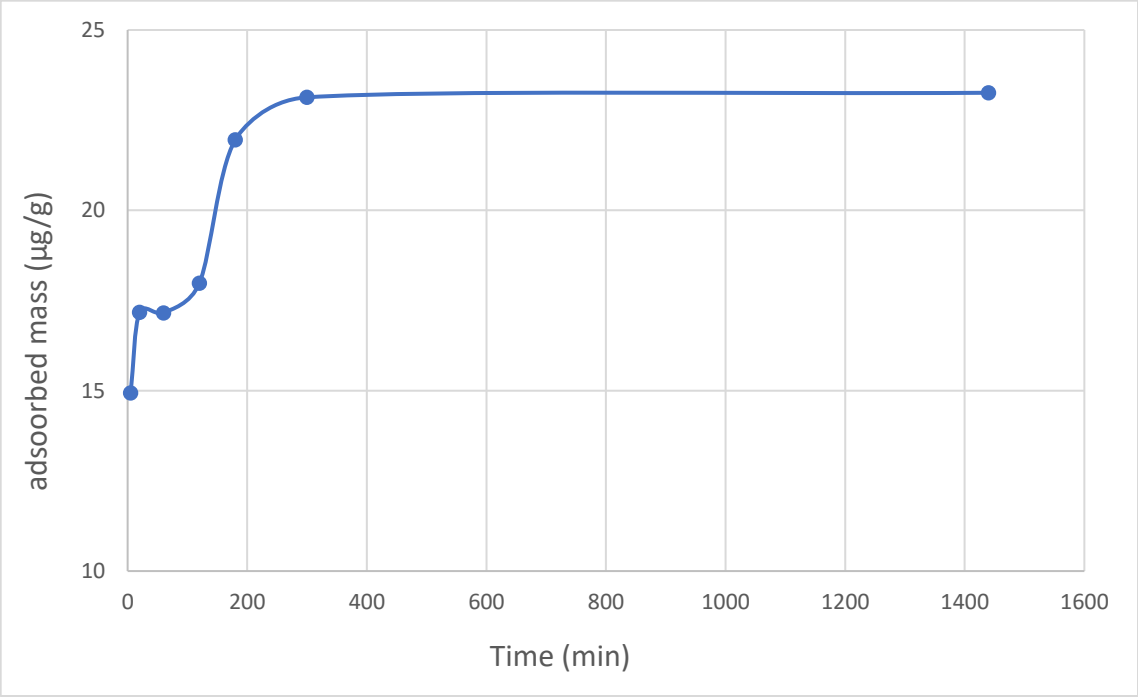

Figure 4-23: Sorption kinetic of local well water

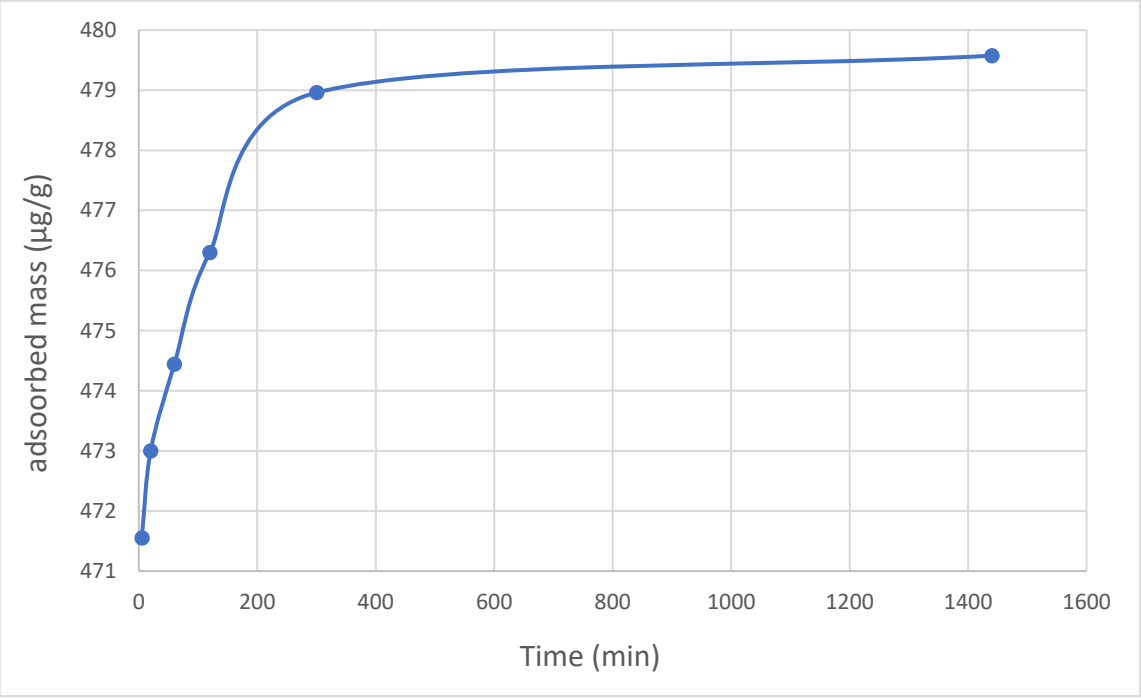

Figure 4-24: Sorption kinetic of synthesized arsenic contaminated water ($Na_2HAsO_4.7H_2O$, 1 ppm)

Pseudo first and pseudo second order kinetic models are usually used for kinetic investigations on activated carbons. Besides, for the porous adsorbents, the diffusional effects are also important, so the mass transfer kinetic models, such as intraparticle diffusion model (the Weber and Morris model) are also applied (Tsibranska & Hristova, 2011). To find out the best model to describe the kinetic of arsenic removal from synthesized water with $Na_2HAsO_4.7H_2O$ (1 ppm) and the local well water, pseudo-first order, pseudo-second order, and intra particle diffusion kinetic models, which used commonly for sorption processes were investigated in this study (Ananta et al., 2015, Chammui *et al.*, 2014).

4.8.1 Pseudo-first order kinetic model

Equation (4-7) presents the pseudo-first kinetic model (Ananta et al., 2015, Sheela *et al.*, 2012):

$$log(q_e - q) = logq_e - (\frac{K_1}{2.303})t \quad (4\text{-}7)$$

In which,

q_e = adsorption capacity, µg/g

q = the amount of adsorbent adsorbed at any time t, µg/g

K_1= rate constant, min^{-1}

t = time, min

By plotting log (q_e-q) versus time, Figure 4-25 and Figure 4-26 for local well water and synthesized water respectively, the value of K_1 is estimated by the value of the slope of the plot. The values of the correlation coefficient (R^2), K_1, and q_e are reported in Table 4-17.

Table 4-17: Parameters of pseudo-first order kinetic model for local well water and synthesized water ($Na_2HAsO_4.7H_2O$, 1 ppm)

Parameter	Value for synthesized water	Value for local well water
K_1	0.0085	0.0136
R^2	0.996	0.91

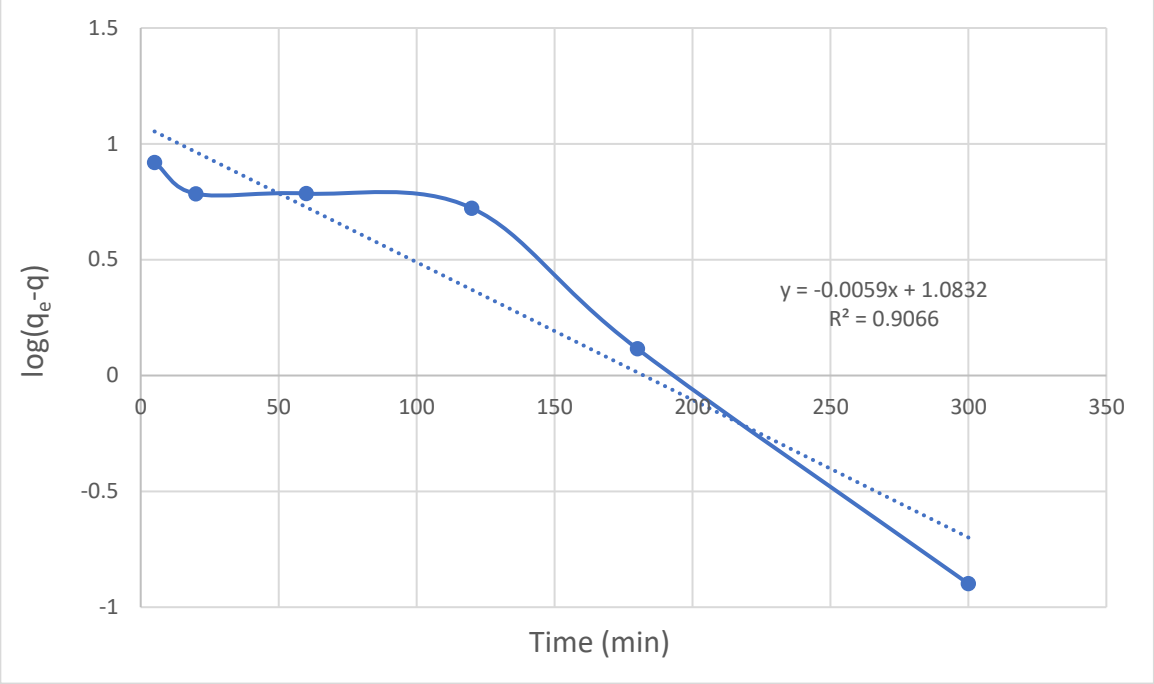

Figure 4-25: Pseudo-first order kinetic model for arsenic removal from local well water

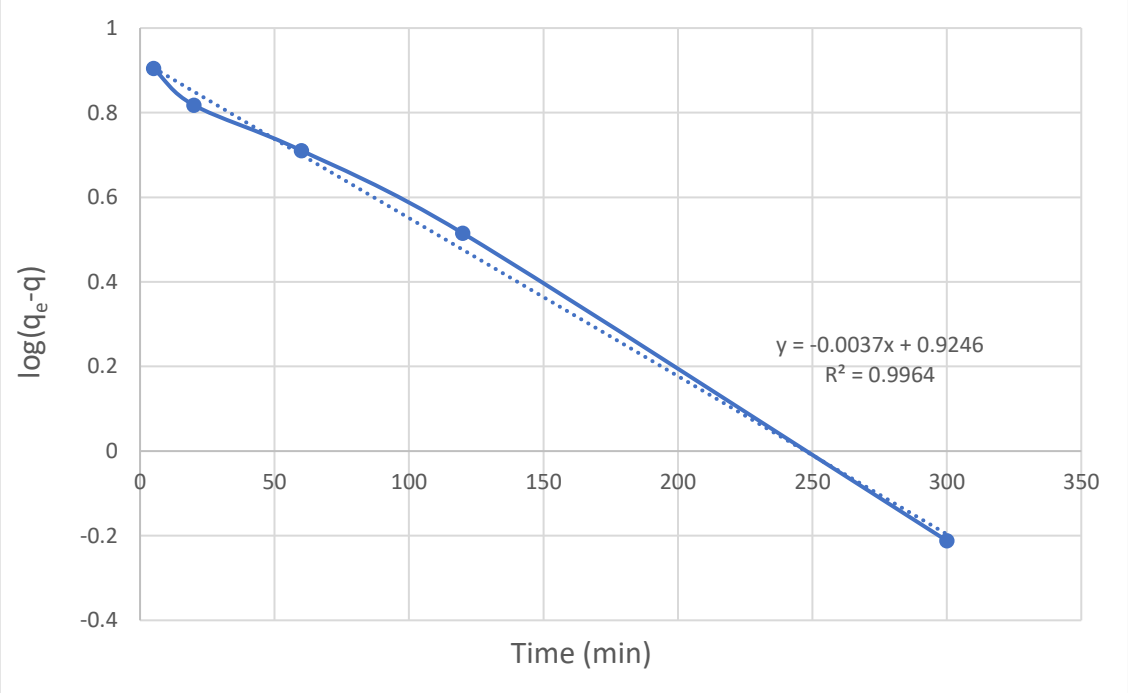

Figure 4-26: Pseudo-first order kinetic model for arsenic removal from synthesized water ($Na_2HAsO_4.7H_2O$, 1 ppm)

4.8.2 Pseudo second order kinetic model

This model is represented by applying Equation (4-8) (Ananta et al., 2015, Figaro *et al.*, 2009, Sheela et al., 2012):

$$\frac{t}{q} = (\frac{1}{K_2 q_e^2}) + (\frac{t}{q_e}) \quad (4\text{-}8)$$

In which

q_e = adsorption capacity, µg/g

q = the amount of adsorbent adsorbed at any time t, µg/g

K_2= rate constant, g. $\mu g^{-1}.min^{-1}$

t = time, min

By plotting t/q versus t, Figure 4-27 and Figure 4-28 for local well water and synthesized water respectively, the value of K_2 is estimated by using the value of plot's intercept. The values of the correlation coefficient (R^2), K_1, and q_e are reported in Table 4-18.

Table 4-18: Parameters of pseudo-second order kinetic model for local well water and synthesized water ($Na_2HAsO_4.7H_2O$, 1 ppm)

Parameter	Value for synthesized water	Value for local well water
K_2	0.004	0.003
R^2	1	0.999

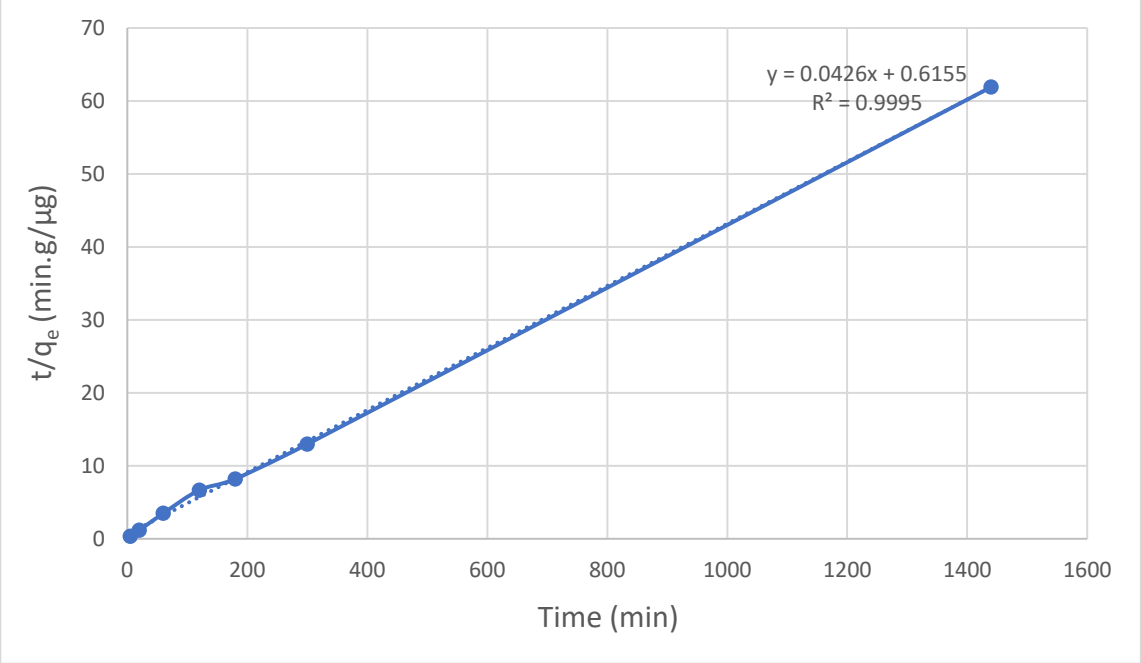

Figure 4-27: Pseudo-second order kinetic model for arsenic removal from local well water

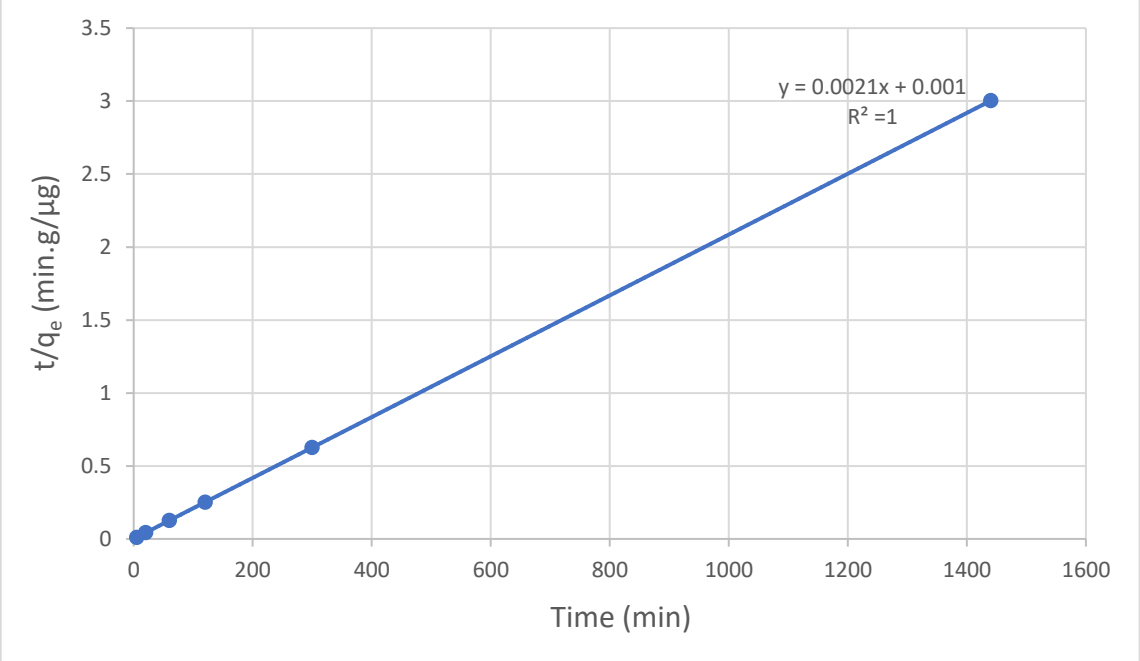

Figure 4-28: Pseudo-second order kinetic model for arsenic removal from synthesized water ($Na_2HAsO_4.7H_2O$, 1 ppm)

4.8.3 Intraparticle diffusion kinetic model (The Weber-Morris model)

The presumption that the adsorbate molecules transported through intraparticle diffusion from the solution to the solid, which is adsorbent, is the major part of intraparticle diffusion model and it is important because determines the adsorption rate in most of liquid systems as it could be controlling step for the rate of the reaction. Equation (4-9) describes intra particle diffusion kinetic model (Ananta et al., 2015, Sheela et al., 2012, Weber & Morris, 1963):

$$q_t = K_{id} t^{0.5} + C \quad (4\text{-}9)$$

In which,

q_t = the amount of adsorbent adsorbed at any time t, µg/g

K_{id}= rate constant of the intra particle diffusion, µg.g^{-1}.min$^{-0.5}$

C = Film thickness

t = time, min

By plotting q_t versus $t^{0.5}$, Figure 4-29 and Figure 4-30 for local well water and synthesized water respectively, the values of K_{id}, which is the slope of the plot, and C, which is the intercept of the plot, are calculated. The values of the correlation coefficient (R^2), K_{id}, and C are reported in Table 4-19.

Table 4-19: Parameters of intra particle diffusion kinetic model for local well water and synthesized water ($Na_2HAsO_4.7H_2O$, 1 ppm)

Parameter	Value for synthesized water	Value for local well water
K_{id}	0.214	0.23
R^2	0.76	0.66
C	472.76	16.32

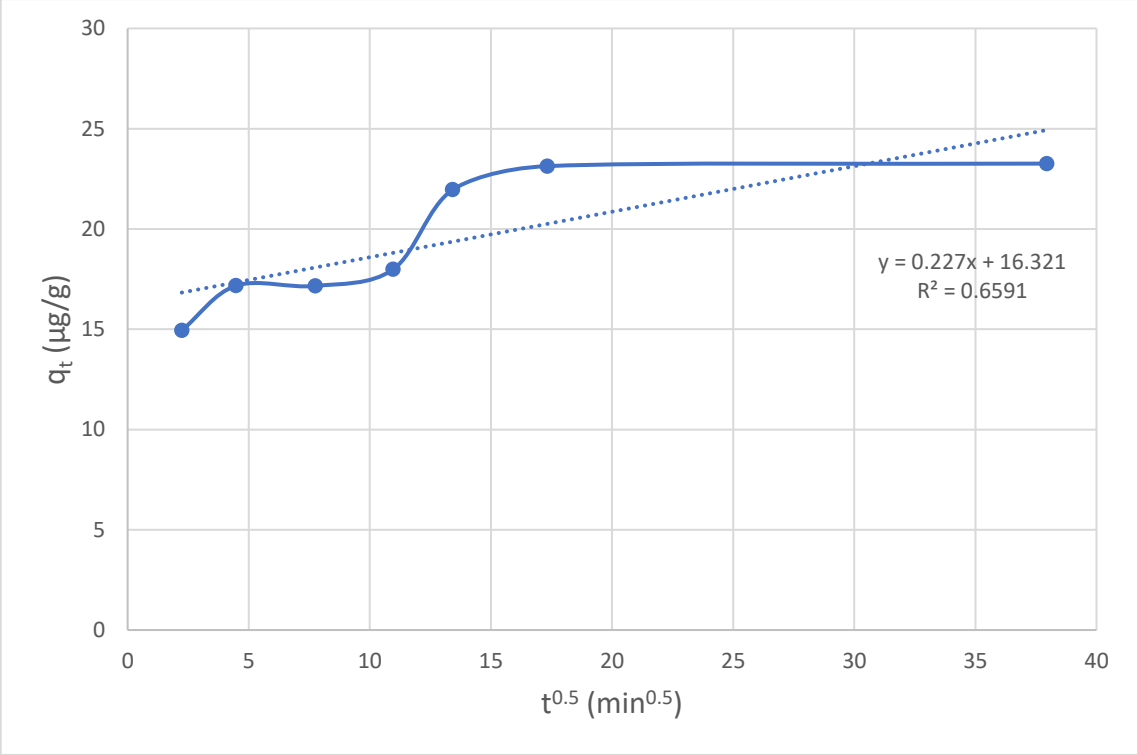

Figure 4-29: Intra particle diffusion kinetic model for arsenic removal from local well water

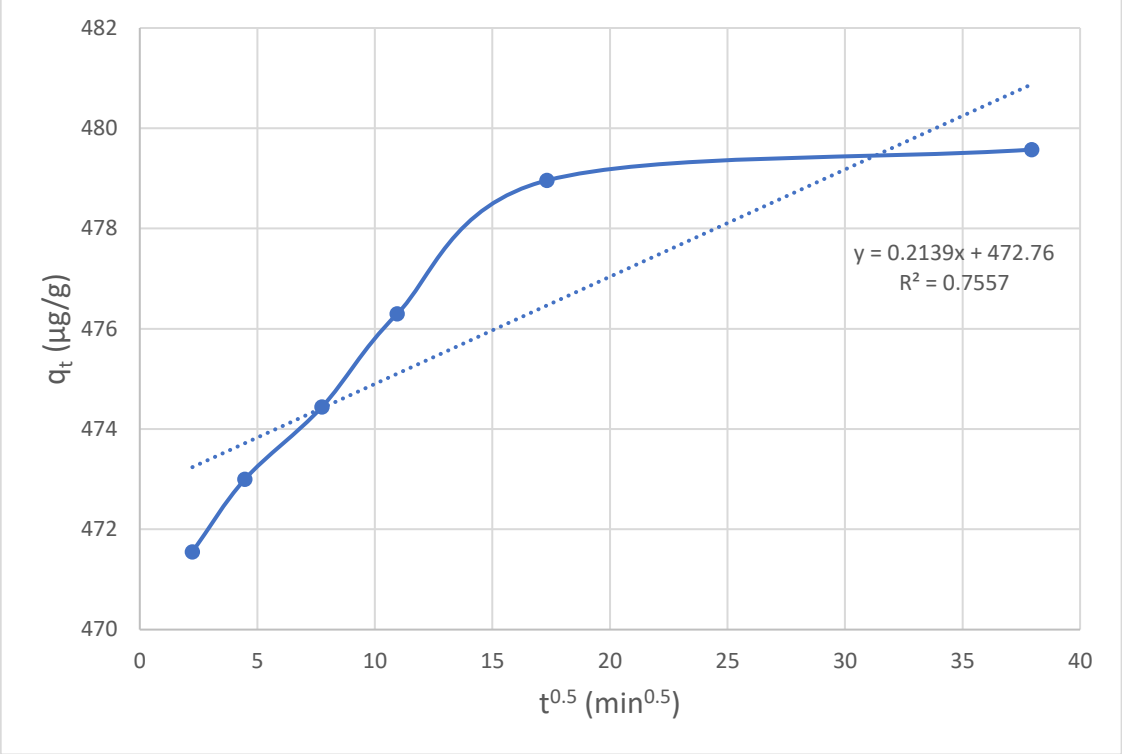

Figure 4-30: Intra particle diffusion kinetic model for arsenic removal from synthesized water ($Na_2HAsO_4.7H_2O$, 1 ppm)

Based on the results achieved from Figure 4-25 to Figure 4-30, it is obvious that, among the kinetic models investigated in this study, pseudo second order kinetic model has the higher correlation coefficient (R^2) and these kinetic data follow the second order kinetic model better than the other models.

5. Conclusions and Recommendations

In this study, a low-cost adsorbent from the ash of Corner Brook Pulp and Paper (CBPP) company was used as a filter media to remove arsenic from drinking water. This low-cost adsorbent processed from the ash which is currently dumped into the landfills. The processed carbon from the ash is found very effective not only to remove arsenic from the arsenic contaminated well waters in the Bell Island but also other components existed in the water. After the cleaning process of CBPP fly ash, two different methods applied for activation: activation with the pure carbon dioxide (CO_2) and, the activation with the mixture of steam and CO_2. Both activations significantly increase the surface area and pore volume of carbon sample. The highest surface area and pore volume achieved with activation at 850^{o}C for 2 hours for both types of activation and at these conditions, the BET surface area of the CBPP fly ash was 847.26m^2/g for the pure CO_2 activation and 1146.25m^2/g for the activation with the mixture of CO_2 and steam, while the surface area of the cleaned and not activated CBPP fly ash was 486.44m^2/g.

The activated CBPP fly ash with the mixture of CO_2 and steam at 850^{o}C for 2 hours, impregnated by iron (III) chloride ($FeCl_3$) solution with different concentrations (0.01 to 1M) and the impregnated samples were applied for arsenic removal. The adsorbent impregnated with 0.1M $FeCl_3$ was the most efficient adsorbent for arsenic removal by removing 99.63% of arsenate and 86.64% of arsenite from synthesized water with concentration of 1ppm of sodium arsenate ($Na_2HAsO_4.7H_2O$) as the source of arsenate and 1 ppm of arsenic (III) oxide (As_2O_3) as the source of arsenite, respectively and applied

for arsenic removal from local well water. Moreover, the BET surface area analysis and scanning electron microscopy images revealed that the impregnation with 0.1M $FeCl_3$ does not significantly decrease the surface area and not causing pore blockage. The iron distribution is also found as an important parameter during the impregnation of activated carbon for arsenic removal.

The Langmuir model better fitted with equilibrium data of arsenic removal from local well water of Bell Island and synthesized water of sodium arsenate (1ppm) than the other models and maximum arsenic adsorption capacity for local well water and synthesized water, according to the Langmuir model, was 35.46µg/g of carbon and 1428.6µg/g of carbon, respectively. Moreover, the pseudo second order kinetic model explained the kinetic behavior of arsenic sorption for both local well water and synthesized water better than the other models.

According to the results of this study, it is notable that by using a small amount of iron for impregnation of activated carbon, the efficiency of arsenic removal significantly increases, and the waste material of the Corner Brook Pulp and Paper company can be processed as a low-cost adsorbent for arsenic removal from the local well water, especially Bell island's well water.

The following recommendations will help in improving the study in future:

a) Multi component adsorption is one of the important issues that could be studied because the existence of some other elements and components in the water affects the arsenic removal efficiency.
b) Desorption of adsorbed elements and especially arsenic could be investigated to find out whether the adsorbent could be reused for treatment or not.
c) The economic aspects of this experiment could be examined through life cycle assessment of the waste material from CBPP.

6. References

Ananta, S., B. Saumen and V. Vijay, 2015: Adsorption isotherm, thermodynamic and kinetic study of arsenic (III) on iron oxide coated granular activated charcoal. *Int. Res. J. Environ. Sci.,* **4,** 64-77.

Arcibar-Orozco, J. A., D.-B. Josue, J. C. Rios-Hurtado and J. R. Rangel-Mendez, 2014: Influence of iron content, surface area and charge distribution in the arsenic removal by activated carbons. *Chemical Engineering Journal,* **249,** 201-209.

Asadullah, M., I. Jahan, M. B. Ahmed, P. Adawiyah, N. H. Malek and M. S. Rahman, 2014: Preparation of microporous activated carbon and its modification for arsenic removal from water. *Journal of Industrial and Engineering Chemistry,* **20,** 887-896.

ASTM D2866-11, 2011: Standard Test Method for Total Ash Content of Activated Carbon, ASTM International, West Conshohocken, PA, 2011, https://doi.org/10.1520/D2866-11.

ASTM D2867-09, 2014: Standard Test Methods for Moisture in Activated Carbon, ASTM International, West Conshohocken, PA, 2014, https://doi.org/10.1520/D2867-09R.

ASTM D3838-05, 2017: Standard Test Method for pH of Activated Carbon, ASTM International, West Conshohocken, PA, 2017, https://doi.org/10.1520/D3838-05R17.

ASTM D4607-14, 2014: Standard Test Method for Determination of Iodine Number of Activated Carbon, ASTM International, West Conshohocken, PA, 2014, https://doi.org/10.1520/D4607-14.

Aworn, A., P. Thiravetyan and W. Nakbanpote, 2008: Preparation and characteristics of agricultural waste activated carbon by physical activation having micro-and mesopores. *Journal of Analytical and Applied Pyrolysis,* **82,** 279-285.

Chammui, Y., P. Sooksamiti, W. Naksata and O.-A. Arqueropanyo, 2014: Kinetic and mechanism of arsenic ions removal by adsorption on leonardite char as low cost adsorbent material. *Journal of the Chilean Chemical Society,* **59,** 2378-2381.

Chang, Q., W. Lin and W.-c. Ying, 2010: Preparation of iron-impregnated granular activated carbon for arsenic removal from drinking water. *Journal of Hazardous Materials,* **184,** 515-522.

Chang, Q., W. Lin and W.-C. Ying, 2012: Impacts of amount of impregnated iron in granular activated carbon on arsenate adsorption capacities and kinetics. *Water Environment Research,* **84,** 514-520.

Chen, W., R. Parette, J. Zou, F. S. Cannon and B. A. Dempsey, 2007: Arsenic removal by iron-modified activated carbon. *Water research,* **41,** 1851-1858.

Dada, A., A. Olalekan, A. Olatunya and O. Dada, 2012: Langmuir, Freundlich, Temkin and Dubinin–Radushkevich isotherms studies of equilibrium sorption of Zn2+ unto phosphoric acid modified rice husk. *IOSR Journal of Applied Chemistry,* **3,** 38-45.

Dehghani, M. H., A. Zarei, A. Mesdaghinia, R. Nabizadeh, M. Alimohammadi and M. Afsharnia, 2017: Response surface modeling, isotherm, thermodynamic and optimization study of arsenic (V) removal from aqueous solutions using modified bentonite-chitosan (MBC). *Korean Journal of Chemical Engineering,* **34,** 757-767.

Department of Municipal Affairs and Environment, 2010: Groundwater Useage Statistics, St. John's, NL. http://www.env.gov.nl.ca/env/waterres/cycle/groundwater/data/useage.html.

Department of Municipal Affairs and Environment, 2016: Arsenic in Well Water, St. John's, NL. http://www.env.gov.nl.ca/env/waterres/cycle/groundwater/well/arsenic.html.

Di Natale, F., A. Erto, A. Lancia and D. Musmarra, 2009: A descriptive model for metallic ions adsorption from aqueous solutions onto activated carbons. *Journal of hazardous materials,* **169,** 360-369.

Erhayem, M., F. Al-Tohami, R. Mohamed and K. Ahmida, 2015: Isotherm, kinetic and thermodynamic studies for the sorption of mercury (II) onto activated carbon from Rosmarinus officinalis leaves. *American Journal of Analytical Chemistry,* **6,** 1.

Fierro, V., G. Muñiz, G. Gonzalez-Sánchez, M. Ballinas and A. Celzard, 2009: Arsenic removal by iron-doped activated carbons prepared by ferric chloride forced hydrolysis. *Journal of Hazardous Materials,* **168,** 430-437.

Figaro, S., J. Avril, F. Brouers, A. Ouensanga and S. Gaspard, 2009: Adsorption studies of molasse's wastewaters on activated carbon: Modelling with a new fractal kinetic equation and evaluation of kinetic models. *Journal of hazardous materials,* **161,** 649-656.

Ghanizadeh, G., M. Ehrampoush and M. Ghaneian, 2010: Application of iron impregnated activated carbon for removal of arsenic from water. *Iranian Journal of Environmental Health Science & Engineering,* **7,** 145.

González, J. F., J. M. Encinar, C. M. González-García, E. Sabio, A. Ramiro, J. L. Canito and J. Gañán, 2006: Preparation of activated carbons from used tyres by gasification with steam and carbon dioxide. *Applied Surface Science,* **252,** 5999-6004.

Gu, Z., B. Deng and J. Yang, 2007: Synthesis and evaluation of iron-containing ordered mesoporous carbon (FeOMC) for arsenic adsorption. *Microporous and mesoporous materials,* **102,** 265-273.

Gu, Z., J. Fang and B. Deng, 2005: Preparation and evaluation of GAC-based iron-containing adsorbents for arsenic removal. *Environmental science & technology,* **39,** 3833-3843.

Ho, Y. and G. McKay, 1998: A comparison of chemisorption kinetic models applied to pollutant removal on various sorbents. *Process safety and environmental protection,* **76,** 332-340.

Jahan, M. I., M. A. Motin, M. Moniuzzaman and M. Asadullah, 2008: Arsenic removal from water using activated carbon obtained from chemical activation of jute stick.

Jenner, G., H. Longerich, S. Jackson and B. Fryer, 1990: ICP-MS—a powerful tool for high-precision trace-element analysis in earth sciences: evidence from analysis of selected USGS reference samples. *Chemical Geology,* **83,** 133-148.

Kinniburgh, D. and P. Smedley, 2001: Arsenic contamination of groundwater in Bangladesh.

Krupa, N. E. and F. S. Cannon, 1996: GAC: pore structure versus dye adsorption. *American Water Works Association. Journal,* **88,** 94.

Li, W.-G., X.-J. Gong, K. Wang, X.-R. Zhang and W.-B. Fan, 2014: Adsorption characteristics of arsenic from micro-polluted water by an innovative coal-based mesoporous activated carbon. *Bioresource technology,* **165,** 166-173.

Lorenzen, L., J. Van Deventer and W. Landi, 1995: Factors affecting the mechanism of the adsorption of arsenic species on activated carbon. *Minerals Engineering,* **8,** 557-569.

Meher, A. K., S. Das, S. Rayalu and A. Bansiwal, 2016: Enhanced arsenic removal from drinking water by iron-enriched aluminosilicate adsorbent prepared from fly ash. *Desalination and Water Treatment,* **57,** 20944-20956.

Mohan, D. and C. U. Pittman, 2007: Arsenic removal from water/wastewater using adsorbents—a critical review. *Journal of Hazardous materials,* **142,** 1-53.

Mondal, P., S. Bhowmick, D. Chatterjee, A. Figoli and B. Van der Bruggen, 2013: Remediation of inorganic arsenic in groundwater for safe water supply: a critical assessment of technological solutions. *Chemosphere,* **92,** 157-170.

Muniz, G., V. Fierro, A. Celzard, G. Furdin, G. Gonzalez-Sánchez and M. Ballinas, 2009: Synthesis, characterization and performance in arsenic removal of iron-doped activated carbons prepared by impregnation with Fe (III) and Fe (II). *Journal of hazardous materials,* **165,** 893-902.

National Standard of the People's Republic of China, 2008: Test method for granular activated carbon from coal-determination of methylene blue adsorption. GB/T 7702.6-2008.

Ouvrard, S., M.-O. Simonnot and M. Sardin, 2002: Reactive behavior of natural manganese oxides toward the adsorption of phosphate and arsenate. *Industrial & engineering chemistry research,* **41,** 2785-2791.

Rageh, O. M., C. A. Coles and L. M. Lye, Statistical analysis of Newfoundland drinking water sources containing arsenic. in Proceedings of the Ottawa Geo2007–60 th Canadian Geotechnical Conference, 2007, p. 2287-2291.

Ray, P. Z. and H. J. Shipley, 2015: Inorganic nano-adsorbents for the removal of heavy metals and arsenic: a review. *RSC Advances,* **5,** 29885-29907.

Raychoudhury, T., F. Schiperski and T. Scheytt, 2015: Distribution of iron in activated carbon composites: assessment of arsenic removal behavior. *Water Science and Technology: Water Supply,* **15,** 990-998.

Rohail, D. B., 2012: Arsenic removal by sand filtration for potable water in rural Newfoundland and Labrador. Memorial University of Newfoundland.

Salbu, B. and E. Steinnes, 1994: *Trace elements in natural waters*. Springer Science & Business.

Sarkar, A., M. Krishnapillai and J. Valcour, 2012: A study of groundwater quality of private wells in Western Newfoundland communities.

Sheela, T., Y. A. Nayaka, R. Viswanatha, S. Basavanna and T. Venkatesha, 2012: Kinetics and thermodynamics studies on the adsorption of Zn (II), Cd (II) and Hg (II) from aqueous solution using zinc oxide nanoparticles. *Powder Technology,* **217,** 163-170.

Smedley, P. and D. Kinniburgh, 2002: A review of the source, behaviour and distribution of arsenic in natural waters. *Applied geochemistry,* **17,** 517-568.

Streat, M., J. Patrick and M. C. Perez, 1995: Sorption of phenol and para-chlorophenol from water using conventional and novel activated carbons. *Water Research,* **29,** 467-472.

Thirunavukkarasu, O., T. Viraraghavan and K. Subramanian, 2001: Removal of arsenic in drinking water by iron oxide-coated sand and ferrihydrite-batch studies. *Water Quality Research Journal of Canada,* **36,** 55-70.

Tsibranska, I. and E. Hristova, 2011: Comparison of different kinetic models for adsorption of heavy metals onto activated carbon from apricot stones. *Bulgarian Chem Commun,* **43,** 370.

U.S.EPA, 2016: National Primary Drinking Water Regulation. http://www.epa.gov/your-drinking-water/table-regulated-drinking-water-contaminants#Inorganic.

Vitela-Rodriguez, A. V. and J. R. Rangel-Mendez, 2013: Arsenic removal by modified activated carbons with iron hydro (oxide) nanoparticles. *Journal of environmental management,* **114,** 225-231.

Wang, X.-s. and Y. Qin, 2005: Equilibrium sorption isotherms for of Cu 2+ on rice bran. *Process Biochemistry,* **40,** 677-680.

Weber, W. J. and J. C. Morris, 1963: Kinetics of adsorption on carbon from solution. *Journal of the Sanitary Engineering Division,* **89,** 31-60.

Xu, C. and A. S. Teja, 2006: Supercritical water synthesis and deposition of iron oxide (α-Fe 2 O 3) nanoparticles in activated carbon. *The Journal of supercritical fluids,* **39,** 135-141.

Yadav, L. S., B. K. Mishra, A. Kumar and K. K. Paul, 2014: Arsenic removal using bagasse fly ash-iron coated and sponge iron char. *Journal of Environmental Chemical Engineering,* **2,** 1467-1473.

Yan, C., C. Wang, J. Yao, L. Zhang and X. Liu, 2009: Adsorption of methylene blue on mesoporous carbons prepared using acid-and alkaline-treated zeolite X as the template. *Colloids and Surfaces A: Physicochemical and Engineering Aspects,* **333,** 115-119.

Yao, S., Z. Liu and Z. Shi, 2014: Arsenic removal from aqueous solutions by adsorption onto iron oxide/activated carbon magnetic composite. *Journal of Environmental Health Science and Engineering,* **12,** 58.

Zhang, F.-S. and H. Itoh, 2006: Photocatalytic oxidation and removal of arsenite from water using slag-iron oxide-TiO 2 adsorbent. *Chemosphere,* **65,** 125-131.

Zhang, H., T. Husain and Y. Chen, 2017: Corner Brook Pulp and Paper Mill Waste Management. The Harris Centre MMSB Waste Management Applied Reasearch Fund 2015/2016, 53 pages.

Zhang, K., D. Zhang and K. Zhang, 2016: Arsenic removal from water using a novel amorphous adsorbent developed from coal fly ash. *Water Science and Technology,* **73,** 1954-1962.

7. Appendixes

Appendix A

BET surface area and porosity analysis report of the cleaned CBPP fly ash (Zhang et al., 2017)

CCRI University of Ottawa

Sample: MU-sample-2
Operator:
File: C:\3Flex\data\Yong Yang data\000-326-MU-sample-2.SMP

Started:	31/08/2016 10:12:37 AM	Analysis adsorptive:	N2
Completed:	01/09/2016 12:42:16 AM	Analysis bath temp.:	77.397 K
Report time:	01/09/2016 9:59:02 AM	Thermal correction:	No
Sample mass:	0.0797 g	Warm free space:	16.6669 cm³ Measured
Cold free space:	59.7874 cm³	Equilibration interval:	10 s
Low pressure dose:	None	Sample density:	1.000 g/cm³
Automatic degas:	No		

Summary Report

Surface Area

Single point surface area at p/p° = 0.300000000:	429.8371 m²/g
BET Surface Area:	486.4352 m²/g
t-Plot Micropore Area:	402.4971 m²/g
t-Plot external surface area:	83.9381 m²/g
BJH Adsorption cumulative surface area of pores between 1.7000 nm and 300.0000 nm width:	68.331 m²/g
BJH Desorption cumulative surface area of pores between 1.7000 nm and 300.0000 nm width:	30.8406 m²/g

Pore Volume

t-Plot micropore volume:	0.181080 cm³/g
BJH Adsorption cumulative volume of pores between 1.7000 nm and 300.0000 nm width:	0.060152 cm³/g
BJH Desorption cumulative volume of pores between 1.7000 nm and 300.0000 nm width:	0.034851 cm³/g

Pore Size

BJH Adsorption average pore width (4V/A):	3.5212 nm
BJH Desorption average pore width (4V/A):	4.5201 nm

Sample: MU-sample-2
Operator:
File: C:\3Flex\data\Yong Yang data\000-326-MU-sample-2.SMP

Started: 31/08/2016 10:12:37 AM
Completed: 01/09/2016 12:42:16 AM
Report time: 01/09/2016 9:59:02 AM
Sample mass: 0.0797 g
Cold free space: 59.7874 cm³
Low pressure dose: None
Automatic degas: No

Analysis adsorptive: N2
Analysis bath temp.: 77.397 K
Thermal correction: No
Warm free space: 16.6669 cm³ Measured
Equilibration interval: 10 s
Sample density: 1.000 g/cm³

Isotherm Tabular Report

Relative Pressure (p/p°)	Absolute Pressure (mmHg)	Quantity Adsorbed (cm³/g STP)	Elapsed Time (h:min)	Saturation Pressure (mmHg)
			01:04	755.715210
0.002872266	2.189735	112.1333	09:42	762.371948
0.006061635	4.634561	117.6243	10:56	764.572815
0.024502589	18.696449	126.8301	11:24	763.039734
0.034419968	26.248293	129.0882	11:32	762.589111
0.044503543	33.930656	130.8206	11:38	762.425964
0.063430268	48.394859	133.1425	11:44	762.961609
0.074003917	56.381454	134.1942	11:48	761.871216
0.107937202	82.356895	136.6731	11:52	763.007507
0.142516749	108.754128	138.5169	11:55	763.097168
0.176791744	134.831879	139.9439	11:59	762.659363
0.200549261	153.008804	140.8386	12:02	762.948730
0.243449753	185.739487	142.0199	12:05	762.947937
0.277439118	211.694412	142.8197	12:08	763.030151
0.311649989	237.604889	143.4657	12:11	762.409424
0.344771410	262.964966	144.0148	12:14	762.722656
0.378955097	288.784485	144.4605	12:17	762.054626
0.411615873	314.226990	144.8711	12:20	763.398621
0.446524428	340.769897	145.1849	12:23	763.160706
0.480018489	366.608643	145.4062	12:26	763.738586
0.513930242	392.765259	145.5823	12:29	764.238464
0.547702577	418.930695	145.7175	12:32	764.887207
0.581988349	445.125427	145.8599	12:35	764.835632
0.616795812	471.225525	145.9906	12:39	763.989502
0.649293574	496.677246	146.1514	12:42	764.950195
0.684135730	523.300781	146.3727	12:45	764.907837
0.718272287	548.975281	146.6805	12:48	764.299683
0.734461496	561.574890	146.8563	12:51	764.607666
0.752439678	574.725220	147.0268	12:54	763.815674
0.769448883	587.383301	147.2278	12:57	763.381836
0.777190535	593.345459	147.3222	13:00	763.449158
0.785846377	599.941956	147.4159	13:03	763.434143
0.819256616	625.429321	148.0140	13:06	763.410767
0.852780025	651.611694	148.7798	13:09	764.102905
0.885856969	677.880310	149.7751	13:12	765.225464
0.921911970	704.842102	151.1068	13:15	764.543823
0.955095729	730.103821	152.8303	13:18	764.429993
0.987991802	754.754761	157.6879	13:22	763.928162

Sample: MU-sample-2
Operator:
File: C:\3Flex\data\Yong Yang data\000-326-MU-sample-2.SMP

Started:	31/08/2016 10:12:37 AM	Analysis adsorptive:	N2
Completed:	01/09/2016 12:42:16 AM	Analysis bath temp.:	77.397 K
Report time:	01/09/2016 9:59:02 AM	Thermal correction:	No
Sample mass:	0.0797 g	Warm free space:	16.6669 cm³ Measured
Cold free space:	59.7874 cm³	Equilibration interval:	10 s
Low pressure dose:	None	Sample density:	1.000 g/cm³
Automatic degas:	No		

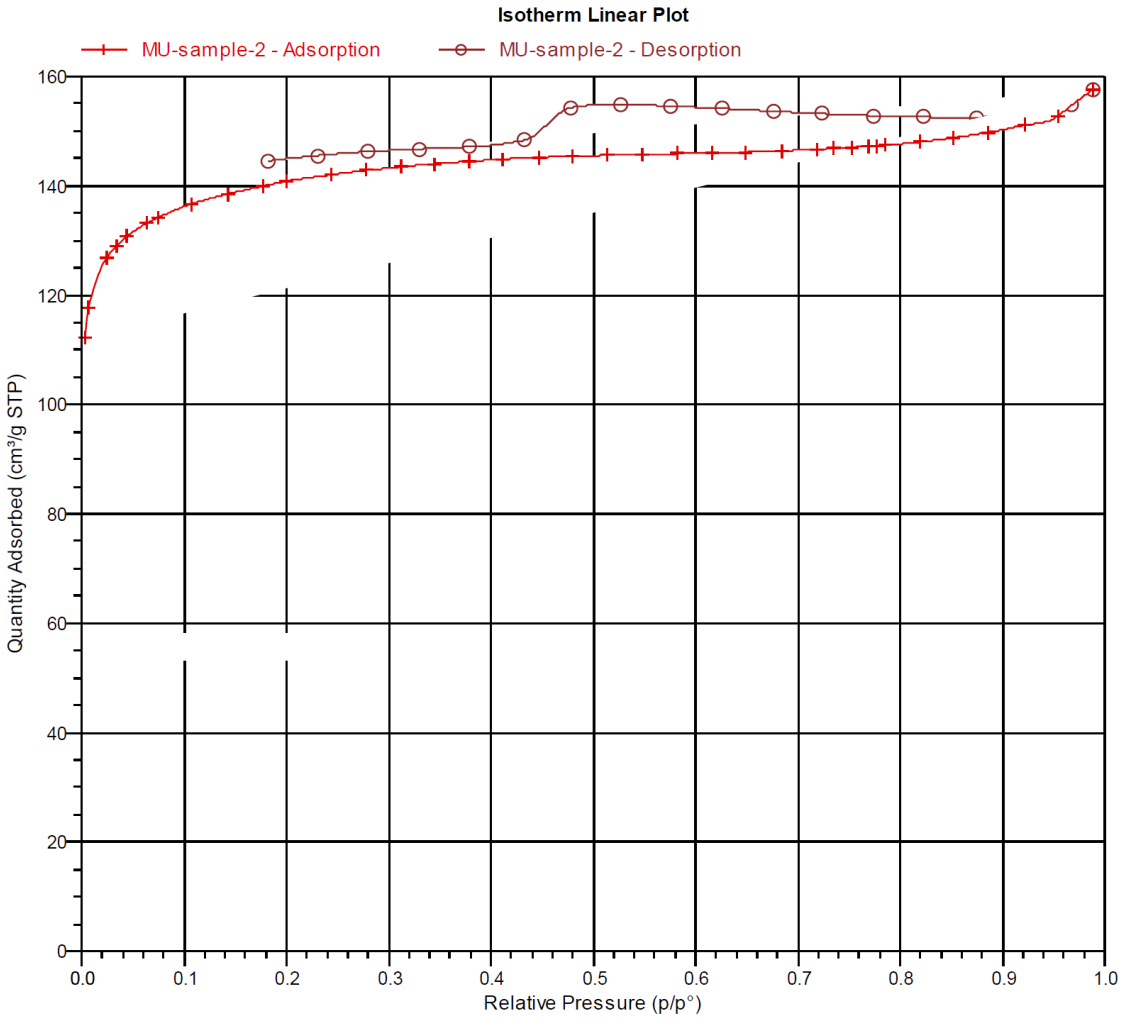

Sample: MU-sample-2
Operator:
File: C:\3Flex\data\Yong Yang data\000-326-MU-sample-2.SMP

Started:	31/08/2016 10:12:37 AM	Analysis adsorptive:	N2
Completed:	01/09/2016 12:42:16 AM	Analysis bath temp.:	77.397 K
Report time:	01/09/2016 9:59:02 AM	Thermal correction:	No
Sample mass:	0.0797 g	Warm free space:	16.6669 cm³ Measured
Cold free space:	59.7874 cm³	Equilibration interval:	10 s
Low pressure dose:	None	Sample density:	1.000 g/cm³
Automatic degas:	No		

BET Report

BET surface area:	486.4352 ± 8.5146 m²/g
Slope:	0.009022 ± 0.000155 g/cm³ STP
Y-intercept:	-0.000074 ± 0.000019 g/cm³ STP
C:	-120.740637
Qm:	111.7579 cm³/g STP
Correlation coefficient:	0.9995547
Molecular cross-sectional area:	0.1620 nm²

Relative Pressure (p/p°)	Quantity Adsorbed (cm³/g STP)	1/[Q(p°/p - 1)]
0.063430268	133.1425	0.000509
0.074003917	134.1942	0.000596
0.107937202	136.6731	0.000885
0.142516749	138.5169	0.001200
0.176791744	139.9439	0.001535

Sample: MU-sample-2
Operator:
File: C:\3Flex\data\Yong Yang data\000-326-MU-sample-2.SMP

Started:	31/08/2016 10:12:37 AM	Analysis adsorptive:	N2
Completed:	01/09/2016 12:42:16 AM	Analysis bath temp.:	77.397 K
Report time:	01/09/2016 9:59:02 AM	Thermal correction:	No
Sample mass:	0.0797 g	Warm free space:	16.6669 cm³ Measured
Cold free space:	59.7874 cm³	Equilibration interval:	10 s
Low pressure dose:	None	Sample density:	1.000 g/cm³
Automatic degas:	No		

BET Surface Area Plot

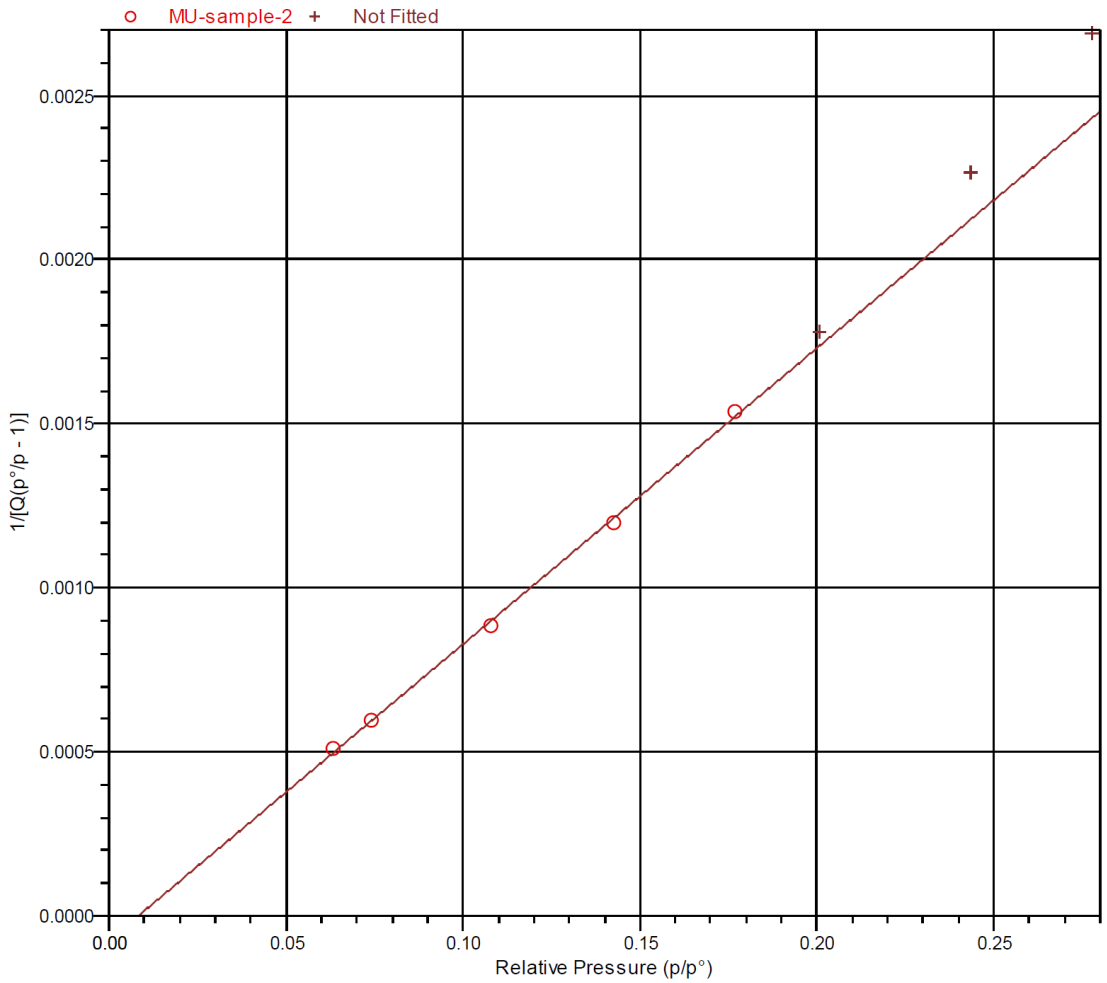

Sample: MU-sample-2
Operator:
File: C:\3Flex\data\Yong Yang data\000-326-MU-sample-2.SMP

Started:	31/08/2016 10:12:37 AM	Analysis adsorptive:	N2
Completed:	01/09/2016 12:42:16 AM	Analysis bath temp.:	77.397 K
Report time:	01/09/2016 9:59:02 AM	Thermal correction:	No
Sample mass:	0.0797 g	Warm free space:	16.6669 cm³ Measured
Cold free space:	59.7874 cm³	Equilibration interval:	10 s
Low pressure dose:	None	Sample density:	1.000 g/cm³
Automatic degas:	No		

t-Plot Report

Micropore volume:	0.181080 cm³/g
Micropore area:	402.4971 m²/g
External surface area:	83.9381 m²/g
Slope:	54.152554 ± 3.752418 cm³/g·nm STP
Y-intercept:	116.823166 ± 1.621664 cm³/g STP
Correlation coefficient:	0.990533
Surface area correction factor:	1.000
Density conversion factor:	0.0015500
Total surface area (BET):	486.4352 m²/g
Thickness range:	0.35000 nm to 0.50000 nm
Thickness equation:	Harkins and Jura

Thickness Curve

t = [13.99 / (0.034 - log(p/p°))] ^ 0.5

t-Plot Report - Data

Relative Pressure (p/p°)	Statistical Thickness (nm)	Quantity Adsorbed (cm³/g STP)	Fitted
0.063430268	0.33702	133.1425	
0.074003917	0.34657	134.1942	
0.107937202	0.37388	136.6731	*
0.142516749	0.39869	138.5169	*
0.176791744	0.42174	139.9439	*
0.200549261	0.43724	140.8386	*
0.243449753	0.46479	142.0199	*
0.277439118	0.48661	142.8197	*
0.311649989	0.50884	143.4657	
0.344771410	0.53084	144.0148	
0.378955097	0.55425	144.4605	
0.411615873	0.57748	144.8711	
0.446524428	0.60347	145.1849	
0.480018489	0.62977	145.4062	
0.513930242	0.65803	145.5823	
0.547702577	0.68812	145.7175	
0.581988349	0.72105	145.8599	
0.616795812	0.75743	145.9906	
0.649293574	0.79463	146.1514	
0.684135730	0.83876	146.3727	

Sample: MU-sample-2
Operator:
File: C:\3Flex\data\Yong Yang data\000-326-MU-sample-2.SMP

Started:	31/08/2016 10:12:37 AM	Analysis adsorptive:	N2
Completed:	01/09/2016 12:42:16 AM	Analysis bath temp.:	77.397 K
Report time:	01/09/2016 9:59:02 AM	Thermal correction:	No
Sample mass:	0.0797 g	Warm free space:	16.6669 cm³ Measured
Cold free space:	59.7874 cm³	Equilibration interval:	10 s
Low pressure dose:	None	Sample density:	1.000 g/cm³
Automatic degas:	No		

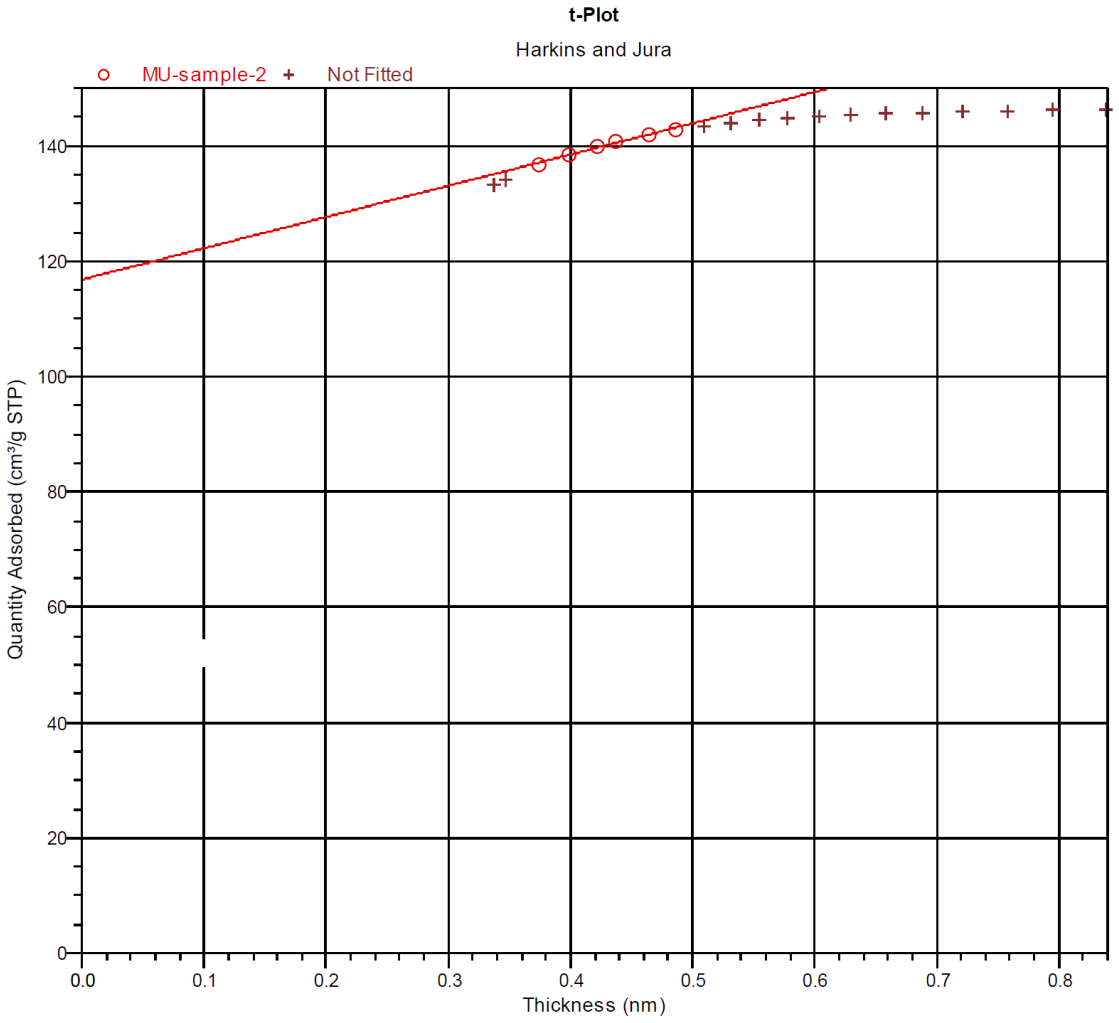

Sample: MU-sample-2
Operator:
File: C:\3Flex\data\Yong Yang data\000-326-MU-sample-2.SMP

Started: 31/08/2016 10:12:37 AM
Completed: 01/09/2016 12:42:16 AM
Report time: 01/09/2016 9:59:02 AM
Sample mass: 0.0797 g
Cold free space: 59.7874 cm³
Low pressure dose: None
Automatic degas: No

Analysis adsorptive: N2
Analysis bath temp.: 77.397 K
Thermal correction: No
Warm free space: 16.6669 cm³ Measured
Equilibration interval: 10 s
Sample density: 1.000 g/cm³

BJH Adsorption Pore Distribution Report

Faas Correction
Kruk-Jaroniec-Sayari
$t = [60.65 / (0.03071 - \log(p/p^\circ))] ^ {0.3968}$

Width range: 1.7000 nm to 300.0000 nm
Adsorbate property factor: 0.95300 nm
Density conversion factor: 0.0015500
Fraction of pores open at both ends: 0.00

Pore Width Range (nm)	Average Width (nm)	Incremental Pore Volume (cm³/g)	Cumulative Pore Volume (cm³/g)	Incremental Pore Area (m²/g)	Cumulative Pore Area (m²/g)
161.6 - 44.8	52.4	0.008586	0.008586	0.655	0.655
44.8 - 26.4	30.9	0.003151	0.011736	0.408	1.063
26.4 - 18.5	21.0	0.002557	0.014293	0.488	1.551
18.5 - 14.5	16.0	0.001992	0.016286	0.499	2.050
14.5 - 11.9	13.0	0.001565	0.017851	0.483	2.534
11.9 - 10.2	10.9	0.001237	0.019088	0.454	2.988
10.2 - 9.8	10.0	0.000173	0.019261	0.069	3.057
9.8 - 9.5	9.6	0.000185	0.019446	0.077	3.134
9.5 - 8.8	9.1	0.000400	0.019846	0.175	3.310
8.8 - 8.3	8.5	0.000323	0.020169	0.151	3.461
8.3 - 7.8	8.0	0.000363	0.020532	0.181	3.642
7.8 - 7.0	7.3	0.000619	0.021150	0.338	3.980
7.0 - 6.3	6.6	0.000389	0.021540	0.237	4.216
6.3 - 5.7	6.0	0.000247	0.021786	0.165	4.381
5.7 - 5.2	5.5	0.000152	0.021938	0.111	4.492
5.2 - 4.8	5.0	0.000218	0.022156	0.174	4.666
4.8 - 4.5	4.6	0.000215	0.022371	0.186	4.852
4.5 - 4.1	4.3	0.000386	0.022757	0.360	5.212
4.1 - 3.9	4.0	0.000584	0.023341	0.586	5.798
3.9 - 3.6	3.7	0.000969	0.024310	1.044	6.842
3.6 - 3.4	3.5	0.001427	0.025737	1.647	8.488
3.4 - 3.1	3.2	0.001575	0.027312	1.944	10.432
3.1 - 2.9	3.0	0.002089	0.029401	2.757	13.189
2.9 - 2.7	2.8	0.002545	0.031945	3.592	16.780
2.7 - 2.6	2.6	0.003338	0.035284	5.047	21.827
2.6 - 2.3	2.4	0.005096	0.040380	8.357	30.184
2.3 - 2.2	2.3	0.004164	0.044544	7.309	37.493
2.2 - 2.1	2.1	0.006660	0.051204	12.516	50.009
2.1 - 1.9	2.0	0.008948	0.060152	18.322	68.331

Sample: MU-sample-2
Operator:
File: C:\3Flex\data\Yong Yang data\000-326-MU-sample-2.SMP

Started:	31/08/2016 10:12:37 AM	Analysis adsorptive:	N2
Completed:	01/09/2016 12:42:16 AM	Analysis bath temp.:	77.397 K
Report time:	01/09/2016 9:59:02 AM	Thermal correction:	No
Sample mass:	0.0797 g	Warm free space:	16.6669 cm³ Measured
Cold free space:	59.7874 cm³	Equilibration interval:	10 s
Low pressure dose:	None	Sample density:	1.000 g/cm³
Automatic degas:	No		

BJH Adsorption Cumulative Pore Volume (Larger)

Kruk-Jaroniec-Sayari : Faas Correction

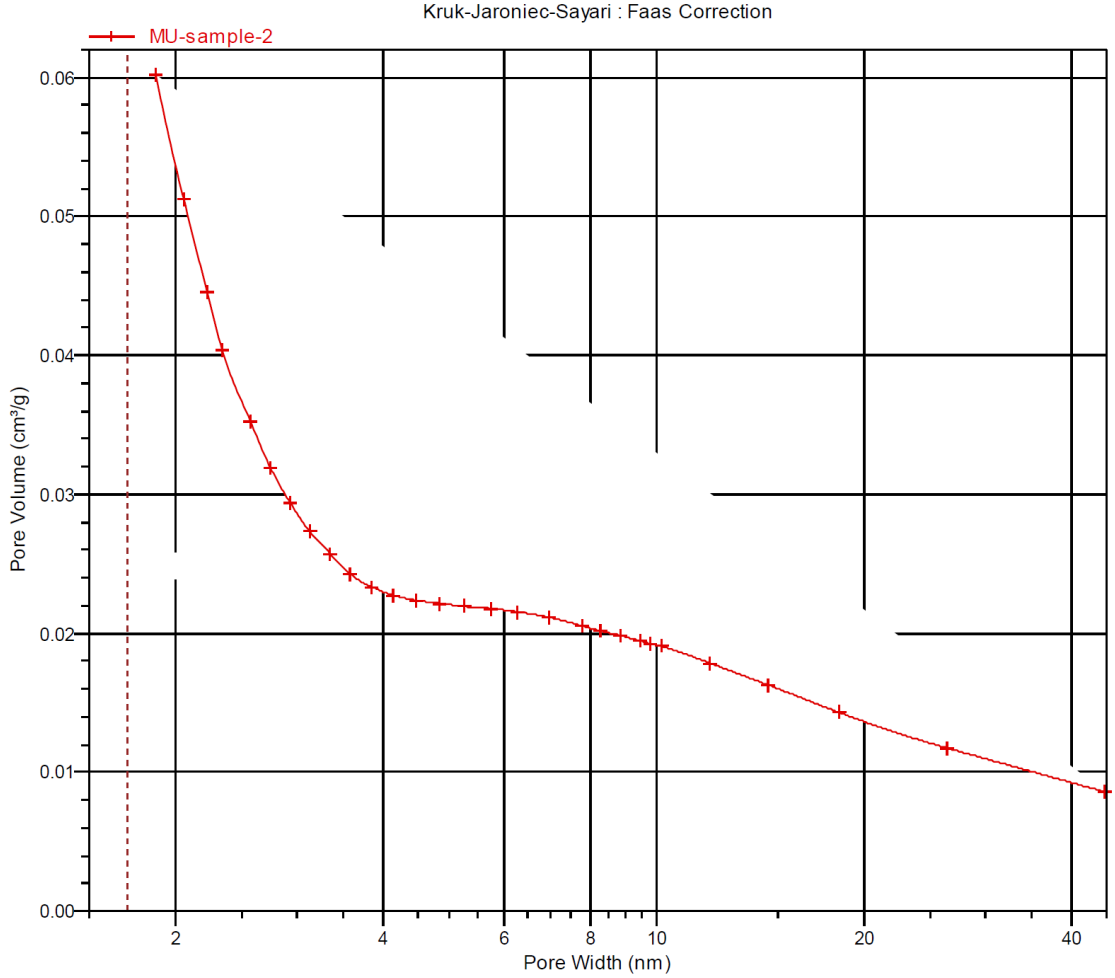

Sample: MU-sample-2
Operator:
File: C:\3Flex\data\Yong Yang data\000-326-MU-sample-2.SMP

Started:	31/08/2016 10:12:37 AM	Analysis adsorptive:	N2
Completed:	01/09/2016 12:42:16 AM	Analysis bath temp.:	77.397 K
Report time:	01/09/2016 9:59:02 AM	Thermal correction:	No
Sample mass:	0.0797 g	Warm free space:	16.6669 cm³ Measured
Cold free space:	59.7874 cm³	Equilibration interval:	10 s
Low pressure dose:	None	Sample density:	1.000 g/cm³
Automatic degas:	No		

BJH Desorption dV/dw Pore Volume

Kruk-Jaroniec-Sayari : Faas Correction

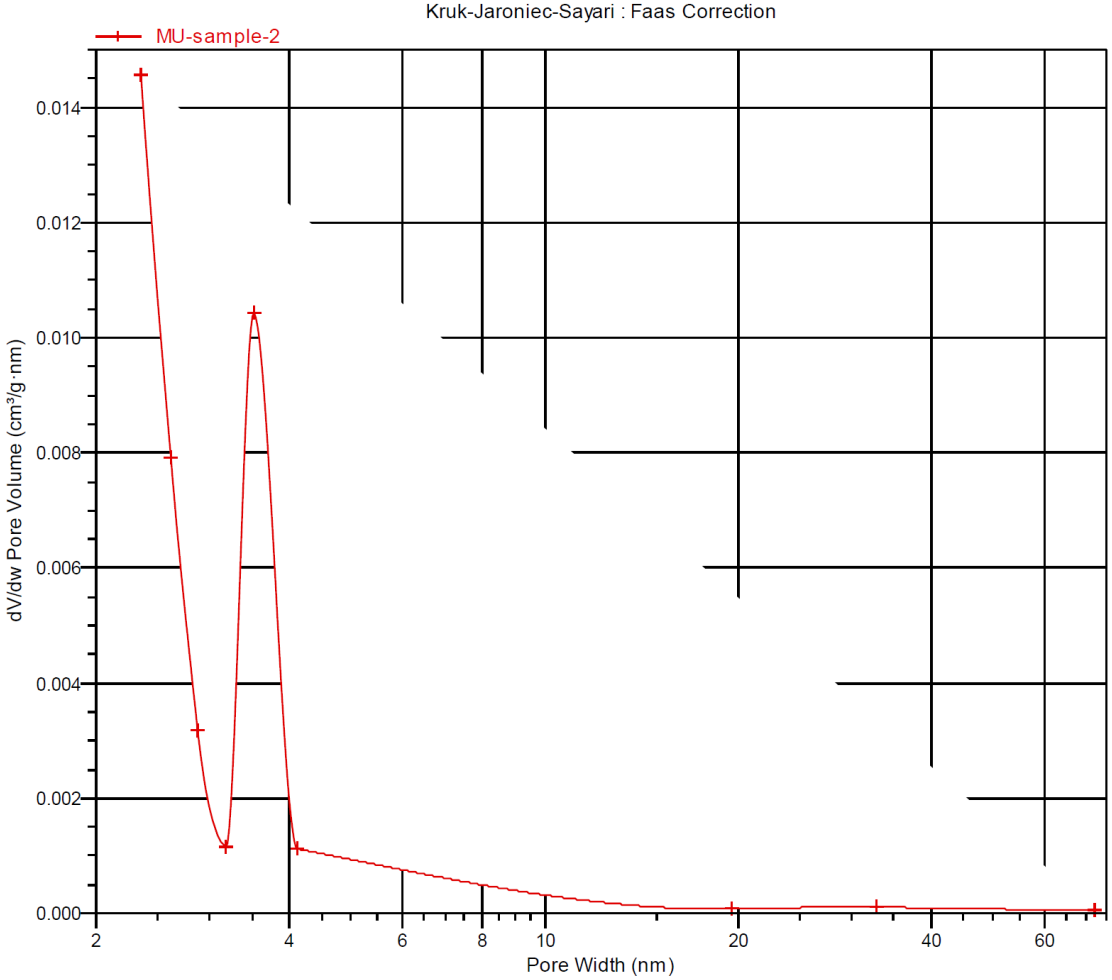

Appendix B

BET surface area and porosity analysis report of the pure CO_2 activated CBPP fly ash at 850°C (CAC) (Zhang et al., 2017)

CCRI University of Ottawa

3Flex 3.01 | 3Flex Version 3.01 Serial # 541 Unit 1 Port 1 | Page 1

Sample: MU-sample-1
Operator:
File: C:\3Flex\data\Yong Yang data\000-325-MU-sample-1.SMP

Started:	31/08/2016 10:12:37 AM	Analysis adsorptive:	N2
Completed:	01/09/2016 12:42:16 AM	Analysis bath temp.:	77.377 K
Report time:	01/09/2016 9:57:09 AM	Thermal correction:	No
Sample mass:	0.0783 g	Warm free space:	17.1518 cm³ Measured
Cold free space:	61.5803 cm³	Equilibration interval:	10 s
Low pressure dose:	None	Sample density:	1.000 g/cm³
Automatic degas:	No		

Summary Report

Surface Area

Single point surface area at p/p° = 0.300000000:	756.1617 m²/g
BET Surface Area:	847.2587 m²/g
t-Plot Micropore Area:	619.4937 m²/g
t-Plot external surface area:	227.7650 m²/g
BJH Adsorption cumulative surface area of pores between 1.7000 nm and 300.0000 nm width:	197.099 m²/g
BJH Desorption cumulative surface area of pores between 1.7000 nm and 300.0000 nm width:	142.9051 m²/g

Pore Volume

t-Plot micropore volume:	0.278697 cm³/g
BJH Adsorption cumulative volume of pores between 1.7000 nm and 300.0000 nm width:	0.215505 cm³/g
BJH Desorption cumulative volume of pores between 1.7000 nm and 300.0000 nm width:	0.186968 cm³/g

Pore Size

BJH Adsorption average pore width (4V/A):	4.3735 nm
BJH Desorption average pore width (4V/A):	5.2333 nm

Sample: MU-sample-1
Operator:
File: C:\3Flex\data\Yong Yang data\000-325-MU-sample-1.SMP

Started: 31/08/2016 10:12:37 AM
Completed: 01/09/2016 12:42:16 AM
Report time: 01/09/2016 9:57:09 AM
Sample mass: 0.0783 g
Cold free space: 61.5803 cm³
Low pressure dose: None
Automatic degas: No

Analysis adsorptive: N2
Analysis bath temp.: 77.377 K
Thermal correction: No
Warm free space: 17.1518 cm³ Measured
Equilibration interval: 10 s
Sample density: 1.000 g/cm³

Isotherm Tabular Report

Relative Pressure (p/p°)	Absolute Pressure (mmHg)	Quantity Adsorbed (cm³/g STP)	Elapsed Time (h:min)	Saturation Pressure (mmHg)
			01:04	755.715210
0.002853270	2.173656	183.9589	04:23	761.812317
0.005805263	4.430001	193.6831	04:36	763.100830
0.021836203	16.652920	211.4856	04:47	762.628906
0.032162341	24.539495	216.7341	04:53	762.988464
0.042912548	32.746700	220.7136	04:58	763.103149
0.061327646	46.729656	225.6686	05:04	761.967224
0.073981690	56.453331	228.3956	05:08	763.071655
0.108227429	82.679375	234.1632	05:13	763.941040
0.144680470	110.314575	238.8225	05:17	762.470398
0.179704454	136.866440	242.5605	05:21	761.619629
0.203758315	155.271484	244.8577	05:25	762.037537
0.245446167	187.027298	248.3693	05:28	761.989075
0.279612647	213.078644	250.9664	05:31	762.049377
0.314283085	239.513367	253.3514	05:36	762.094360
0.347047902	264.267975	255.4514	05:39	761.474060
0.379510806	289.409882	257.4207	05:42	762.586670
0.413647464	315.649017	259.3439	05:47	763.087036
0.448185672	341.710938	261.1817	05:50	762.431641
0.480748189	367.049805	262.8412	05:53	763.497009
0.514210600	392.793030	264.4838	05:58	763.875793
0.549634456	419.566803	266.1120	06:01	763.356079
0.583566191	445.140045	267.6359	06:04	762.792725
0.618156015	470.834503	269.2112	06:07	761.675842
0.652735752	496.200165	270.7693	06:12	760.185364
0.683128134	519.772034	272.3278	06:15	760.870483
0.716843830	546.045593	274.1682	06:18	761.735779
0.734856680	559.664856	275.1790	06:21	761.597290
0.751895907	573.061890	276.1241	06:26	762.155884
0.768466627	585.702759	277.0729	06:29	762.170715
0.777371381	592.391296	277.5921	06:32	762.044128
0.786724682	598.810181	278.0577	06:35	761.143250
0.818280308	622.763855	280.3083	06:38	761.064209
0.850679066	649.224670	283.2351	06:42	763.184021
0.886639268	676.587585	287.1024	06:46	763.092285
0.921384981	702.105591	292.5147	06:50	762.011108
0.951571227	725.475952	302.0846	06:54	762.397949
0.984673751	749.979431	320.3032	07:00	761.652710

Sample: MU-sample-1
Operator:
File: C:\3Flex\data\Yong Yang data\000-325-MU-sample-1.SMP

Started:	31/08/2016 10:12:37 AM	Analysis adsorptive:	N2
Completed:	01/09/2016 12:42:16 AM	Analysis bath temp.:	77.377 K
Report time:	01/09/2016 9:57:09 AM	Thermal correction:	No
Sample mass:	0.0783 g	Warm free space:	17.1518 cm³ Measured
Cold free space:	61.5803 cm³	Equilibration interval:	10 s
Low pressure dose:	None	Sample density:	1.000 g/cm³
Automatic degas:	No		

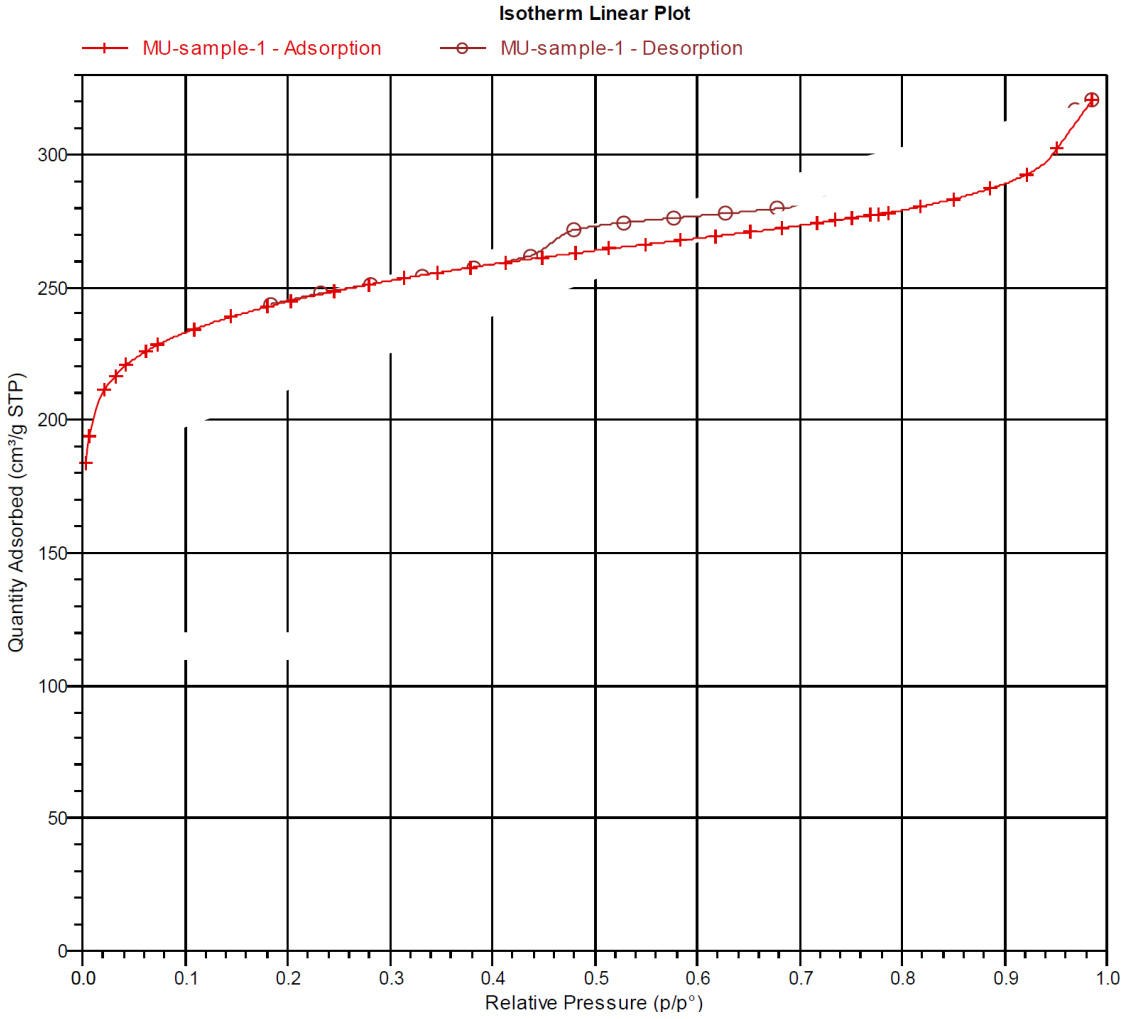

Sample: MU-sample-1
Operator:
File: C:\3Flex\data\Yong Yang data\000-325-MU-sample-1.SMP

Started:	31/08/2016 10:12:37 AM	Analysis adsorptive:	N2
Completed:	01/09/2016 12:42:16 AM	Analysis bath temp.:	77.377 K
Report time:	01/09/2016 9:57:09 AM	Thermal correction:	No
Sample mass:	0.0783 g	Warm free space:	17.1518 cm³ Measured
Cold free space:	61.5803 cm³	Equilibration interval:	10 s
Low pressure dose:	None	Sample density:	1.000 g/cm³
Automatic degas:	No		

BET Report

BET surface area:	847.2587 ± 13.5370 m²/g
Slope:	0.005171 ± 0.000081 g/cm³ STP
Y-intercept:	-0.000034 ± 0.000010 g/cm³ STP
C:	-153.312025
Qm:	194.6567 cm³/g STP
Correlation coefficient:	0.9996278
Molecular cross-sectional area:	0.1620 nm²

Relative Pressure (p/p°)	Quantity Adsorbed (cm³/g STP)	1/[Q(p°/p - 1)]
0.061327646	225.6686	0.000290
0.073981690	228.3956	0.000350
0.108227429	234.1632	0.000518
0.144680470	238.8225	0.000708
0.179704454	242.5605	0.000903

Sample: MU-sample-1
Operator:
File: C:\3Flex\data\Yong Yang data\000-325-MU-sample-1.SMP

Started:	31/08/2016 10:12:37 AM	Analysis adsorptive:	N2
Completed:	01/09/2016 12:42:16 AM	Analysis bath temp.:	77.377 K
Report time:	01/09/2016 9:57:09 AM	Thermal correction:	No
Sample mass:	0.0783 g	Warm free space:	17.1518 cm³ Measured
Cold free space:	61.5803 cm³	Equilibration interval:	10 s
Low pressure dose:	None	Sample density:	1.000 g/cm³
Automatic degas:	No		

BET Surface Area Plot

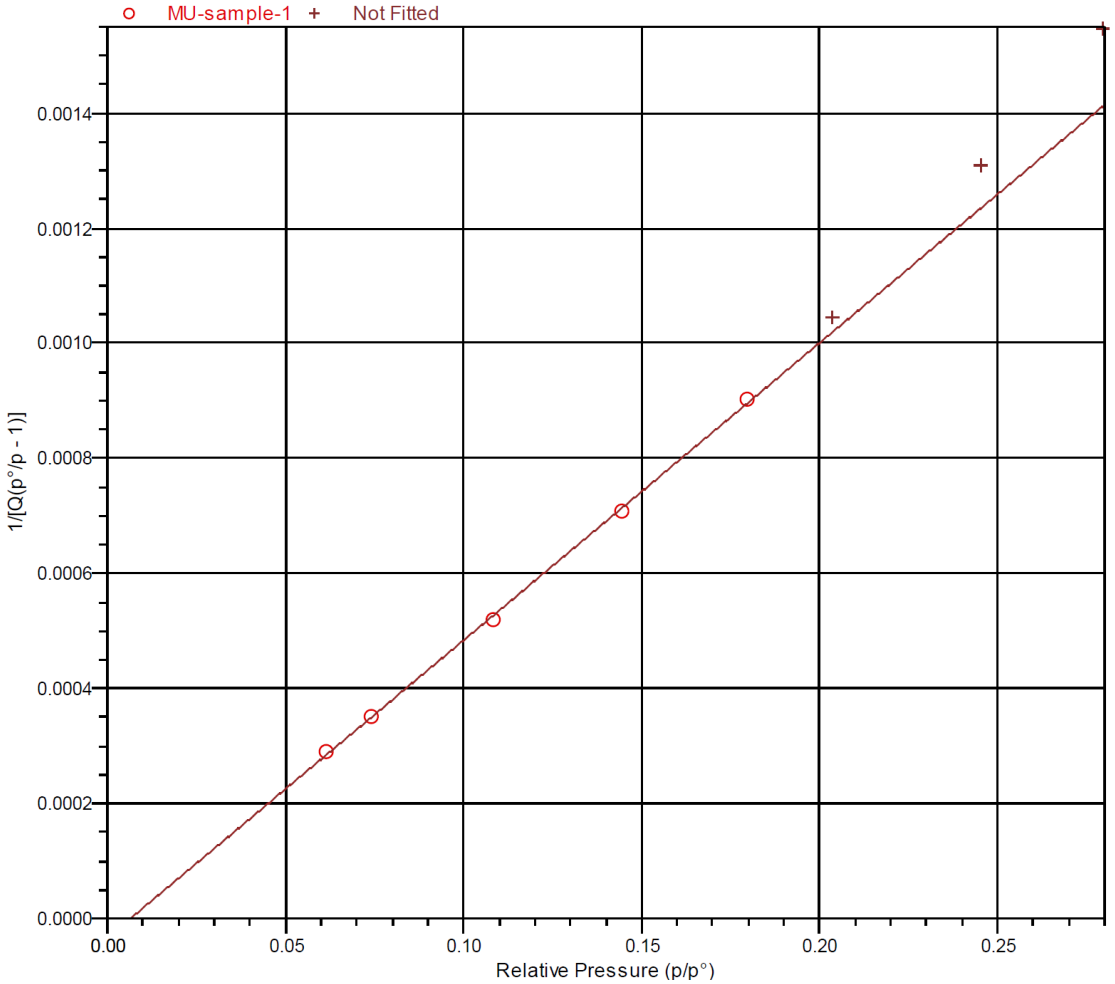

Sample: MU-sample-1
Operator:
File: C:\3Flex\data\Yong Yang data\000-325-MU-sample-1.SMP

Started:	31/08/2016 10:12:37 AM	Analysis adsorptive:	N2
Completed:	01/09/2016 12:42:16 AM	Analysis bath temp.:	77.377 K
Report time:	01/09/2016 9:57:09 AM	Thermal correction:	No
Sample mass:	0.0783 g	Warm free space:	17.1518 cm³ Measured
Cold free space:	61.5803 cm³	Equilibration interval:	10 s
Low pressure dose:	None	Sample density:	1.000 g/cm³
Automatic degas:	No		

t-Plot Report

Micropore volume:	0.278697 cm³/g
Micropore area:	619.4937 m²/g
External surface area:	227.7650 m²/g
Slope:	146.958047 ± 5.903053 cm³/g·nm STP
Y-intercept:	179.820610 ± 2.559442 cm³/g STP
Correlation coefficient:	0.996789
Surface area correction factor:	1.000
Density conversion factor:	0.0015499
Total surface area (BET):	847.2587 m²/g
Thickness range:	0.35000 nm to 0.50000 nm
Thickness equation:	Harkins and Jura

Thickness Curve

t = [13.99 / (0.034 - log(p/p°))] ^ 0.5

t-Plot Report - Data

Relative Pressure (p/p°)	Statistical Thickness (nm)	Quantity Adsorbed (cm³/g STP)	Fitted
0.061327646	0.33503	225.6686	
0.073981690	0.34655	228.3956	
0.108227429	0.37410	234.1632	*
0.144680470	0.40018	238.8225	*
0.179704454	0.42366	242.5605	*
0.203758315	0.43931	244.8577	*
0.245446167	0.46607	248.3693	*
0.279612647	0.48801	250.9664	*
0.314283085	0.51057	253.3514	
0.347047902	0.53237	255.4514	
0.379510806	0.55464	257.4207	
0.413647464	0.57896	259.3439	
0.448185672	0.60474	261.1817	
0.480748189	0.63036	262.8412	
0.514210600	0.65827	264.4838	
0.549634456	0.68991	266.1120	
0.583566191	0.72263	267.6359	
0.618156015	0.75892	269.2112	
0.652735752	0.79878	270.7693	
0.683128134	0.83741	272.3278	

Sample: MU-sample-1
Operator:
File: C:\3Flex\data\Yong Yang data\000-325-MU-sample-1.SMP

Started:	31/08/2016 10:12:37 AM	Analysis adsorptive:	N2
Completed:	01/09/2016 12:42:16 AM	Analysis bath temp.:	77.377 K
Report time:	01/09/2016 9:57:09 AM	Thermal correction:	No
Sample mass:	0.0783 g	Warm free space:	17.1518 cm³ Measured
Cold free space:	61.5803 cm³	Equilibration interval:	10 s
Low pressure dose:	None	Sample density:	1.000 g/cm³
Automatic degas:	No		

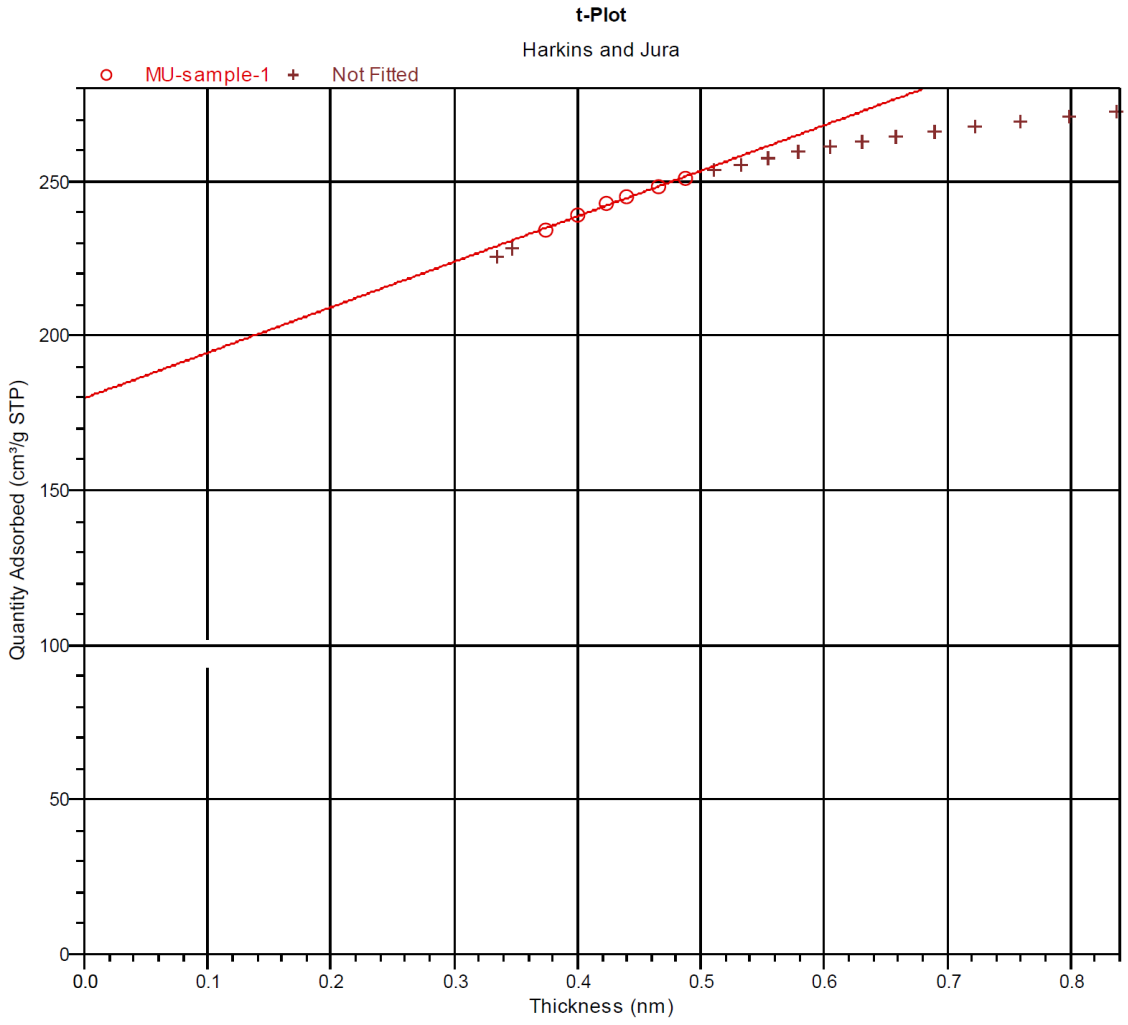

Sample: MU-sample-1
Operator:
File: C:\3Flex\data\Yong Yang data\000-325-MU-sample-1.SMP

Started:	31/08/2016 10:12:37 AM	Analysis adsorptive:	N2
Completed:	01/09/2016 12:42:16 AM	Analysis bath temp.:	77.377 K
Report time:	01/09/2016 9:57:09 AM	Thermal correction:	No
Sample mass:	0.0783 g	Warm free space:	17.1518 cm³ Measured
Cold free space:	61.5803 cm³	Equilibration interval:	10 s
Low pressure dose:	None	Sample density:	1.000 g/cm³
Automatic degas:	No		

BJH Adsorption Pore Distribution Report

Faas Correction
Kruk-Jaroniec-Sayari
t = [60.65 / (0.03071 - log(p/p°))] ^ 0.3968

Width range: 1.7000 nm to 300.0000 nm
Adsorbate property factor: 0.95300 nm
Density conversion factor: 0.0015499
Fraction of pores open at both ends: 0.00

Pore Width Range (nm)	Average Width (nm)	Incremental Pore Volume (cm³/g)	Cumulative Pore Volume (cm³/g)	Incremental Pore Area (m²/g)	Cumulative Pore Area (m²/g)
127.2 - 41.7	49.3	0.032419	0.032419	2.631	2.631
41.7 - 26.3	30.4	0.017796	0.050216	2.339	4.970
26.3 - 18.6	21.0	0.010312	0.060528	1.962	6.932
18.6 - 14.3	15.8	0.007571	0.068099	1.911	8.843
14.3 - 11.9	12.8	0.005928	0.074027	1.846	10.689
11.9 - 10.2	10.9	0.004602	0.078629	1.689	12.378
10.2 - 9.8	10.0	0.000890	0.079519	0.357	12.734
9.8 - 9.4	9.6	0.001061	0.080580	0.442	13.176
9.4 - 8.8	9.1	0.001974	0.082554	0.867	14.044
8.8 - 8.3	8.5	0.002003	0.084557	0.940	14.983
8.3 - 7.8	8.0	0.002208	0.086766	1.105	16.088
7.8 - 6.9	7.3	0.004147	0.090912	2.272	18.360
6.9 - 6.3	6.6	0.003590	0.094502	2.172	20.532
6.3 - 5.8	6.0	0.003573	0.098075	2.375	22.907
5.8 - 5.3	5.5	0.003782	0.101857	2.758	25.665
5.3 - 4.8	5.0	0.003774	0.105631	2.997	28.662
4.8 - 4.5	4.6	0.004209	0.109840	3.628	32.290
4.5 - 4.2	4.3	0.004486	0.114326	4.177	36.467
4.2 - 3.9	4.0	0.004704	0.119030	4.704	41.172
3.9 - 3.6	3.7	0.005405	0.124435	5.801	46.973
3.6 - 3.4	3.5	0.005882	0.130317	6.771	53.743
3.4 - 3.2	3.3	0.006281	0.136598	7.729	61.472
3.2 - 3.0	3.0	0.006896	0.143493	9.055	70.527
3.0 - 2.8	2.8	0.008091	0.151585	11.367	81.894
2.8 - 2.6	2.7	0.009180	0.160764	13.819	95.713
2.6 - 2.4	2.5	0.012844	0.173608	20.940	116.653
2.4 - 2.2	2.3	0.008701	0.182309	15.172	131.826
2.2 - 2.1	2.1	0.014504	0.196813	27.099	158.925
2.1 - 1.9	2.0	0.018692	0.215505	38.175	197.099

Sample: MU-sample-1
Operator:
File: C:\3Flex\data\Yong Yang data\000-325-MU-sample-1.SMP

Started:	31/08/2016 10:12:37 AM	Analysis adsorptive:	N2
Completed:	01/09/2016 12:42:16 AM	Analysis bath temp.:	77.377 K
Report time:	01/09/2016 9:57:09 AM	Thermal correction:	No
Sample mass:	0.0783 g	Warm free space:	17.1518 cm³ Measured
Cold free space:	61.5803 cm³	Equilibration interval:	10 s
Low pressure dose:	None	Sample density:	1.000 g/cm³
Automatic degas:	No		

BJH Desorption dV/dw Pore Volume

Kruk-Jaroniec-Sayari : Faas Correction

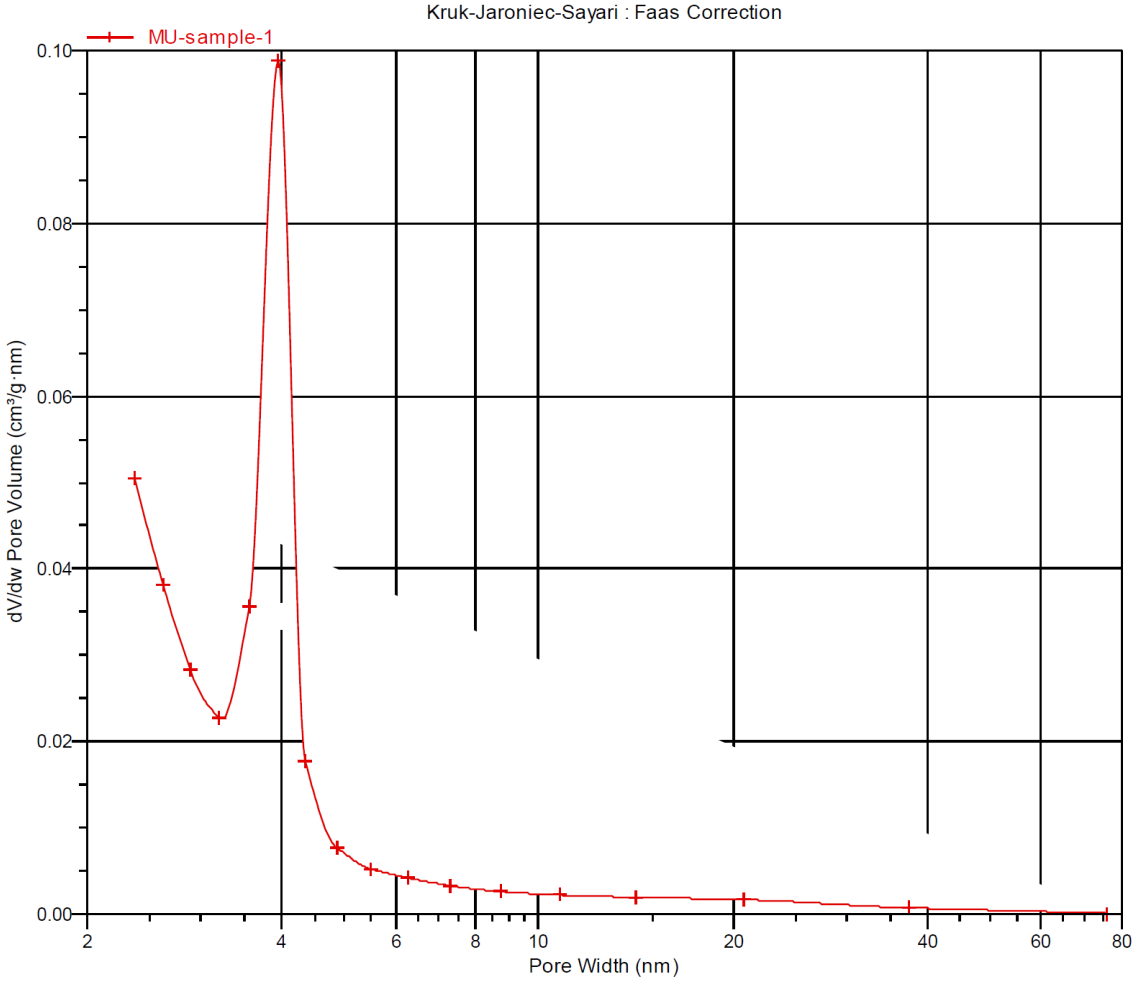

Appendix C

BET surface area and porosity analysis report of the mixture of CO_2 and steam activated CBPP fly ash at 850°C (CSAC)

CCRI University of Ottawa

Sample: UM-6
Operator:
File: C:\3Flex\data\Yong Yang data\000-717-UM-6.SMP

Started:	16/06/2017 3:51:00 PM	Analysis adsorptive:	N2
Completed:	17/06/2017 7:56:54 AM	Analysis bath temp.:	77.297 K
Report time:	19/06/2017 1:24:15 PM	Thermal correction:	No
Sample mass:	0.0720 g	Warm free space:	17.0137 cm³ Measured
Cold free space:	58.9353 cm³	Equilibration interval:	10 s
Low pressure dose:	None	Sample density:	1.000 g/cm³
Automatic degas:	No		

Summary Report

Surface Area

Single point surface area at p/p° = 0.300000000:	1,039.6474 m²/g
BET Surface Area:	1,146.2469 m²/g
t-Plot Micropore Area:	648.8924 m²/g
t-Plot external surface area:	497.3544 m²/g
BJH Adsorption cumulative surface area of pores between 1.7000 nm and 300.0000 nm width:	469.624 m²/g
BJH Desorption cumulative surface area of pores between 1.7000 nm and 300.0000 nm width:	394.1650 m²/g

Pore Volume

t-Plot micropore volume:	0.288730 cm³/g
BJH Adsorption cumulative volume of pores between 1.7000 nm and 300.0000 nm width:	0.765571 cm³/g
BJH Desorption cumulative volume of pores between 1.7000 nm and 300.0000 nm width:	0.730644 cm³/g

Pore Size

BJH Adsorption average pore width (4V/A):	6.5207 nm
BJH Desorption average pore width (4V/A):	7.4146 nm

CCRI University of Ottawa

3Flex 3.01

3Flex Version 3.01
Serial # 541 Unit 1 Port 3

Sample: UM-6
Operator:
File: C:\3Flex\data\Yong Yang data\000-717-UM-6.SMP

Started: 16/06/2017 3:51:00 PM
Completed: 17/06/2017 7:56:54 AM
Report time: 19/06/2017 1:24:15 PM
Sample mass: 0.0720 g
Cold free space: 58.9353 cm³
Low pressure dose: None
Automatic degas: No

Analysis adsorptive: N2
Analysis bath temp.: 77.297 K
Thermal correction: No
Warm free space: 17.0137 cm³ Measured
Equilibration interval: 10 s
Sample density: 1.000 g/cm³

Isotherm Tabular Report

Relative Pressure (p/p°)	Absolute Pressure (mmHg)	Quantity Adsorbed (cm³/g STP)	Elapsed Time (h:min)	Saturation Pressure (mmHg)
			01:16	755.214478
0.001426008	1.076703	204.4907	09:21	755.046753
0.002853986	2.155049	219.4280	09:43	755.101501
0.005875093	4.436430	235.0276	09:57	755.125000
0.029890923	22.568089	271.6550	10:05	755.014771
0.040301565	30.426710	278.9887	10:13	754.975891
0.058297420	44.009674	288.3431	10:19	754.916321
0.072820727	54.977222	294.2970	10:25	754.966675
0.108439960	81.864975	305.7726	10:31	754.933655
0.143668005	108.447807	314.8699	10:37	754.850098
0.178478134	134.712418	322.6693	10:43	754.783875
0.203304374	153.459152	327.8222	10:47	754.824646
0.245800192	185.518295	336.1317	10:52	754.752441
0.281048748	212.132813	342.7082	10:58	754.790100
0.315616731	238.257614	349.0118	11:04	754.895386
0.347769419	262.510681	354.7424	11:10	754.841187
0.377845754	285.211761	360.0619	11:16	754.836487
0.411333885	310.499390	366.1059	11:20	754.859741
0.445648102	336.393188	372.3519	11:25	754.840393
0.480646324	362.845642	378.9594	11:31	754.911926
0.514858600	388.642761	385.4141	11:36	754.853394
0.548330399	413.943634	392.1186	11:42	754.916443
0.582389223	439.582153	399.5012	11:47	754.791016
0.616201140	465.157318	407.6490	11:52	754.879028
0.650177236	490.727539	416.5891	11:57	754.759644
0.683872585	516.143066	426.5576	12:04	754.735718
0.717308596	541.368042	437.7015	12:10	754.721252
0.735530236	555.039673	444.3767	12:15	754.611633
0.752103507	567.577087	450.8738	12:20	754.652893
0.767658233	579.309509	457.4458	12:25	754.645081
0.776863891	586.276428	461.5210	12:30	754.670715
0.785420106	592.658386	465.2798	12:34	754.575012
0.818233755	617.239258	481.7902	12:42	754.355652
0.850610133	641.653320	500.9620	12:50	754.344788
0.883958498	666.846497	524.3551	12:58	754.386658
0.916867991	691.646118	553.2194	13:07	754.357361
0.953903775	719.696411	600.0544	13:22	754.474854
0.988995743	746.424194	667.7265	13:39	754.729431

CCRI University of Ottawa

3Flex 3.01

3Flex Version 3.01
Serial # 541 Unit 1 Port 3

Sample: UM-6
Operator:
File: C:\3Flex\data\Yong Yang data\000-717-UM-6.SMP

Started: 16/06/2017 3:51:00 PM
Completed: 17/06/2017 7:56:54 AM
Report time: 19/06/2017 1:24:15 PM
Sample mass: 0.0720 g
Cold free space: 58.9353 cm³
Low pressure dose: None
Automatic degas: No

Analysis adsorptive: N2
Analysis bath temp.: 77.297 K
Thermal correction: No
Warm free space: 17.0137 cm³ Measured
Equilibration interval: 10 s
Sample density: 1.000 g/cm³

Isotherm Tabular Report

Relative Pressure (p/p°)	Absolute Pressure (mmHg)	Quantity Adsorbed (cm³/g STP)	Elapsed Time (h:min)	Saturation Pressure (mmHg)
0.971214928	733.059204	654.2115	13:46	754.785767
0.936876766	707.171326	607.5987	14:00	754.817871
0.891353358	672.835449	557.1761	14:13	754.847046
0.834359017	629.769287	516.1848	14:26	754.794128
0.794264431	599.562073	492.8368	14:35	754.864563
0.745251238	562.637756	468.7174	14:43	754.963867
0.693872579	523.886841	446.9121	14:51	755.018799
0.642515998	485.189423	427.9898	14:59	755.139832
0.590593039	445.919373	411.9238	15:06	755.036621
0.538958284	406.999756	398.3679	15:12	755.160034
0.487652379	368.214722	386.3840	15:19	755.076233
0.442070895	333.810852	370.1778	15:26	755.107056
0.388337542	293.235138	358.4216	15:32	755.103760
0.336388705	254.025314	349.5138	15:37	755.154114
0.286574086	216.400970	341.0384	15:43	755.130981
0.237091291	179.050507	332.3947	15:48	755.196472
0.187958664	141.942749	323.3093	15:53	755.180664

CCRI University of Ottawa

3Flex 3.01

3Flex Version 3.01
Serial # 541 Unit 1 Port 3

Sample: UM-6
Operator:
File: C:\3Flex\data\Yong Yang data\000-717-UM-6.SMP

Started:	16/06/2017 3:51:00 PM	Analysis adsorptive:	N2
Completed:	17/06/2017 7:56:54 AM	Analysis bath temp.:	77.297 K
Report time:	19/06/2017 1:24:15 PM	Thermal correction:	No
Sample mass:	0.0720 g	Warm free space:	17.0137 cm³ Measured
Cold free space:	58.9353 cm³	Equilibration interval:	10 s
Low pressure dose:	None	Sample density:	1.000 g/cm³
Automatic degas:	No		

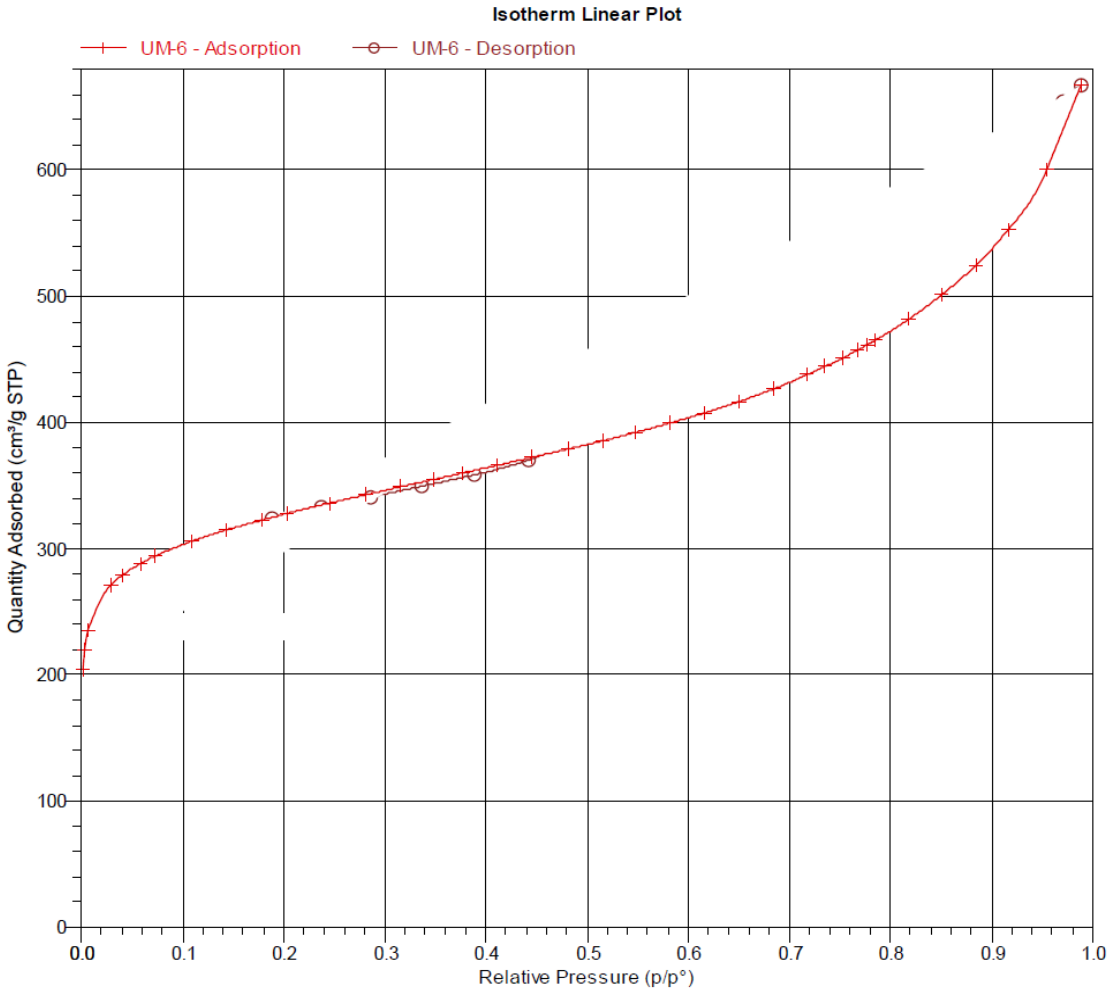

CCRI University of Ottawa

3Flex 3.01

3Flex Version 3.01
Serial # 541 Unit 1 Port 3

Sample: UM-6
Operator:
File: C:\3Flex\data\Yong Yang data\000-717-UM-6.SMP

Started:	16/06/2017 3:51:00 PM	Analysis adsorptive:	N2
Completed:	17/06/2017 7:56:54 AM	Analysis bath temp.:	77.297 K
Report time:	19/06/2017 1:24:15 PM	Thermal correction:	No
Sample mass:	0.0720 g	Warm free space:	17.0137 cm³ Measured
Cold free space:	58.9353 cm³	Equilibration interval:	10 s
Low pressure dose:	None	Sample density:	1.000 g/cm³
Automatic degas:	No		

BET Report

BET surface area:	1146.2469 ± 14.0576 m²/g
Slope:	0.003808 ± 0.000046 g/cm³ STP
Y-intercept:	-0.000011 ± 0.000006 g/cm³ STP
C:	-355.160822
Qm:	263.3489 cm³/g STP
Correlation coefficient:	0.9997790
Molecular cross-sectional area:	0.1620 nm²

Relative Pressure (p/p°)	Quantity Adsorbed (cm³/g STP)	1/[Q(p°/p - 1)]
0.058297420	288.3431	0.000215
0.072820727	294.2970	0.000267
0.108439960	305.7726	0.000398
0.143668005	314.8699	0.000533
0.178478134	322.6693	0.000673

CCRI University of Ottawa

3Flex 3.01

3Flex Version 3.01
Serial # 541 Unit 1 Port 3

Sample: UM-6
Operator:
File: C:\3Flex\data\Yong Yang data\000-717-UM-6.SMP

Started:	16/06/2017 3:51:00 PM	Analysis adsorptive:	N2
Completed:	17/06/2017 7:56:54 AM	Analysis bath temp.:	77.297 K
Report time:	19/06/2017 1:24:15 PM	Thermal correction:	No
Sample mass:	0.0720 g	Warm free space:	17.0137 cm³ Measured
Cold free space:	58.9353 cm³	Equilibration interval:	10 s
Low pressure dose:	None	Sample density:	1.000 g/cm³
Automatic degas:	No		

BET Surface Area Plot

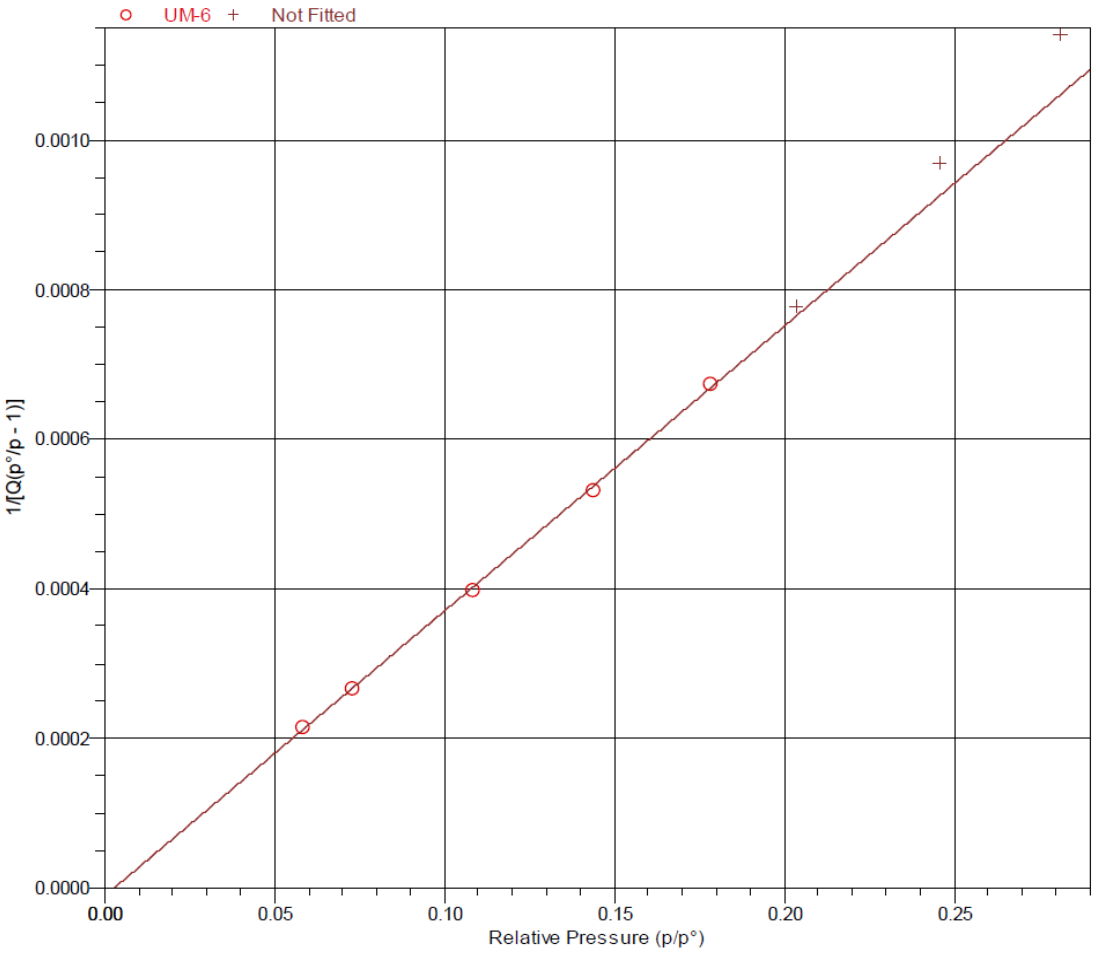

CCRI University of Ottawa

3Flex 3.01

3Flex Version 3.01
Serial # 541 Unit 1 Port 3

Sample: UM-6
Operator:
File: C:\3Flex\data\Yong Yang data\000-717-UM-6.SMP

Started:	16/06/2017 3:51:00 PM	Analysis adsorptive:	N2
Completed:	17/06/2017 7:56:54 AM	Analysis bath temp.:	77.297 K
Report time:	19/06/2017 1:24:15 PM	Thermal correction:	No
Sample mass:	0.0720 g	Warm free space:	17.0137 cm³ Measured
Cold free space:	58.9353 cm³	Equilibration interval:	10 s
Low pressure dose:	None	Sample density:	1.000 g/cm³
Automatic degas:	No		

t-Plot Report

Micropore volume:	0.288730 cm³/g
Micropore area:	648.8924 m²/g
External surface area:	497.3544 m²/g
Slope:	321.034558 ± 6.644752 cm³/g·nm STP
Y-intercept:	186.370675 ± 2.880695 cm³/g STP
Correlation coefficient:	0.999144
Surface area correction factor:	1.000
Density conversion factor:	0.0015492
Total surface area (BET):	1146.2469 m²/g
Thickness range:	0.35000 nm to 0.50000 nm
Thickness equation:	Harkins and Jura

Thickness Curve

$t = [\ 13.99 / (\ 0.034 - \log(p/p^\circ)\ )\ ]^{\wedge} 0.5$

t-Plot Report - Data

Relative Pressure (p/p°)	Statistical Thickness (nm)	Quantity Adsorbed (cm³/g STP)	Fitted
0.058297420	0.33212	288.3431	
0.072820727	0.34554	294.2970	
0.108439960	0.37425	305.7726	*
0.143668005	0.39948	314.8699	*
0.178478134	0.42285	322.6693	*
0.203304374	0.43902	327.8222	*
0.245800192	0.46630	336.1317	*
0.281048748	0.48893	342.7082	*
0.315616731	0.51144	349.0118	
0.347769419	0.53286	354.7424	
0.377845754	0.55348	360.0619	
0.411333885	0.57728	366.1059	
0.445648102	0.60280	372.3519	
0.480646324	0.63027	378.9594	
0.514858600	0.65883	385.4141	
0.548330399	0.68870	392.1186	
0.582389223	0.72145	399.5012	
0.616201140	0.75678	407.6490	
0.650177236	0.79569	416.5891	
0.683872585	0.83841	426.5576	

CCRI University of Ottawa

3Flex 3.01

3Flex Version 3.01
Serial # 541 Unit 1 Port 3

Sample: UM-6
Operator:
File: C:\3Flex\data\Yong Yang data\000-717-UM-6.SMP

Started:	16/06/2017 3:51:00 PM	Analysis adsorptive:	N2
Completed:	17/06/2017 7:56:54 AM	Analysis bath temp.:	77.297 K
Report time:	19/06/2017 1:24:15 PM	Thermal correction:	No
Sample mass:	0.0720 g	Warm free space:	17.0137 cm³ Measured
Cold free space:	58.9353 cm³	Equilibration interval:	10 s
Low pressure dose:	None	Sample density:	1.000 g/cm³
Automatic degas:	No		

t-Plot

Harkins and Jura

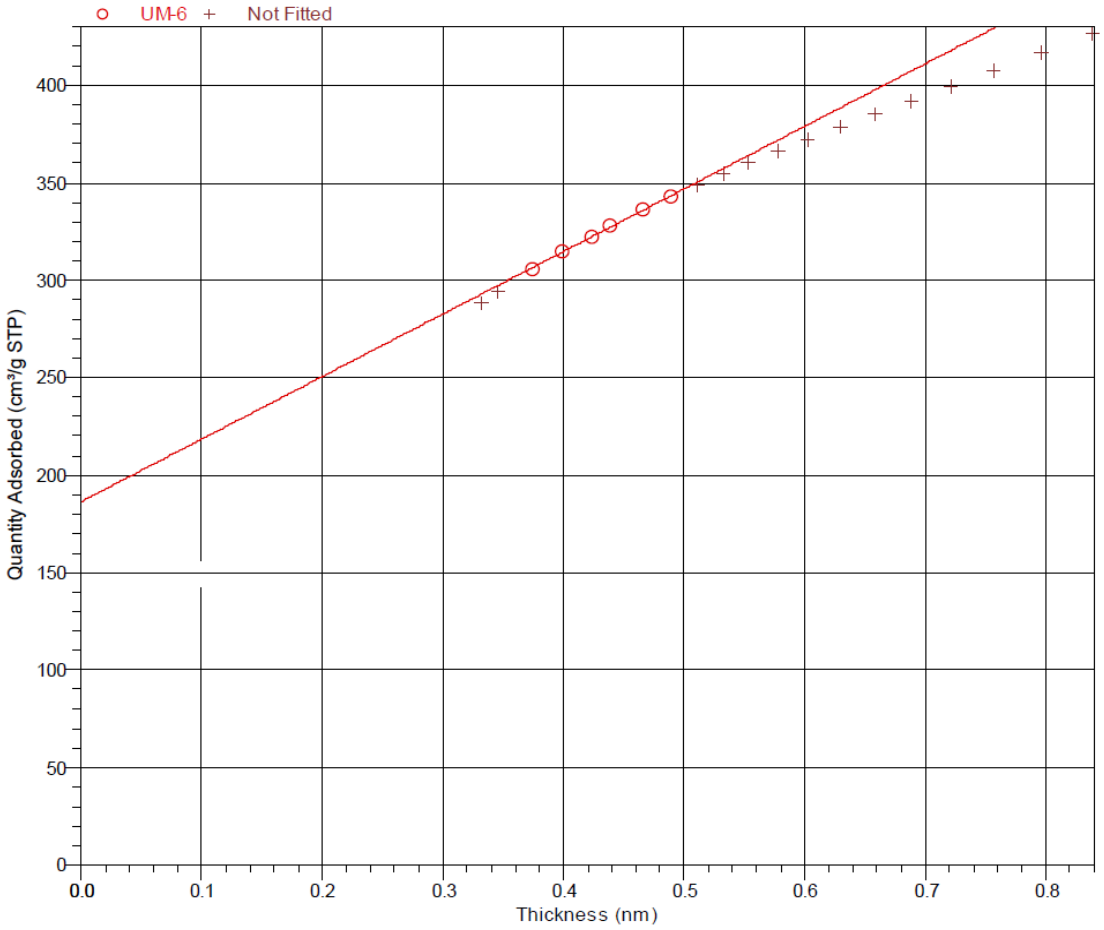

CCRI University of Ottawa

3Flex 3.01

3Flex Version 3.01
Serial # 541 Unit 1 Port 3

Sample: UM-6
Operator:
File: C:\3Flex\data\Yong Yang data\000-717-UM-6.SMP

Started:	16/06/2017 3:51:00 PM	Analysis adsorptive:	N2
Completed:	17/06/2017 7:56:54 AM	Analysis bath temp.:	77.297 K
Report time:	19/06/2017 1:24:15 PM	Thermal correction:	No
Sample mass:	0.0720 g	Warm free space:	17.0137 cm³ Measured
Cold free space:	58.9353 cm³	Equilibration interval:	10 s
Low pressure dose:	None	Sample density:	1.000 g/cm³
Automatic degas:	No		

BJH Desorption Pore Distribution Report

Faas Correction
Kruk-Jaroniec-Sayari
t = [60.65 / (0.03071 - log(p/p°))] ^ 0.3968

Width range: 1.7000 nm to 300.0000 nm
Adsorbate property factor: 0.95300 nm
Density conversion factor: 0.0015492
Fraction of pores open at both ends: 0.00

Pore Width Range (nm)	Average Width (nm)	Incremental Pore Volume (cm³/g)	Cumulative Pore Volume (cm³/g)	Incremental Pore Area (m²/g)	Cumulative Pore Area (m²/g)
176.1 - 68.8	82.3	0.022863	0.022863	1.111	1.111
68.8 - 32.4	38.5	0.085325	0.108187	8.866	9.977
32.4 - 19.3	22.5	0.099337	0.207525	17.633	27.610
19.3 - 13.0	14.8	0.085559	0.293084	23.087	50.697
13.0 - 10.6	11.5	0.050540	0.343623	17.596	68.293
10.6 - 8.6	9.4	0.054164	0.397787	23.171	91.464
8.6 - 7.2	7.7	0.050632	0.448419	26.144	117.608
7.2 - 6.2	6.6	0.044997	0.493416	27.359	144.967
6.2 - 5.4	5.7	0.038223	0.531639	26.857	171.824
5.4 - 4.7	5.0	0.031807	0.563446	25.463	197.287
4.7 - 4.2	4.4	0.027875	0.591322	25.145	222.432
4.2 - 3.8	4.0	0.047831	0.639152	47.893	270.325
3.8 - 3.4	3.6	0.027006	0.666158	30.036	300.361
3.4 - 3.1	3.2	0.015874	0.682032	19.635	319.996
3.1 - 2.8	2.9	0.015227	0.697259	20.837	340.832
2.8 - 2.5	2.6	0.015993	0.713252	24.184	365.017
2.5 - 2.3	2.4	0.017392	0.730644	29.149	394.165

CCRI University of Ottawa

3Flex 3.01

3Flex Version 3.01
Serial # 541 Unit 1 Port 3

Sample: UM-6
Operator:
File: C:\3Flex\data\Yong Yang data\000-717-UM-6.SMP

Started:	16/06/2017 3:51:00 PM	Analysis adsorptive:	N2
Completed:	17/06/2017 7:56:54 AM	Analysis bath temp.:	77.297 K
Report time:	19/06/2017 1:24:15 PM	Thermal correction:	No
Sample mass:	0.0720 g	Warm free space:	17.0137 cm³ Measured
Cold free space:	58.9353 cm³	Equilibration interval:	10 s
Low pressure dose:	None	Sample density:	1.000 g/cm³
Automatic degas:	No		

BJH Desorption Cumulative Pore Volume (Larger)

Kruk-Jaroniec-Sayari : Faas Correction

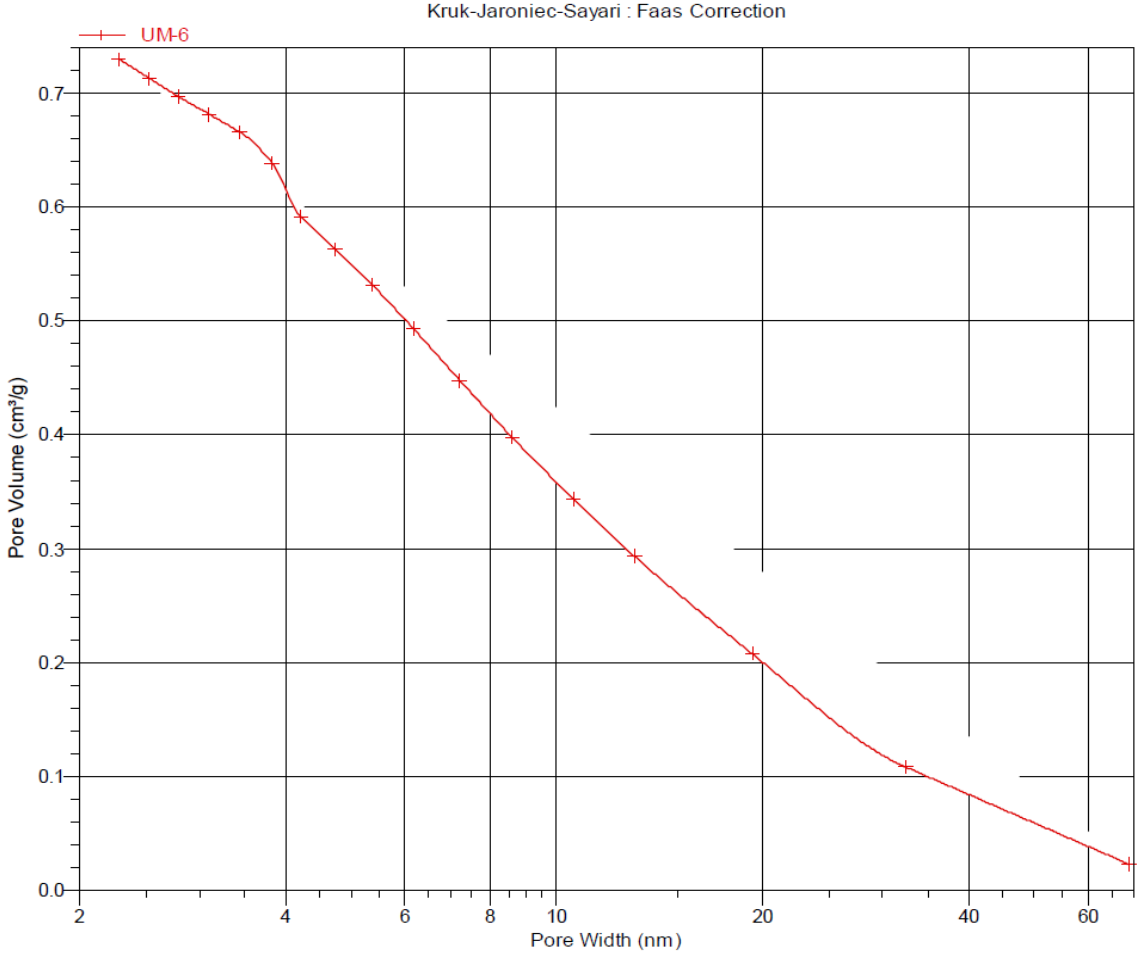

CCRI University of Ottawa

3Flex 3.01

3Flex Version 3.01
Serial # 541 Unit 1 Port 3

Sample: UM-6
Operator:
File: C:\3Flex\data\Yong Yang data\000-717-UM-6.SMP

Started:	16/06/2017 3:51:00 PM	Analysis adsorptive:	N2
Completed:	17/06/2017 7:56:54 AM	Analysis bath temp.:	77.297 K
Report time:	19/06/2017 1:24:15 PM	Thermal correction:	No
Sample mass:	0.0720 g	Warm free space:	17.0137 cm³ Measured
Cold free space:	58.9353 cm³	Equilibration interval:	10 s
Low pressure dose:	None	Sample density:	1.000 g/cm³
Automatic degas:	No		

BJH Desorption dV/dw Pore Volume

Kruk-Jaroniec-Sayari : Faas Correction

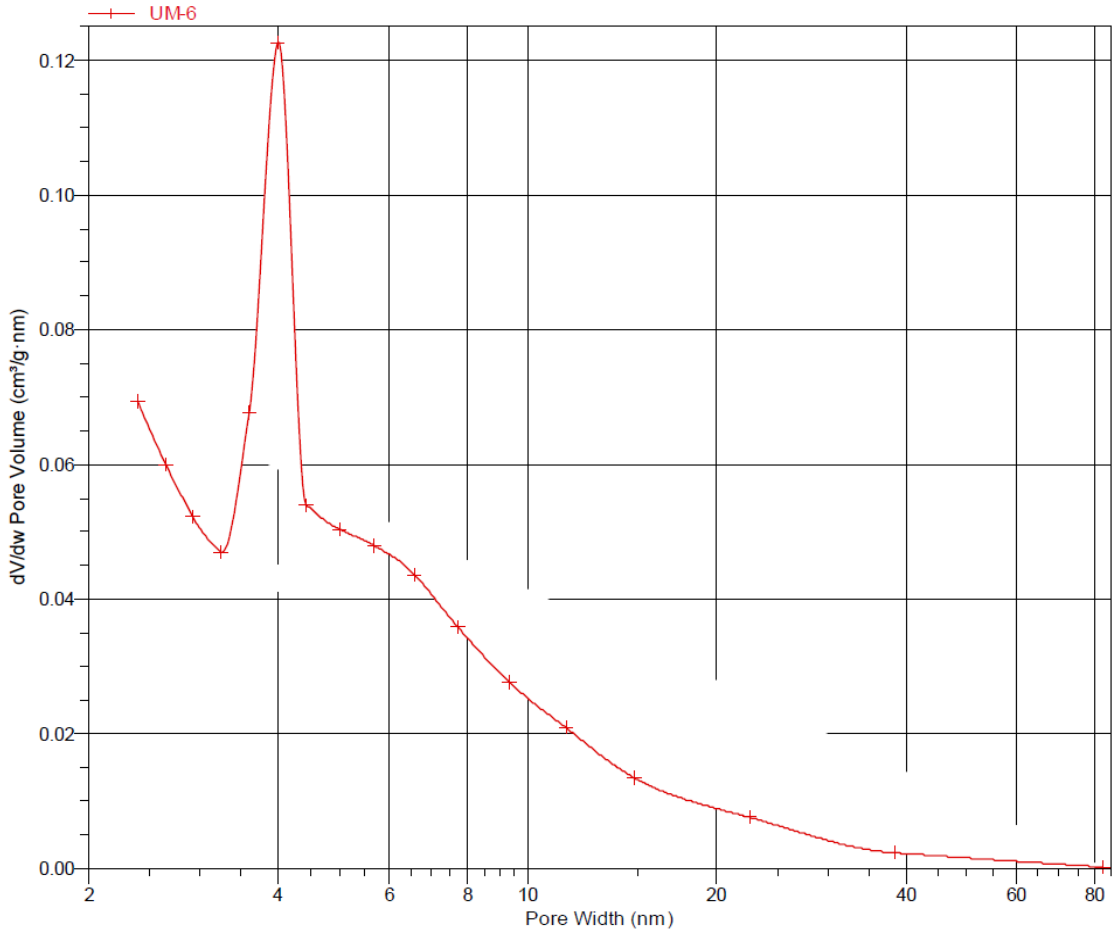

Appendix D

BET surface area and porosity analysis report of the mixture of CO_2 and steam activated CBPP fly ash at *850°C (CSAC)* impregnated with 0.1M $FeCl_3$

CCRI University of Ottawa

3Flex 3.01 | 3Flex Version 3.01 Serial # 541 Unit 1 Port 2 | Page 1

Sample: UM-7
Operator:
File: C:\3Flex\data\Yong Yang data\000-718-UM-7.SMP

Started:	28/06/2017 10:47:09 AM	Analysis adsorptive:	N2
Completed:	28/06/2017 8:05:40 PM	Analysis bath temp.:	77.353 K
Report time:	29/06/2017 3:15:30 PM	Thermal correction:	No
Sample mass:	0.0742 g	Warm free space:	16.9888 cm³ Measured
Cold free space:	60.2111 cm³	Equilibration interval:	10 s
Low pressure dose:	None	Sample density:	1.000 g/cm³
Automatic degas:	No		

Summary Report

Surface Area

Single point surface area at p/p° = 0.300000000:	980.3574 m²/g
BET Surface Area:	1,074.4514 m²/g
t-Plot Micropore Area:	572.8437 m²/g
t-Plot external surface area:	501.6078 m²/g
BJH Adsorption cumulative surface area of pores between 1.7000 nm and 300.0000 nm width:	475.647 m²/g
BJH Desorption cumulative surface area of pores between 1.7000 nm and 300.0000 nm width:	408.6617 m²/g

Pore Volume

t-Plot micropore volume:	0.254708 cm³/g
BJH Adsorption cumulative volume of pores between 1.7000 nm and 300.0000 nm width:	0.740973 cm³/g
BJH Desorption cumulative volume of pores between 1.7000 nm and 300.0000 nm width:	0.706137 cm³/g

Pore Size

BJH Adsorption average pore width (4V/A):	6.2313 nm
BJH Desorption average pore width (4V/A):	6.9117 nm

Sample: UM-7
Operator:
File: C:\3Flex\data\Yong Yang data\000-718-UM-7.SMP

Started:	28/06/2017 10:47:09 AM	Analysis adsorptive:	N2
Completed:	28/06/2017 8:05:40 PM	Analysis bath temp.:	77.353 K
Report time:	29/06/2017 3:15:30 PM	Thermal correction:	No
Sample mass:	0.0742 g	Warm free space:	16.9888 cm³ Measured
Cold free space:	60.2111 cm³	Equilibration interval:	10 s
Low pressure dose:	None	Sample density:	1.000 g/cm³
Automatic degas:	No		

Isotherm Tabular Report

Relative Pressure (p/p°)	Absolute Pressure (mmHg)	Quantity Adsorbed (cm³/g STP)	Elapsed Time (h:min)	Saturation Pressure (mmHg)
			00:59	761.256714
0.001427707	1.084983	189.4132	04:26	759.948242
0.002886104	2.193282	203.7087	04:43	759.945557
0.005860124	4.453998	217.9121	04:53	760.051819
0.028990615	22.030735	251.3698	05:00	759.926453
0.040570046	30.830112	259.1595	05:04	759.923035
0.059028945	44.855549	268.2458	05:08	759.890747
0.072658820	55.210827	273.6340	05:12	759.864075
0.108144218	82.177223	284.8044	05:16	759.885498
0.142610893	108.371727	293.6187	05:20	759.911987
0.177625662	134.989822	301.5226	05:24	759.968018
0.202299849	153.730698	306.7121	05:28	759.915039
0.244329737	185.659164	315.0500	05:32	759.871338
0.279835795	212.639969	321.8269	05:35	759.874084
0.313849501	238.484589	328.2604	05:39	759.869263
0.346587015	263.346710	334.3279	05:43	759.828552
0.378224325	287.382294	340.2317	05:46	759.819702
0.412306895	313.267578	346.6016	05:50	759.792236
0.446275770	339.020264	352.9942	05:54	759.665405
0.480027676	364.638123	359.5733	05:58	759.618958
0.513836345	390.286804	366.3290	06:02	759.554688
0.547687971	416.017151	373.4205	06:06	759.587891
0.581358967	441.639679	380.9840	06:10	759.667786
0.615257268	467.410767	389.2156	06:14	759.699707
0.648994165	493.109680	398.2983	06:18	759.806030
0.683260354	519.117188	408.4927	06:22	759.764832
0.717057572	544.778625	420.0124	06:27	759.741821
0.734732682	558.230286	426.4385	06:31	759.773315
0.751461240	570.933960	432.8873	06:35	759.765015
0.767991979	583.566467	439.9163	06:40	759.860107
0.777284687	590.618469	443.7901	06:43	759.848328
0.785409582	596.768860	447.4409	06:47	759.818665
0.818870864	622.192017	464.2285	06:54	759.817017
0.851631297	647.061340	483.0947	07:00	759.790466
0.885294814	672.665955	505.7629	07:06	759.821411
0.917980253	697.551758	533.5639	07:12	759.876648
0.950591741	722.424194	571.4585	07:20	759.973145
0.986908120	750.514893	629.1495	07:31	760.470886

Sample: UM-7
Operator:
File: C:\3Flex\data\Yong Yang data\000-718-UM-7.SMP

Started:	28/06/2017 10:47:09 AM	Analysis adsorptive:	N2
Completed:	28/06/2017 8:05:40 PM	Analysis bath temp.:	77.353 K
Report time:	29/06/2017 3:15:30 PM	Thermal correction:	No
Sample mass:	0.0742 g	Warm free space:	16.9888 cm³ Measured
Cold free space:	60.2111 cm³	Equilibration interval:	10 s
Low pressure dose:	None	Sample density:	1.000 g/cm³
Automatic degas:	No		

Isotherm Tabular Report

Relative Pressure (p/p°)	Absolute Pressure (mmHg)	Quantity Adsorbed (cm³/g STP)	Elapsed Time (h:min)	Saturation Pressure (mmHg)
0.969236083	736.957153	616.8786	07:37	760.348450
0.942503366	716.669861	588.1718	07:44	760.389709
0.886629529	674.358276	533.5122	07:53	760.586304
0.844859841	642.002258	504.5636	08:00	759.892029
0.794612863	603.637817	476.5146	08:06	759.662781
0.742729919	564.324280	451.5096	08:13	759.797424
0.691054784	524.983826	429.9907	08:19	759.684814
0.639283310	485.611877	411.3563	08:24	759.619202
0.588029584	446.687500	395.4671	08:29	759.634399
0.536970827	407.880798	381.9595	08:34	759.595825
0.486403931	369.424438	369.7367	08:39	759.501343
0.439614473	333.853760	353.4572	08:45	759.423950
0.386644010	293.643524	341.5602	08:49	759.467407
0.335407595	254.721863	332.2481	08:53	759.439758
0.285813898	217.073807	323.2452	08:58	759.493530
0.236327704	179.476395	314.1050	09:02	759.438660
0.187118624	142.108383	304.5014	09:06	759.456116

Sample: UM-7
Operator:
File: C:\3Flex\data\Yong Yang data\000-718-UM-7.SMP

Started:	28/06/2017 10:47:09 AM	Analysis adsorptive:	N2
Completed:	28/06/2017 8:05:40 PM	Analysis bath temp.:	77.353 K
Report time:	29/06/2017 3:15:30 PM	Thermal correction:	No
Sample mass:	0.0742 g	Warm free space:	16.9888 cm³ Measured
Cold free space:	60.2111 cm³	Equilibration interval:	10 s
Low pressure dose:	None	Sample density:	1.000 g/cm³
Automatic degas:	No		

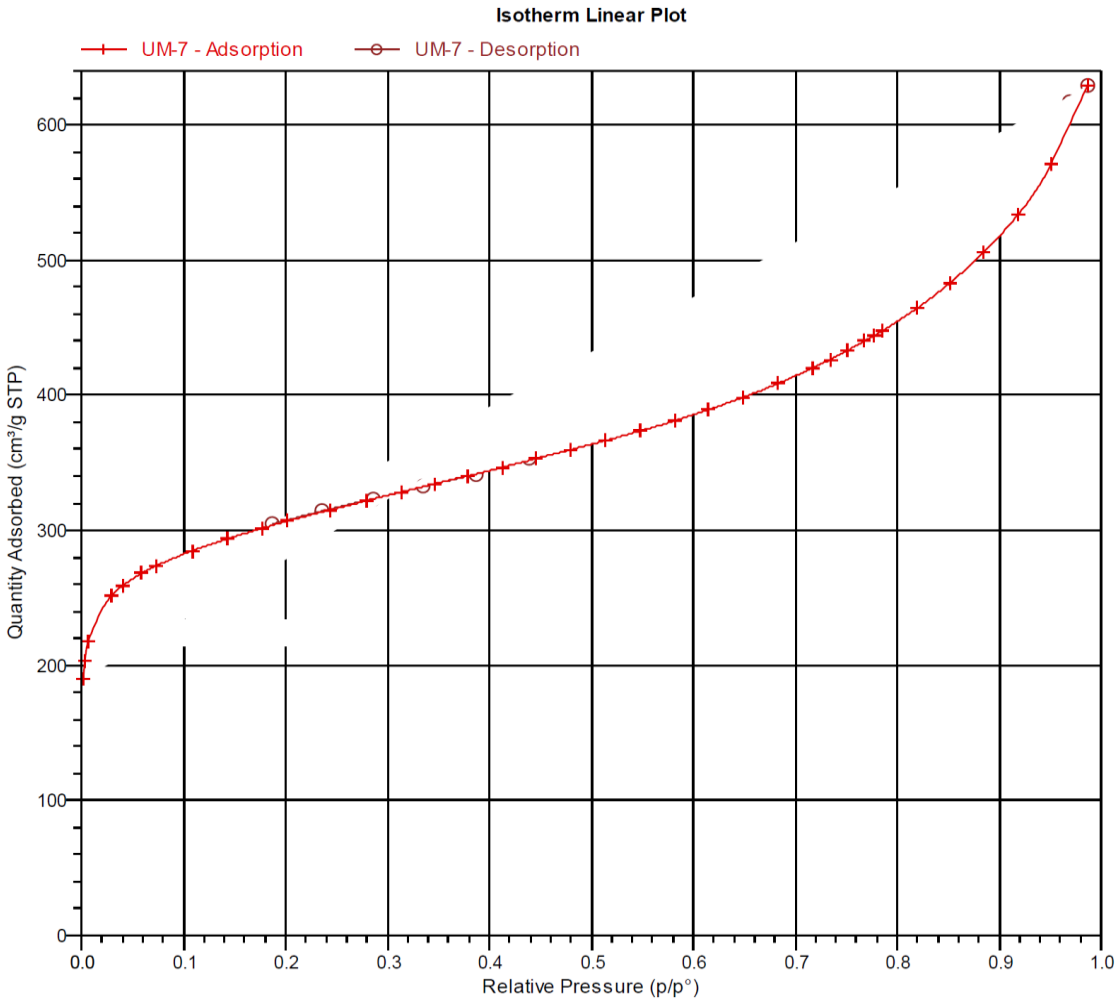

Sample: UM-7
Operator:
File: C:\3Flex\data\Yong Yang data\000-718-UM-7.SMP

Started:	28/06/2017 10:47:09 AM	Analysis adsorptive:	N2
Completed:	28/06/2017 8:05:40 PM	Analysis bath temp.:	77.353 K
Report time:	29/06/2017 3:15:30 PM	Thermal correction:	No
Sample mass:	0.0742 g	Warm free space:	16.9888 cm³ Measured
Cold free space:	60.2111 cm³	Equilibration interval:	10 s
Low pressure dose:	None	Sample density:	1.000 g/cm³
Automatic degas:	No		

BET Report

BET surface area:	1074.4514 ± 12.0525 m²/g
Slope:	0.004060 ± 0.000045 g/cm³ STP
Y-intercept:	-0.000009 ± 0.000005 g/cm³ STP
C:	-449.131147
Qm:	246.8540 cm³/g STP
Correlation coefficient:	0.9998148
Molecular cross-sectional area:	0.1620 nm²

Relative Pressure (p/p°)	Quantity Adsorbed (cm³/g STP)	1/[Q(p°/p - 1)]
0.059028945	268.2458	0.000234
0.072658820	273.6340	0.000286
0.108144218	284.8044	0.000426
0.142610893	293.6187	0.000566
0.177625662	301.5226	0.000716

Sample: UM-7
Operator:
File: C:\3Flex\data\Yong Yang data\000-718-UM-7.SMP

Started:	28/06/2017 10:47:09 AM	Analysis adsorptive:	N2
Completed:	28/06/2017 8:05:40 PM	Analysis bath temp.:	77.353 K
Report time:	29/06/2017 3:15:30 PM	Thermal correction:	No
Sample mass:	0.0742 g	Warm free space:	16.9888 cm³ Measured
Cold free space:	60.2111 cm³	Equilibration interval:	10 s
Low pressure dose:	None	Sample density:	1.000 g/cm³
Automatic degas:	No		

BET Surface Area Plot

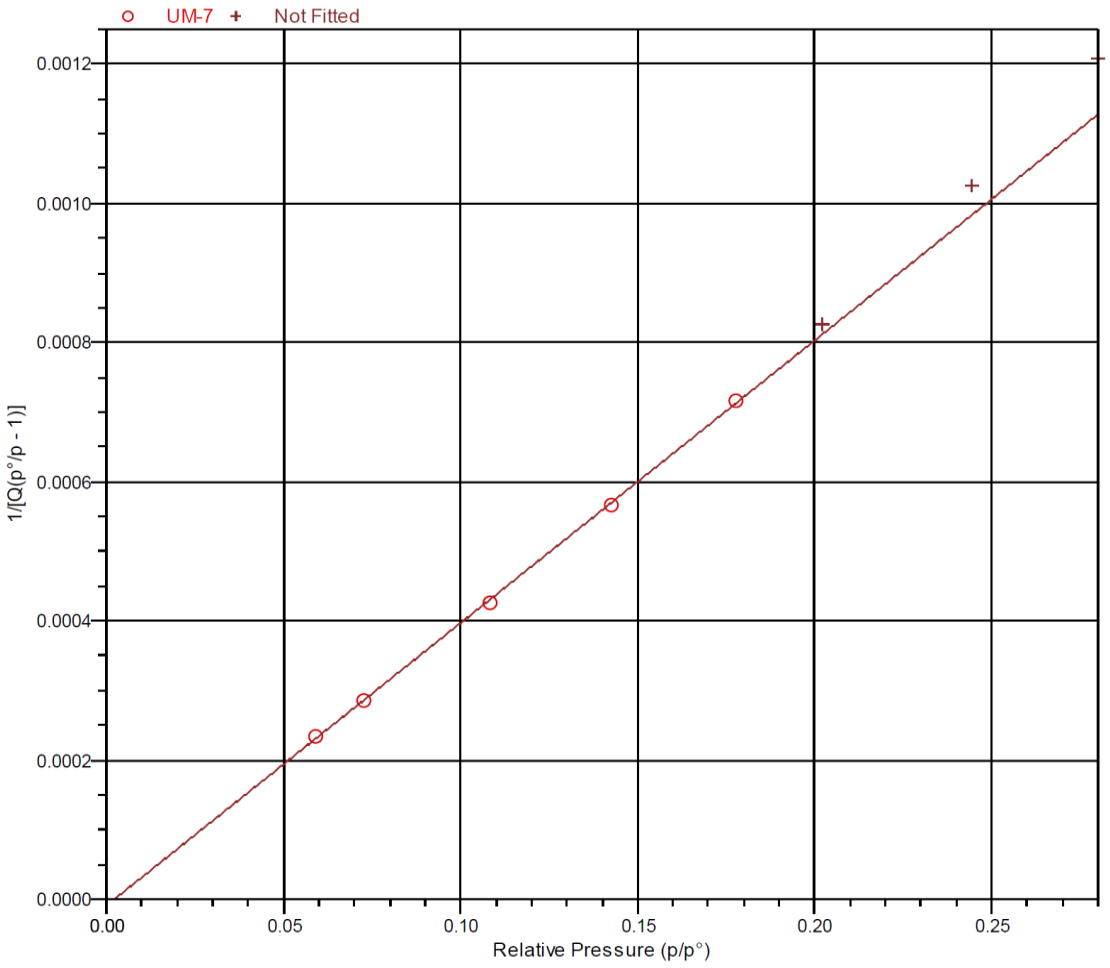

Sample: UM-7
Operator:
File: C:\3Flex\data\Yong Yang data\000-718-UM-7.SMP

Started:	28/06/2017 10:47:09 AM	Analysis adsorptive:	N2
Completed:	28/06/2017 8:05:40 PM	Analysis bath temp.:	77.353 K
Report time:	29/06/2017 3:15:30 PM	Thermal correction:	No
Sample mass:	0.0742 g	Warm free space:	16.9888 cm³ Measured
Cold free space:	60.2111 cm³	Equilibration interval:	10 s
Low pressure dose:	None	Sample density:	1.000 g/cm³
Automatic degas:	No		

t-Plot Report

Micropore volume:	0.254708 cm³/g
Micropore area:	572.8437 m²/g
External surface area:	501.6078 m²/g
Slope:	323.685933 ± 5.705627 cm³/g·nm STP
Y-intercept:	164.362181 ± 2.469788 cm³/g STP
Correlation coefficient:	0.999379
Surface area correction factor:	1.000
Density conversion factor:	0.0015497
Total surface area (BET):	1074.4514 m²/g
Thickness range:	0.35000 nm to 0.50000 nm
Thickness equation:	Harkins and Jura

Thickness Curve

$t = [13.99 / (0.034 - \log(p/p^\circ))] ^ 0.5$

t-Plot Report - Data

Relative Pressure (p/p°)	Statistical Thickness (nm)	Quantity Adsorbed (cm³/g STP)	Fitted
0.059028945	0.33283	268.2458	
0.072658820	0.34539	273.6340	
0.108144218	0.37403	284.8044	*
0.142610893	0.39875	293.6187	*
0.177625662	0.42229	301.5226	*
0.202299849	0.43837	306.7121	*
0.244329737	0.46536	315.0500	*
0.279835795	0.48815	321.8269	*
0.313849501	0.51028	328.2604	
0.346587015	0.53206	334.3279	
0.378224325	0.55374	340.2317	
0.412306895	0.57798	346.6016	
0.446275770	0.60328	352.9942	
0.480027676	0.62977	359.5733	
0.513836345	0.65795	366.3290	
0.547687971	0.68810	373.4205	
0.581358967	0.72042	380.9840	
0.615257268	0.75575	389.2156	
0.648994165	0.79427	398.2983	
0.683260354	0.83759	408.4927	

Sample: UM-7
Operator:
File: C:\3Flex\data\Yong Yang data\000-718-UM-7.SMP

Started:	28/06/2017 10:47:09 AM	Analysis adsorptive:	N2
Completed:	28/06/2017 8:05:40 PM	Analysis bath temp.:	77.353 K
Report time:	29/06/2017 3:15:30 PM	Thermal correction:	No
Sample mass:	0.0742 g	Warm free space:	16.9888 cm³ Measured
Cold free space:	60.2111 cm³	Equilibration interval:	10 s
Low pressure dose:	None	Sample density:	1.000 g/cm³
Automatic degas:	No